# INVESTIGATING THE IMPACT OF METALS AND METHANOBACTIN ON GENE EXPRESSION IN *METHYLOSINUS TRICHOSPORIUM* OB3B

By

**Bhagyalakshmi Kalidass**

A dissertation submitted in partial fulfillment
of the requirements for the degree of
Doctor of Philosophy
(Environmental Engineering)
in The University of Michigan
2016

Doctoral Committee:
Professor Jeremy D. Semrau, Chair
Professor Alan A. DiSpirito
Assistant Professor Brian Robert Ellis
Professor Thomas M. Schmidt

**ACKNOWLEDGEMENTS**

I take this opportunity to thank my advisor, Professor Jeremy D. Semrau for his constant guidance, encouragement and inspiration. I have been motivated by his dedication to perfection, thoroughness and critical thinking, and greatly value his comments and criticisms that helped with the successful completion of my research. I am thankful to my committee members, Professors Alan A. DiSpirito, Thomas M. Schmidt, Brian Robert Ellis for their valuable suggestions and inputs towards the doctoral degree.

I am thankful to my former labmates, Sheeja Jagadevan and Alexey Vorobev, for all the help in learning laboratory experimental techniques, and my current labmates, Muhammad Farhan Ul Haque and Wenyu Gu, for all their suggestions and thoughtful discussions throughout the project. Special thanks to Muhammad Farhan Ul Haque for the RT-qPCR data collected for my work. I sincerely thank Thomas Yavaraski for all the help he extended for the use of Inductively Coupled Plasma –Mass Spectrometry.

I would like to convey my hearty thanks to my roommates, Manaswini Malladi, Nalini Nadupalli and Prannda Sharma, and friends, Divya Garikapati, Parameshwaran Pasupathy and Kavya Raja for their moral support at tough times.

I am indebted to my parents, Selvanayagi Kalidass and Kalidass Elumalai, siblings, Bhagheerathi Vyakarnam, Bhuvaneswari Sivapalani and Balachandran Kalidass, and thank all my family members for their continuous motivation and support at all times. I would like to thank my fiancé, Ramkumar Sugumar, for helping me putting this all together.

Last but not least, I would like to dedicate this to my late grandfather, Govindan Ramaswamy, who had sparked the interest in me for science and technology, and is a constant source of inspiration. He shall always be remembered.

## TABLE OF CONTENTS

## LIST OF TABLES

## LIST OF FIGURES

## ABSTRACT

With the rise in the atmospheric concentration of methane, a very potent greenhouse gas, its mitigation requires the utmost attention (EPA, 2006). Methanotrophs are a unique set of bacteria capable of mitigating methane emissions by converting methane to carbon dioxide which has a lower global warming potential. Studies on methanotrophs mainly focus on understanding the physiological and biochemical properties of methanotrophs to best model them for field scale applications. While methanotrophs are well known to be sensitive to copper as its concentration affects the expression and activities of the two forms of methane monooxygenase, information about the effect of other abundant metal ions available in the environment is scarce. Due to the ubiquitous nature of methanotrophs, understanding their behavioral response to the diverse environments is vital for exploiting them in bioremediation.

The first set of experiments described here focus on understanding if metals other than copper can affect the expression and activity of methane monooxygenase. Herein, gold was shown to affect the "copper-switch" by competing with copper for uptake by a copper chelating molecule, methanobactin, secreted by few methanotrophs. In other words, while it is well known that presence of copper alone suppresses the activity of soluble methane monooxygenase (sMMO), gold actually induces sMMO activity in *Methylosinus trichosporium* OB3b, even in the presence of copper. This clearly indicates the need for understanding how the relative abundance of metals in the environment affects methanotrophic activity.

The second set of experiments target at determining what metals can affect the expression and activity of methanol dehydrogenase, the second enzyme in the methane oxidation pathway. The study indicates that the rare earth element, cerium, acts as a switch between the two forms of methanol dehydrogenase in *M. trichosporium* OB3b. Such information will likely prove important when designing systems where one form of methanol dehydrogenase that has a catalytic advantage over the other form is preferred for system performance.

Thirdly, it was hypothesized that if metals could have a drastic impact on expression and activities of key enzyme, so might methanobactin since methanobactin acts as a means of uptake mechanism for metals like copper and gold. When *M. trichosporium* OB3b was grown in media supplemented with copper and methanobactin from *Methylocystis* sp. strain SB2, sMMO activity was induced. This shows that "cross-talk" can occur between methanotrophs and thus methanobactin qualifies as a signaling molecule affecting the gene expression in a methanotroph that did not secrete the methanobactin.

Lastly, this study attempted to identify the complete regulatory basis of the "copper-switch" as competing models currently exist. A series of electro-mobility shift assays were performed between DNA upstream of genes and the gene products to determine if any specific gene product activates or suppresses the expression of the gene by binding to its upstream consensus region. The results are not confirmative at this point and thus more work is needed to fully define the mechanism underlying the "copper-switch" in methanotrophs.

# CHAPTER I: INTRODUCTION

## I.1. Introduction

Anthropogenic use of fossil fuels has led to a continued increase in methane emissions, a major contributor to global warming. Innovative technologies have been proposed to: (1) reduce methane emissions and (2) utilize methane emissions for production of hydrogen and organic chemicals such as methanol, formaldehyde, chloroform and biodiesel (Fujimoto et al., 1994; Silverman et al., 2014). Given that methanotrophs are ubiquitous in the environment, and the high specificity these microbes exhibit for methane, methanotrophs are ideal natural catalysts for use in both reducing methane emissions and product development.

Extensive research on methanotrophs has disclosed its prospective commercial use in production of single cell protein, biopolymers (polyhydroxyalkanoates and polyhydroxybutyrate), osmoprotectants, biofuels, human health supplements, soluble metabolic products such as methanol, formaldehyde and organic acids, and catalytic systems for electrochemistry (Overland et al., 2010; Fei et al., 2014; Karthikeyan et al., 2014; Trotsenko et al., 2005; Silverman et al.,

2014; Mueller et al., 2005; Kalyuzhnaya et al., 2013; Dominguez-Benetton et al., 2013), but there are still significant challenges to achieve these potential applications of methanotrophs at an industrial scale. The challenges include, for example, the solubility of methane in water, mass transfer limitations as well as the fact that much is unknown as to how methanotrophs sense and respond to their environment (Jiang et al., 2010). Further, the key details of methanotrophic physiology are still unclear. This study attempts to fill gaps in our understanding of methanotrophs, as this would be of great value for tweaking the methanotrophs in both natural and engineered systems for expanding the biotechnological applications for human benefit.

### *I.1.1. Greenhouse gases*

The Earth's average surface temperature is increasing steadily with a global warming rate > 0.2 ºC per decade (Smith et al., 2015). This increase is substantially accounted for by the anthropogenic emissions of greenhouse gases (GHGs) (Climate Change 2014). Naturally occurring GHGs in the atmosphere include carbon dioxide ($CO_2$), methane ($CH_4$), water vapor ($H_2O$), ozone ($O_3$) and nitrous oxide ($N_2O$), while synthetic GHGs include chlorofluorocarbons (CFCs), hydrofluorocarbons (HFCs), perfluorocarbons (PFCs) and sulfur hexafluoride ($SF_6$). Increasing awareness of the effect of GHGs on climate change has led to control of synthetic GHGs by Montreal protocol, thereby limiting their global emissions. Atmospheric levels of naturally occurring GHGs continue to rise since their anthropogenic emissions are linked to the daily needs of mankind, e.g., as domestic and industrial fuel. The anthropogenic sources of these predominant GHGs are fossil fuel consumption, oil flaring, natural gas fracking, deforestation, enteric fermentation and landfills among several other contributors (Subak et al., 1993). With the human population exceeding seven billion and increasing dependence on fossil fuels, the

atmospheric concentrations of GHGs pose a potential threat to our climate. The anthropogenic emissions of important GHGs available from 2008 are listed in Table I.1.

**Table I.1** Anthropogenic emissions, percentage increase since 1750 and global warming potential for 20 years' time horizon of predominant greenhouse gases.

| Greenhouse gas | Anthropogenic emissions [a] (Gt $CO_2$-eq $yr^{-1}$) | Percentage increase since 1750 [b,c,d,e] | Global warming potential over a 20 year period [f] |
|---|---|---|---|
| $CO_2$ | 35 | 41.2 % | 1 |
| $CH_4$ | 8.5 | 170.4 % | 86 |
| $N_2O$ | 3.1 | 20.7 % | 268 |

[a] Montzka et al., 2011; [b,c,d,e] Prentice et al., 2001; http://www.esrl.noaa.gov/gmd/ccgg/trends; Prinn et al., 2000; IPCC 2007; [f] IPCC 2013

Although the anthropogenic emissions of $CO_2$ are the highest among all GHGs due to the increased rate of fossil fuel burning, the increase in its atmospheric concentration is strongly affected by the fluctuations in land and ocean sinks for $CO_2$ and land use (Gruber et al., 2009; Feely et al., 2004).

Given this, it is very difficult to reduce its emissions in the near future. While efforts like capping $CO_2$ emissions and/or a tax on fossil fuel usage are being taken to mitigate $CO_2$ emissions, simultaneous measures to abate the non-$CO_2$ GHG emissions must also be taken. The key non-$CO_2$ GHGs of concern are $CH_4$ and $N_2O$. $N_2O$ emissions are primarily from fossil fuel combustion and biomass burning (Muzio and Kramlich, 1988). Most of the reactive nitrogen is fixed using nitrogen-fixing crops, nitrogen mineralization as ammonia and nitrate, and biogeochemical cycling of nitrogen, thus leading to very little contribution of anthropogenic $N_2O$ to atmospheric levels (Van Groenigen et al., 2010; Seitzinger et al., 2000). Methane, on the other

hand, is the focus of this study as it is the most abundant non-$CO_2$ GHG with about 170% elevated atmospheric concentration since 1750.

*I.1.1.1. Methane*

Methane ($CH_4$) is an essential component of the global carbon cycle and an important greenhouse gas that is produced from many natural and anthropogenic sources such as agriculture, fossil fuel exploitation, waste treatment and biomass burning (Anderson et al., 2010; Parker et al., 2011). The globally averaged atmospheric methane concentration in 2011 was 1803 ± 2 ppb (IPCC, 2013) and has been increasing in recent years. The main reasons for elevated global methane emissions are methane leaks from natural gas collection and distribution systems, melting of permafrost and increased emissions from wetlands, landfills and ruminants amongst others (Bousquet et al., 2006; Ohara et al., 2007; Bloom et al., 2010; Dlugokencky et al., 2011). It is now recognized as a potent greenhouse gas with the latest IPCC estimate of the global warming potential of methane to be about 86 and 34 times that of carbon dioxide over a 20- and 100-year period respectively, making methane emission a global concern over a short time horizon (IPCC, 2013). The various contributions of methane emissions are listed in Table I.2.

**Table I.2** Annual contributions of methane emissions (Kirschke et al., 2013)

| **Methane emissions** | | **Tg methane $yr^{-1}$** |
|---|---|---|
| **Anthropogenic activities** | Agriculture and waste | 209 |
| | Biomass burning | 30 |
| | Fossil fuels | 96 |
| | Subtotal | **335** |
| **Natural emissions** | Wetlands | 175 |
| | Lakes, rivers, oceans, wild fires, permafrost, ruminants | 43 |
| | Subtotal | **218** |
| **Total** | | **553** |

The natural sinks for atmospheric methane include: (1) reaction with hydroxyl radical to form methyl radical and water vapour; (2) reaction with chlorine in the atmosphere to form chloromethane and hydrochloric acid, and; (3) removal via methanotrophic activity (Clark and Jim, 2006). The main sink of atmospheric methane is the reaction with the hydroxyl radical (Montzka et al., 2011). However, the chemical coupling between OH• and $CH_4$ reduces the atmospheric concentrations of both the species leading to slowing down of methane removal by negative feedback (Fuglestvedt et al., 1995; Prinn et al., 1995).

About 90% of methane produced in anaerobic soils, however, is removed through microbiological oxidation by methanotrophic bacteria, a unique group of methane oxidizing prokaryotes that thrive on methane as their sole source of carbon and energy (Yoon et al., 2009; Chowdhury and Dick, 2013).

### *I.1.2. Methanotrophs*

Methanotrophs are a bacterial subset of methylotrophs that primarily use reduced one-carbon compounds and multi-carbon compounds with no carbon-carbon bonds for growth. The ability of methanotrophs to break the stable, non-reactive tetrahedral carbon-hydrogen bond (435 kJ $mol^{-1}$ bond dissociation energy) present in methane under ambient growth conditions makes it unique (Chauhan et al., 2008). This process of activating the C-H bond in methane otherwise requires extreme temperatures and pressures and is not economically feasible (Arakawa et al., 2001).

Methanotrophs are found in a wide variety of locations, including volcanic mudpots, Antarctic lakes, coral reefs, acidic forest soils, hydrothermal vents, agricultural soils, etc. (Schnell and King, 1995; Semrau et al., 2010). Methanotrophs in nature obtain their carbon from methane produced by anaerobic digestion of methanogenic archaea in environments like swamps, wetlands, intestinal tract of mammals (Michael et al, 2003) and from abiotic sources such as fossil fuels and geothermal/volcanic $CH_4$. The residual methane that is not consumed by methanotrophs is released as atmospheric methane and has increased the rate of global warming (Ehalt, 1974; Ehalt and Schmidt, 1978; Anderson et al., 2010).

There is a resurgence of interest in methanotrophs, in part due to their role in methane removal from the atmosphere as well as their ability to catalyze reactions of industrial and environmental importance. Agricultural and forest soils have shown to be strong methane sinks in the past decade (Price et al., 2004; Castaldi et al., 2007; Dunfield, 2007). Further, Yoon et al., (2009) have developed a model of a biotrickling filtration system composed of methanotrophs for removal of atmospheric methane. Their study showed that the use of methanotrophic biotrickling

filters for controlling methane emissions is technically feasible and if a carbon tax is implemented, these systems could be economically attractive.

*I.1.2.1. Applications of methanotrophy*

Methanotrophs have significant potential in bioremediation of pollutants (e.g., halogenated hydrocarbons) via co-metabolism, biotransformation of diverse organic substrates into more valuable products (e.g., propylene to epoxypropane, production of chiral alcohols), greenhouse gas removal, production of commercially relevant compounds (e.g., single cell protein, poly-3-hydroxybutyrate, astaxanthin) and biofuel production (Jiang et al., 2010; Wackett and Professor, 2014). BioProtein, a bacterial single-cell protein synthesized by the industry Norferm Danmark in Denmark, is a fermentation product of natural gas with the methanotroph, *Methylococcus capsulatus* Bath. BioProtein is currently used as a protein supplement in animal and fish feed and is a potential protein source in human diets (Christensen et al., 2003; Sikkeland et al., 2007). Methanotrophs have also shown great potential in methanol production from methane, for easier use as liquid fuel, using the enzyme methane monooxygenase. Industrial-scale production, however, is yet to be achieved for any of these processes (Xin et al., 2004).

The recent discovery of a metal chelator named methanobactin, produced by some methanotrophs, has further broadened the potential application of methanotrophy (Kim et al., 2004). Methanobactin could play an important role in processes ranging from copper extraction from insoluble minerals (Kulczycki et al., 2007), extraction of copper from wastewater and treatment of Wilson's disease (Ruiz and Ogden, 2004; Summer et al., 2011; Zischka et al., 2011), a human disorder of copper metabolism resulting in excess copper deposits in liver, kidney, brain and eyes leading to chronic oxidative stress and subsequent hepatitis (Summer et al., 2011). The

most commonly used chelator for treating Wilson's disease is D-penicillamine, which affects brain and nervous system functions (Brewer, 1999). Methanobactin, however, has been shown to have no observable side effects (Summer et al., 2011). Methanobactin also has antibacterial properties against Gram-positive bacteria (Kim et al., 2004). Further, a study by Choi et al., (2006b) found that methanobactin from *M. trichosporium* OB3b could produce gold nanoparticles by reducing Au (III) to elemental gold, Au (0), suggesting another potential application of methanobactin. Methanobactin from *M. trichosporium* OB3b also was shown to bind mercury as Hg (II) and reduce to it to Hg (0), thereby reducing mercury toxicity (Vorobev et al., 2013). This suggests that methanobactin might be crucial for manipulating the community structure and diversity of both methanotrophs and non-methanotrophs for survival in metal-polluted environments where proteins like methanobactin would provide protection against other similar toxic metals.

*I.1.2.2. Methanotrophic diversity*

Methanotrophs use either oxygen under aerobic conditions or utilize terminal electrons such as nitrite, nitrate and sulphate under anaerobic conditions to oxidize methane. The aerobic proteobacterial methanotrophs use the enzyme, methane monooxygenase, to oxidize methane to methanol and subsequently convert methanol to formaldehyde, which is incorporated into biomass via the serine or ribulose monophosphate (RuMP) pathway (Figure I.1). Formaldehyde can be further oxidized to carbon dioxide to obtain energy. Methane oxidation pathway under aerobic conditions is discussed below in more detail (Section *I.1.3*).

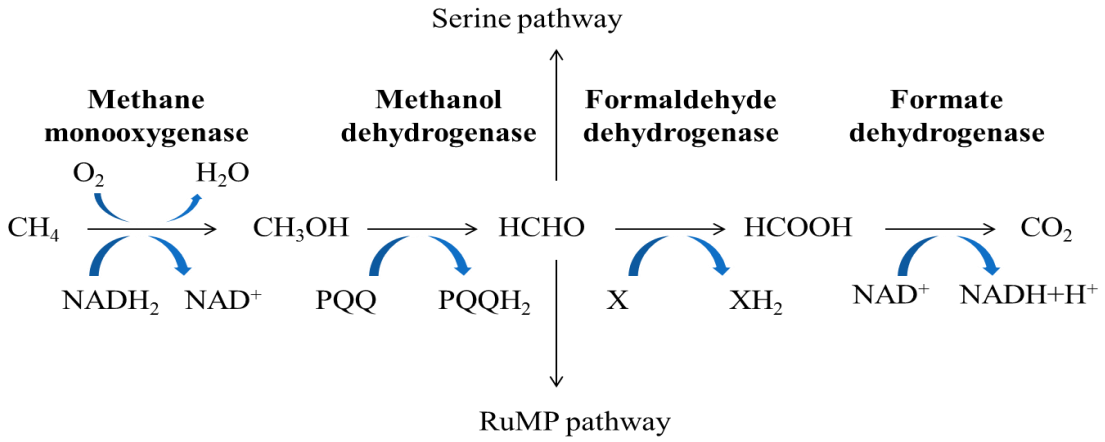


**Figure I.1** The metabolic pathway of methane oxidation to carbon dioxide in aerobic methanotrophs. MMO- Methane monooxygenase; MDH- Methanol dehydrogenase; FADH- Formaldehyde dehydrogenase; FDH- Formate dehydrogenase.

Aerobic methanotrophs from the phyla Verrucomicrobia and NC 10 phyla, also use methane monooxygenase for methane oxidation, but utilize Calvin-Benson-Bassham cycle for fixing carbon into their biomass (Khadem et al., 2011; Rasigraf et al., 2014). The recently characterized methanotroph from the NC 10 phylum, *Ca.* Methylomirabilis oxyfera, is peculiar in the way it gets its oxygen for methane oxidation. It was found to couple methane oxidation to nitrite reduction (Hu et al., 2011). *Ca.* Methylomirabilis oxyfera oxidizes methane using reactions similar to those used by aerobic methanotrophs; however, it does so in the complete absence of external oxygen. Instead, nitrite is reduced to nitric oxide, and the latter is dismutated to molecular nitrogen and oxygen (Ettwig et al., 2010, 2012). The internally produced oxygen can then be used for methane oxidation by methane monooxygenase.

Anaerobic methanotrophs have been shown to couple methane oxidation to not only nitrite reduction (Ettwig et al., 2010) but also to sulphate reduction (Hinrichs and Boetius, 2002; Reeburgh, 2007; Haroon et al., 2013). Syntrophic coupling between the consortia of

methanotrophic archaea (ANME) and sulfate-reducing bacteria (SRB) facilitates anaerobic oxidation of methane with sulphate as terminal electron acceptor to reduce it to hydrogen sulphide (Schreiber et al., 2010). The archaeal groups, ANME-1 and ANME-2 have been most studied for anaerobic methanotrophy in conjunction with SRB. It has been proposed that ANME archaea oxidize methane via a reversal of the methanogenic pathway (Hallam et al., 2004; Meyerdierks et al., 2010; Thauer, 2011; Stokke et al., 2012) but how the electrons from methane oxidation are transferred to the SRB -bacteria still remains controversial (Milucka et al., 2012; Kojima et al., 2014). Figure I.2 shows the proposed pathway for reverse methanogenesis as adopted from Stokke et al., 2012.

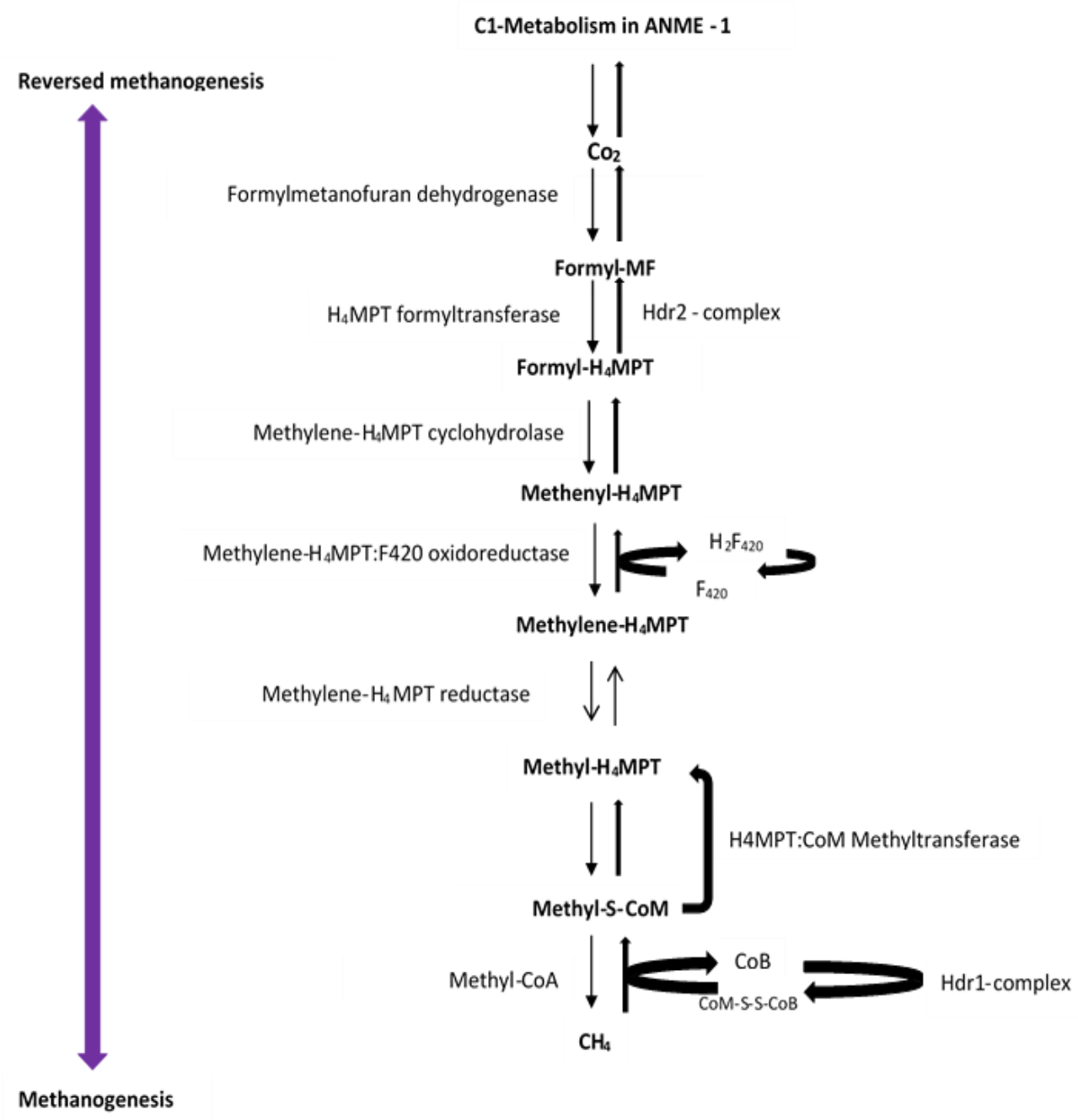


**Figure I.2** Proposed reverse methanogenesis pathway in ANME-1 as adapted from Stokke et al., 2012.

The key enzymes in reverse methanogenesis include heterodisulfide reductases (Hdr) that catalyse the formation of CoM-CoB heterodisulfide, an electron-accepting, non-CoM-CoB heterosulphide complex, and $F_{420}H_2$:quinone oxidoreductase (Fqo) complex that is involved in

recycling of electron carrier coenzyme $F_{420}$. Once the CoM-CoB heterodisulphide is formed, it is reduced to CoB by accepting electrons from methane (Meyerdierks et al., 2010). Methane is first oxidized to methyl-S-CoM, which is subsequently oxidized to methylenyl-$H_4$MPT from methylene-$H_4$MPT via the Fqo complex.

The second mechanism of anaerobic methane oxidation couples methane oxidation with nitrate reduction, facilitated by a consortia of ANME archaea and anammox bacteria (Haroon et al., 2013). A novel denitrifying methanotroph, *Candidatus* Methanoperedens nitroreducens of the family *Candidatus* Methanoperedenaceae was discovered from ANME-2d archaeal group and was shown to perform complete oxidation of methane to $CO_2$ using reverse methanogenesis. This pathway was found to constitute the key enzymes, methyl coenzyme M reductase A and F420-dependet 5, 10-methenyltetrahydromethanopterin reductase along with nitrate reductase.

There is also evidence of anaerobic methane oxidation coupled to metal reduction. Initial microcosm experiments conducted by Beal et al. (2009) showed the potential for iron- and manganese-driven anaerobic methane oxidation with methane-seep sediments from Eel River Basin in California. Sivan et al., (2014) show that the presence of oxidized forms of iron stimulated sulphate-reduction mediated anaerobic methane oxidation. This shows the dissimilatory processes that methanotrophs use to generate energy through the decomposition of substrates in adverse conditions such as anoxic deep ocean.

### I.2. Central methane oxidation pathway

This review will focus on aerobic methanotrophs since they are widely distributed in the environment and are better characterized than anaerobic methanotrophs. The oxidation of

methane to carbon dioxide includes a set of four enzymes (Figure I.3). The first step is the conversion of methane to methanol by methane monooxygenase (MMO).

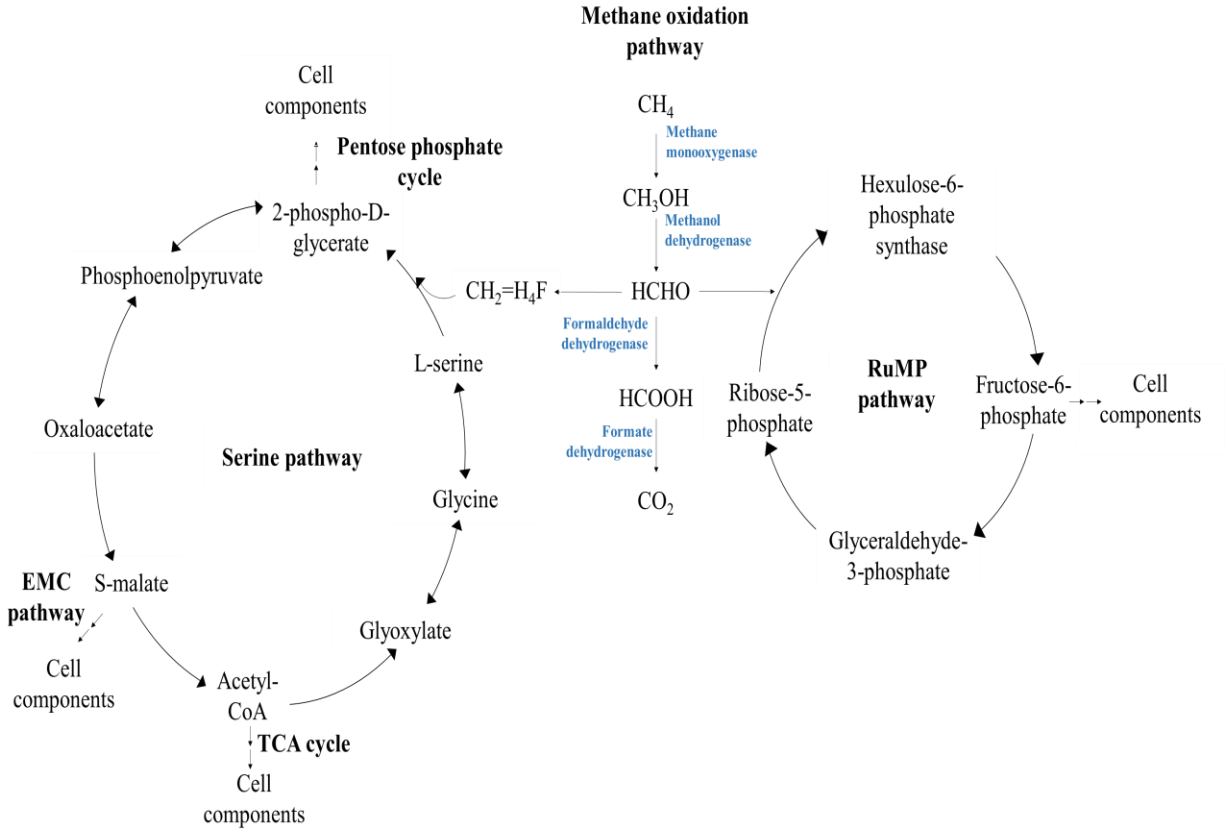


**Figure I.3** Methane oxidation pathway in conjunction with carbon assimilation via serine and ribulose monophosphate pathways. TCA: tricharboxylic acid; EMC: Ethylmalonyl CoA pathway; RuMP: Ribulose monophosphate pathway

Methanol is subsequently oxidized to formaldehyde by a periplasmic pyrroloquinoline quinine (PQQ)-dependent methanol dehydrogenase (MDH). Conversion of formaldehyde to formic acid and formic acid to carbon dioxide is catalyzed by formaldehyde dehydrogenase (FADH) and $NAD^+$(P) formate dehydrogenase (FDH) respectively. Figure I.3 also highlights the carbon assimilation pathways via serine and ribulose monophosphate pathway (RuMP). The following sections will focus on the methane monooxygenase, since it catalyses the first and rate limiting

step of methane oxidation by methanotrophs, and methanol dehydrogenase, following the discovery of two forms of methanol dehydrogenase.

## I.3. Methane monooxygenase

The enzyme methane monooxygenase (MMO) which catalyzes the first step of methane oxidation, is a characteristic feature of most methanotrophs (i.e., aerobic methanotrophs and those of phylum Verrucomicrobia and NC 10). MMO is known to occur as two distinct forms: a soluble or cytoplasmic form (sMMO) and a particulate or membrane-associated form (pMMO).

### *I.3.1. Soluble methane monooxygenase*

The soluble form of methane monooxygenase is found in some methanotrophs, and oxidizes a wide range of substrate e.g., primary alkanes, secondary alcohols, aromatic hydrocarbons like naphthalene and biphenyl, carbon monoxide and ammonia. sMMO is a well characterized enzyme with three components: (i) a 250-kDa hydroxylase protein (MMOH composed of a dimer of 3 subunits of α, β, and γ as $\alpha_3\beta_3\gamma_3$), (ii) a 39-kDa NAD(P)H-dependent oxoreductase (MMOR with flavin adenine dinucleotide and $Fe_2S_2$ prosthetic groups) and (iii) a 16-kDa regulatory component (MMOB) known as protein B or the coupling/gating protein that does not contain any metal ions (Colby and Dalton, 1978; Fox et al., 1989; Wallar and Lipscomb, 1996, 2001). Figure I.4 shows the ribbon diagram representation of sMMO from *Methylococcus capsulatus* (Bath). The reductase (MMOR) transfers electrons from NADH to MMOH (Merkx et al., 2001). The regulatory protein, MMOB, interacts with MMOH to directly affect access to and from the active site (Lee et al., 2013a). Also, MMOB ensures that sMMO acts as a monooxygenase and not an NADH oxidase (Green and Dalton. 1985; Lipscomb, 1994; Lee et

al., 2013a; Wang et al., 2014). sMMO is expressed only under copper limitation (Stanley et al., 1983; Murrell et al., 2000; Merkx et al., 2001).

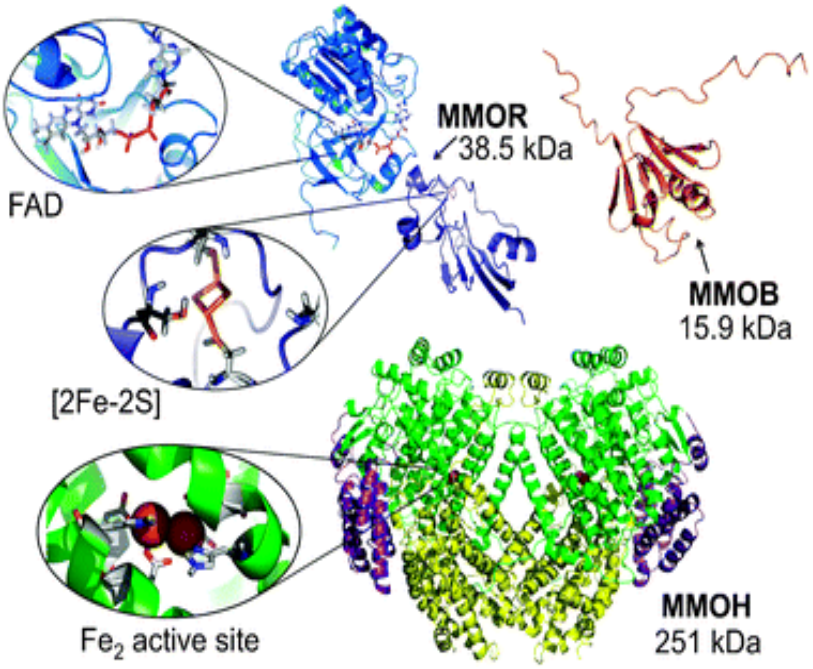


**Figure I.4** The structure of sMMO from *Methylococcus capsulatus* (Bath) consisting of a hydroxylase (MMOH), an oxidoreductase (MMOR; consisting of FAD and [2Fe2S]-Fd domain), and a regulatory protein (MMOB). The ribbon diagram representation of MMOH is based on X-ray coordinates and those of MMOB and the two truncated MMOR fragments, on NMR structures (Friedle et al., 2010).

Based on spectroscopic and X ray crystallographic studies, MMOH, the hydroxylase component, is found to have a catalytic oxygen-bridged diiron complex at its active metal centre as the site for methane oxidation (Rosenzweig et al., 1993; Elango et al., 1997). The metal active site is present in a four helix bundle of the α-subunit of MMOH. By molecular docking studies, the hydrophobic active site of sMMO has been found to be favourable for binding of methane and can accommodate a wide range of substrates including ethane, methanol, acetonitrile, 1,1-dimethylcyclopropane, methylcubane and aromatics (Colby et al., 1977; Valentine et al., 1999).

The resting state of MMOH (oxidized MMOH, $MMOH_{ox}$) includes diiron (III) held together by hydroxide ligands. The catalytic cycle of MMOH as studied in *Methylococcus capsulatus* (Bath) begins with rapid reaction of oxygen with the reduced diiron (II) center, followed by movement of water molecules increasing the Fe-Fe distance resulting in an open coordination site. (Figure I.5; Tinberg and Lippard, 2010).

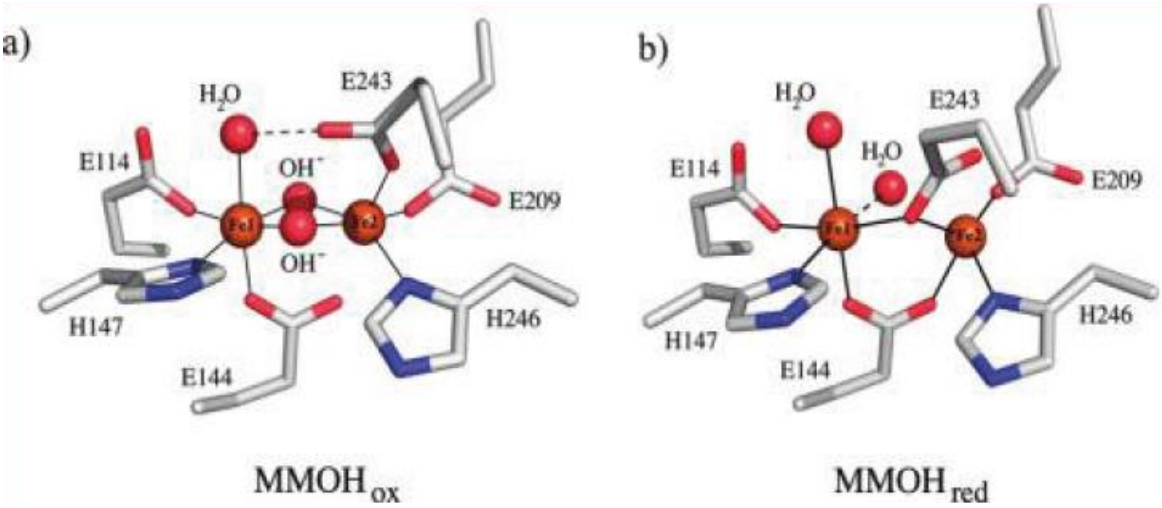


**Figure I.5** Active site of (a) oxidized MMOH ($MMOH_{ox}$) and (b) reduced MMOH ($MMOH_{red}$) of *Methylococcus capsulatus* (Bath) (Tinberg and Lippard, 2010).

It was proposed that the sequential transfer of two protons to the distal oxygen atom of dioxygen unit bound to the diiron centre cleaves the O-O bond resulting in formation of diiron (IV) unit which is responsible for oxidation of methane to methanol. The electrons to reduce $MMOH_{ox}$ are transferred from MMOR and are critical for the activity of sMMO. Studies on involvement of MMOB in methane oxidation show that the N-terminal of MMOB binds to the α-subunit of MMOH increasing the turnover and specificity of substrate hydroxylation (Froland et al., 1992; Liu et al., 1995). The Leu residue at 110 in the side chain in the α-subunit manages the aperture size by acting as a gate with two conformations, one to allow a 2.6 - Å diameter channel to the active site and another to block (Rosenzweig et al., 1997). Thus, MMOB controls the methane,

proton and oxygen access to the active site of sMMO, coupling electron movement to substrate hydroxylation (Lee et al., 2013a).

The binding of MMOR to MMOH has been unclear until recently. Wang et al., (2014), based on mass spectrometry (HDX-MS) studies, show that the ferredoxin domain of MMOR binds to a structure of C2 symmetry termed as a "canyon" present on each side of the MMOH protein dimer of sMMO from *M. capsulatus* (Bath). Also, the ferredoxin domain of MMOR shares the same binding site as the MMOB core implying competitive binding with MMOB to MMOH. In contrast to findings of Lee et al. (2013a), Wang et al., (2014) propose that MMOB inhibits electron transfer. The current finding splits the process of reductive oxygen activation to two steps: Firstly, MMOR displaces MMOB from the MMOH canyon to initiate the catalytic cycle reducing diiron (III) to diiron (II) and secondly, MMOB rebinds MMOH displacing MMOR to initiate oxygen activation for catalytic oxidation of methane.

*I.3.1.a. Genetic organization of soluble methane monooxygenase*

The sMMO gene cluster from *Methylococcus capsulatus* (Bath) and *Methylosinus trichosporium* OB3b has been extensively studied (Murrell, 1994). sMMO is chromosomally encoded by a six-gene operon *mmoXYBZDC*. The gene organization for the sMMO gene cluster (*mmo* operon) in *M. trichosporium* OB3b is shown in Figure I.6.

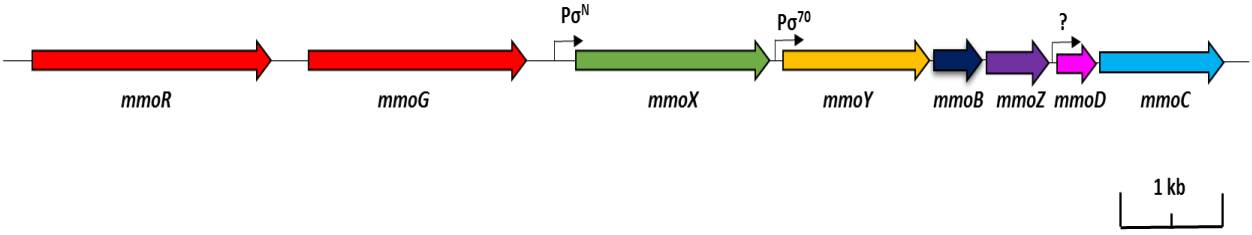


**Figure I.6** The gene structure of *mmo* operon in *M. trichosporium* OB3b with the promoter sites as identified by Nielsen et al., 1997 and Murrell, 1990.

Genes *mmoX*, *mmoY* and *mmoZ* encode the α-, β- and γ-subunits of hydroxylase subunit of sMMO respectively. The reductase subunit is encoded by *mmoC*, and *mmoB* codes for the regulatory component. *mmoD* encodes for a protein that was recently found to regulate expression of MMOs (Semrau et al., 2013), but is not essential for sMMO activity since it was not found in active preparations of sMMO (Fox et al., 1989). The sMMO genes are highly conserved in the genera of methanotrophs with nucleotide sequences being 55–94% identical and amino acid sequences 47–96% identical (Murrell et al., 2000).

The major transcription start sites for the sMMO cluster from *M. trichosporium* OB3b have been identified upstream of *mmoX* and *mmoY* (Murrell, 1994). Nielson et al., (1997) identified a $\sigma^{54}$ - like and $\sigma^{70}$- like promoter upstream of *mmoX* and *mmoY* respectively for the transcription of *mmo* operon of *M. trichosporium* OB3b. Further, Murrell (1994), based on primer extension analysis suggested a third transcription initiation site upstream of *mmoD* although its precise location is not known. There are also two regulatory elements, *mmoR* and *mmoG*, upstream of the structural *mmo* genes encoding for a methane monooxygenase regulator and a methane monooxygenase-associated GroEL homologue respectively and control the expression of *mmo* operon (Stafford et al., 2003).

### *I.3.2. Particulate methane monooxygenase*

The particulate methane monooxygenase is a transmembrane protein that catalyses conversion of methane to methanol and is present in most aerobic methanotrophs except *Methylocella* and *Methyloferula* species (Dedysh et al., 2000; Dedysh et al., 1998; Dunfield et al., 2003). In methanotrophs that possess both forms of MMO, pMMO activity is induced at high copper concentrations (Murrell et al., 2000; Choi et al., 2003; Semrau et al., 2010). Unlike sMMO,

pMMO has a narrow range of substrate specificity, i.e., pMMO can oxidize alkanes and alkenes up to five carbon chain length but not aromatic or cyclic compounds (Stirling et al., 1979; Burrows et al., 1984; Brusseau et al., 1990; Miyaji et al., 2011).

pMMO was first isolated from *Methylococcus capsulatus* Bath by Zahn and DiSpirito (1996) and was found to consist of three major subunits, PmoA (β), PmoB (α) and PmoC (γ) of molecular masses 27 kDa, 47 kDa and 25 kDa respectively. Due to the problems involved in isolation and studying integral membrane proteins, the structure of pMMO was not known until recently. The enzyme's first X-ray crystal structure is shown in Figure I.7, as deduced by Lieberman and Rosenzweig (2005) from the methanotroph *M. capsulatus* Bath with a resolution of 2.8 Å. Since then, crystal structures of pMMOs from three other methanotrophs have been resolved- pMMO from *M. trichosporium* OB3b resolved at 3.9 Å (Hakemian et al., 2008), *Methylocystis* sp. strain M resolved at 2.68 Å (Smith et al., 2011) and *Methylocystis* sp. strain Rockwell solved to 2.6 Å (Sirajuddin et al., 2014). All four crystal structures have the same architecture i.e., all the structures are composed of trimer of the three subunits.

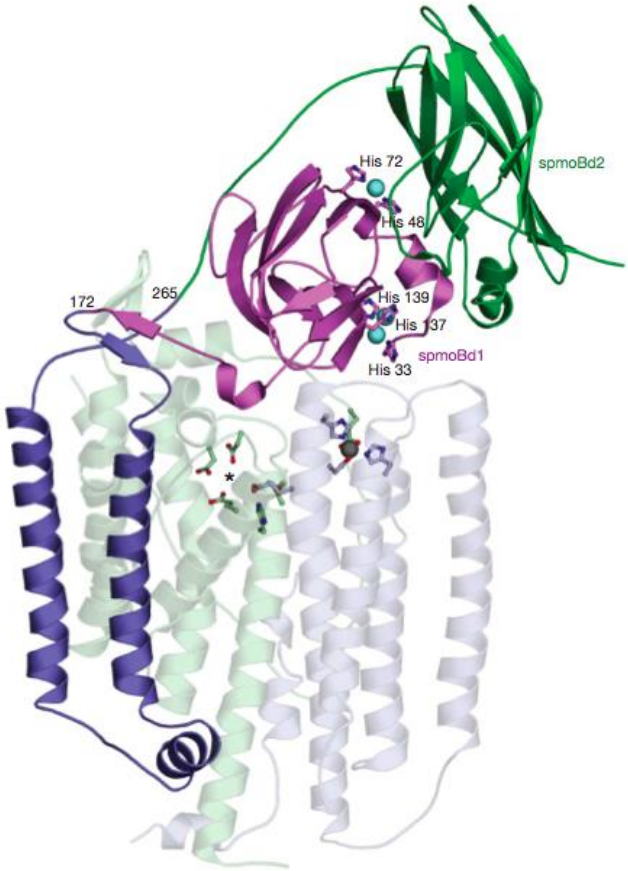


**Figure I.7** The crystal structure of pMMO protomer from *Methylococcus capsulatus* (Bath). The amino terminal cupredoxin domain of PmoB is shown in green; two transmembrane helices are shown in blue; copper ions are shown as cyan spheres and ligands are shown as ball and stick representations. The PmoA and PmoC subunits are faint light green and faint light blue in colour. The asterisk is the hydrophilic group of residues that is proposed to be the site of a tricopper centre. Grey spheres are the zinc sites (Balasubramanian et al., 2010).

The crystal structure of pMMO from *M. capsulatus* Bath indicates that the hydrophobic regions corresponding to six β-barrels are present primarily in PmoB (Lieberman and Rosenzweig, 2005). There are two anti-parallel β-barrels separated by β-hairpins followed by two transmembrane helices, whereas PmoA and PmoC are primarily comprised of transmembrane helices and embedded in the membrane suggesting that they are hydrophobic too. PmoB is structurally similar to cytochrome c oxidase subunit II, indicating that PmoB may play a role in

electron transfer. Studies on the physiological reductant for pMMO, though not affirmative, suggest that quinones reduced by a type 2 NADH:quinone oxidoreductase may be involved (Cook and Shiemke, 2002; Choi et al., 2003; Shiemke et al., 2004).

There are three metal centers identified in the pMMO structure of *M. capsulatus* (Bath) by anomalous difference electron density maps (Sommerhalter e al., 2005). The metal centers include a mononuclear and a dinuclear copper center in the periplasmic domain of PmoB and a third metal center that is subject to some controversy but may be occupied by copper or iron that is coordinated by amino acid residues from PmoC. The mononuclear copper site is found only in PmoB of *M. capsulatus* Bath coordinated by two histidine at His 48 and His 72 (Figure I.8). The His 48 residue seems critical for coordinating copper at this site since on its replacement by an asparagine in pMMO of *M. trichosporium* OB3b and *Methylocystis* sp. strain M, copper is no longer associated at this site (Hakemian et al., 2008; Smith et al., 2011). The dinuclear metal center comprises of His 33, His 137, and His 139 in *M. capsulatus* (Bath) and His 29, His 133, and His 135 in *Methylocystis* sp. strain M. These three histidines are conserved in PmoB of all methanotrophs except the Verrucomicrobial methanotrophs (Op den Camp et al., 2009). Based on X-ray absorption fine structure (EXAFS) data, the Cu-Cu interaction was determined to be 2.5-2.6 Å (Lieberman et al., 2003, 2006).

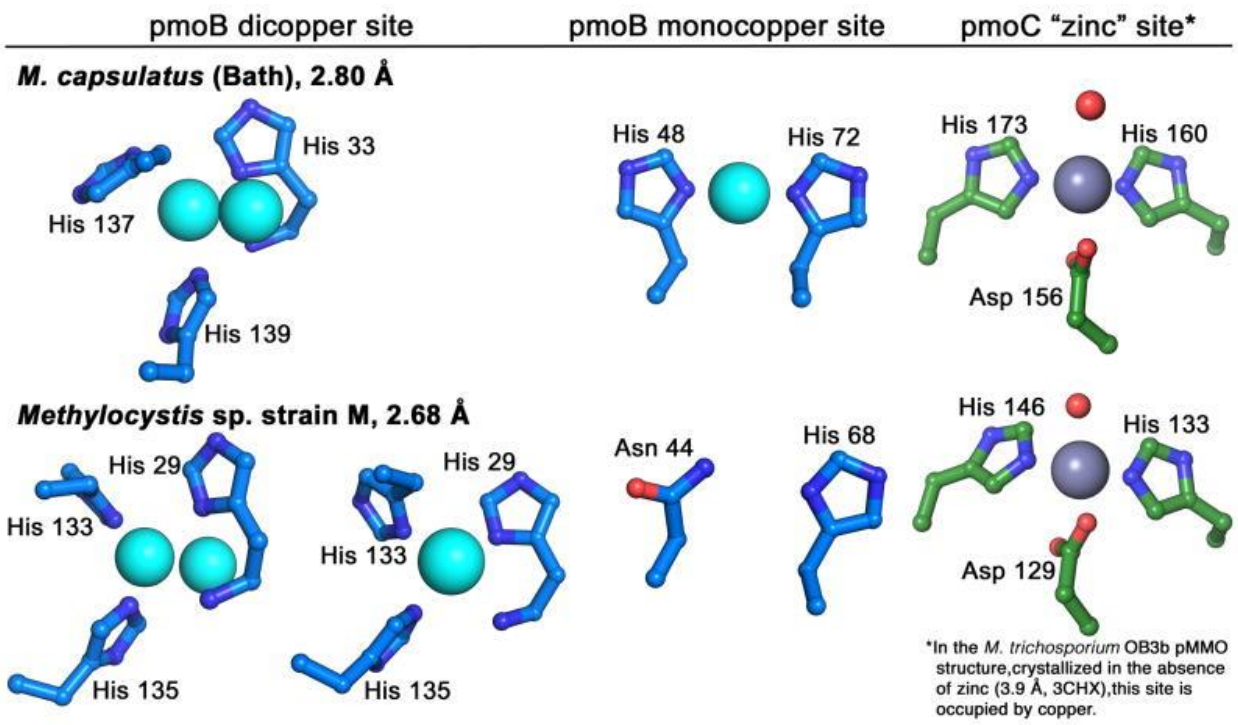


**Figure I.8** Metal centers as modeled in pMMO crystal structures of *M. capsulatus* (Bath) and *Methylocystis* sp. strain M (Culpepper and Rosenzweig, 2012)

The third metal center was initially thought to contain a zinc atom, but was later found to be derived from the crystallization buffer (Lieberman and Rosenzweig, 2005). Several models for pMMO active site and the number of metal ions, copper or iron, per kDa of pMMO protomer have been proposed (Nguyen et al., 1994, 1998; Chan et al., 2004; Lemos et al., 2000; Miyaji et al., 2002; Hakemian et al., 2008; Zahn and Dispirito, 1996). The earliest study performed by Nguyen et al., (1994) suggests the presence of a trinuclear Cu (II) complexes followed by a similar finding from Chan et al., (2004). Nguyen et al. (1998) later proposed 12–15 coppers ion per protomer, while Zahn and Dispirito, (1996) identified that the active protein preparations contained 2.5 iron atoms and 14.5 copper atoms per 99,000 Da of pMMO. Subsequent electron paramagnetic resonance analyses suggested presence of 2 copper ions per pMMO protomer from

*Methylococcus capsulatus* (Bath), *Methylomicrobium album* BG8 (Lemos et al., 2000) and *Methylosinus trichosporium* OB3b (Miyaji et al., 2002; Hakemian et al., 2008). Finally, Mössbauer studies on sMMO from *M. trichosporium* OB3b and pMMO from *M. capsulatus* Bath suggest that pMMO has a diiron centre that is similar to that of sMMO (Figure I.9; Martinho et al., 2007).

Further, this site has His 160, His 173, Asp 156, and Glu 195 residues that are conserved in all pMMOs sequences and is similar to the sMMO-diiron centre suggesting the third metal active site of pMMO may have diiron.

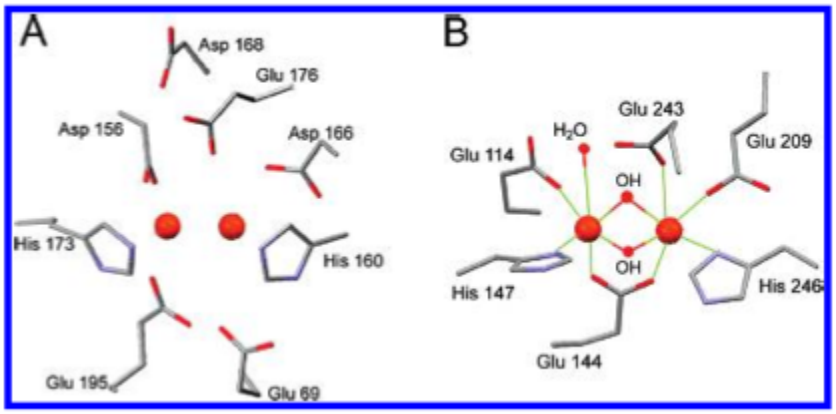


**Figure I.9** Similarities observed between A) the di-iron center of pMMO in *Methylococcus capsulatus* Bath (Lieberman and Rosenzweig, 2005) and B) the diiron centre of sMMO from *M. trichosporium* OB3b (Martinho et al., 2007).

*I.3.2.a. Genetic organization of particulate methane monooxygenase*

The pMMO gene clusters from many methanotrophs have been studied extensively and are known to contain at least three genes *pmoA* (encoding PmoA), *pmoB* (encoding PmoB) and *pmoC* (encoding PmoC) (Smith and Dalton, 1989; Nguyen et al., 1994, 1998; Semrau et al., 1995; Zahn and DiSpirito, 1996). Genes encoding polypeptides associated with pMMO in *Methylococcus capsulatus* (Bath) are known to be clustered with in 3kb region on chromosome in the order *pmoCAB* (Gilbert et al., 2000; Figure I.10). In most methanotrophs there are two virtually identical sets of pMMO genes (*pmoCAB*) which are functionally equivalent along with a third separate copy of *pmoC* (Stolyar et al., 1999; Gilbert et al., 2000).

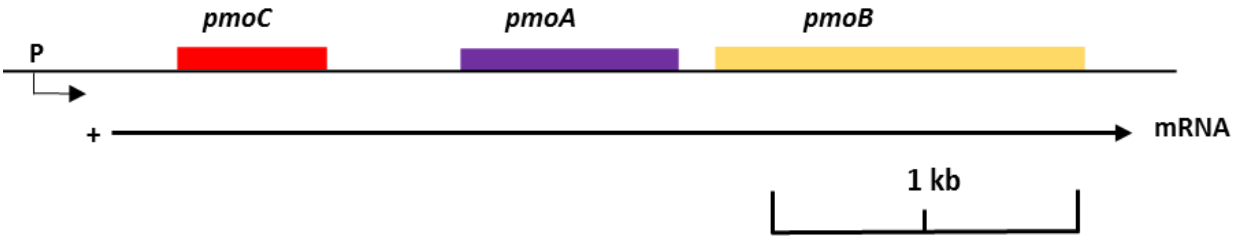


**Figure I.10** Gene structure of *pmo* operon with mRNA transcript of pMMO genes in *M. capsulatus* (Bath) at high copper concentration (modified from Costello et al., 1995; Semrau et al., 1995).

*pmoCAB* gene clusters are transcribed into a polycistronic mRNA of 3.3 kb from a single transcriptional start site located 300 bp upstream of *pmoC*, initiating at a putative $\sigma^{70}$ promoter that is activated by copper ions and is negatively regulated under low-copper conditions, when these bacteria are expressing sMMO (Gilbert et al., 2000).

## I.4. Methanol dehydrogenase

Methanol dehydrogenase catalyzes the second step in methane oxidation, i.e., the conversion of methanol to formaldehyde. In gram-positive bacteria, methanol dehydrogenase is present as a nicotinoprotein in the cytoplasm using NAD (P) H as electron acceptor. In many gram-negative methylotrophs and methanotrophs, methanol dehydrogenase is a soluble quino-enzyme found in the periplasm harboring pyrroloquinoline quinone (PQQ) as a cofactor (Anthony, 1986; Parker et al., 1987). As a PQQ-dependent enzyme, methanol dehydrogenase transfers two electrons sequentially to cytochrome $c_L$ as its primary electron acceptor. Subsequent oxidation of $c_L$ and production of proton motive force results in the creation of one molecule of ATP per molecule of methanol oxidized (Dijkstra et al., 1989).

The crystal structure of methanol dehydrogenase has been resolved from seven strains: *Methylacidiphilum fumariolicum* SolV (Pol et al., 2014), *Methylophaga aminisulfidivorans* MP (T) (Choi et al., 2011), *Hyphomicrobium denitrificans* (Nojiri et al., 2006), *Methylobacterium extorquens* (Williams et al., 2005; Ghosh et al., 1995), *Paracoccus denitrificans* (Xia et al., 2003), *Methylophilus* W3A1 (Xia et al., 1996, 1999), *Methylophilus methylotrophus* (Xia et al., 1992). They show high structural similarity. The atomic resolution structure of methanol dehydrogenase from *Methylobacterium extorquens* as identified by Williams et al. (2005) shows that the heterotetrameric ($\alpha_2\beta_2$) enzyme has a large 66 kDa subunit (α) consisting of a single domain with a β-propeller fold and a small ~8 kDa subunit (β) wrapped around the α-subunit mainly as a α-helical structure (Figure I.11). The active site for catalysis resides at the α-subunit consisting of PQQ prosthetic group located in the centre, a calcium ion and the catalytic amino acid Asp303 (Afolabi et al., 2001; Anthony & Zatman, 1964; Williams et al., 2005).

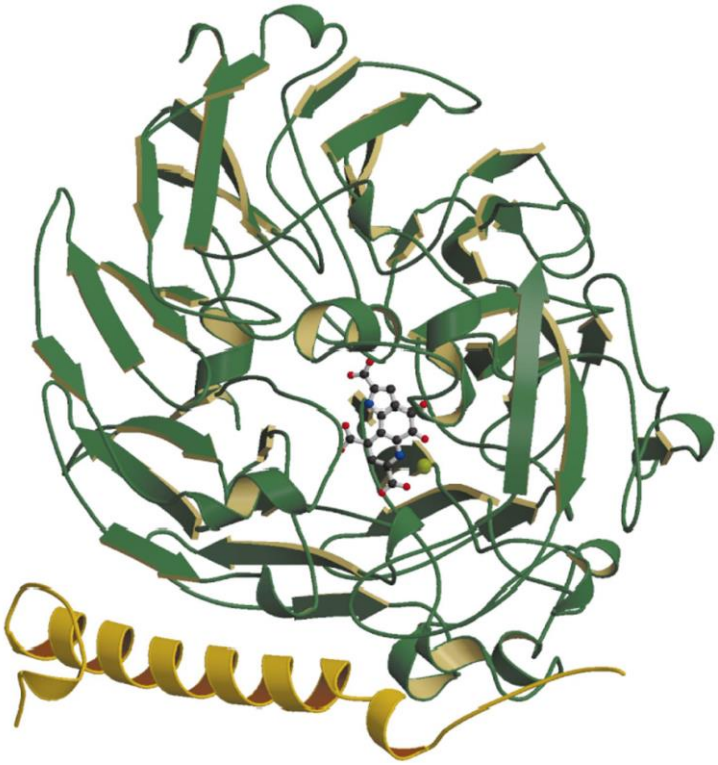

**Figure I.11** A monomer (αβ) unit of methanol dehydrogenase from *Methylobacterium extorquens*. The α-subunit (shown in green) is folded into a β-propeller structure, with calcium ion (green sphere) at the center of this fold; the small β-subunit (yellow) wraps around the side of the α-subunit (Williams et al., 2005).

The catalytic site in some methanol dehydrogenases harbors rare earth metals like cerium as in *M. fumariolicum* SolV (Pol et al., 2014). This form of the enzyme is widely referred to as Xox-MDH while the former with $Ca^{2+}$ in its active site is referred to as Mxa-MDH, named after the genes encoding the two forms. The known protein sizes of the large and small subunit of Mxa-MDH and the only subunit of Xox-MDH for various methylotrophs and methanotrophs are listed in Table I.3.

**Table I.3** Mxa-MDH and Xox-MDH sizes of various characterized methylotroph and methanotrophs.

| Strain | Mxa-MDH | Xox-MDH |
|---|---|---|
| *Methylobacterium extorquens* AM1 | 66 kDa, 8.5 kDa (Nunn et al., 1989) | 61 kDa (Nakagawa et al., 2012) |
| *Paracoccus denitrificans* | 67 kDa; 9.5 kDa (Xia et al., 2003) | ND |
| *Methylobacterium radiotolerans* NBRC15690 | 60 kDa; 10 kDa (Hibi et al., 2011) | 63 kDa (Hibi et al., 2011) |
| *Methylophaga aminisulfidivorans* $MP^T$ | 65.98 kDa; 7.58 kDa<br>65.98 kDa; 27.86 kDa; 7.58 kDa<br>(Kim et al., 2012) | ND |
| *Methylacidiphilum fumariolicum* SolV | ND | 63.5 kDa (Pol et al., 2014) |
| *Methylosinus trichosporium* OB3b | 66 kDa; 8.5 kDa (Schmidt et al., 2010) | 65 kDa |
| *Acetobacter methanolicus* | 62 kDa, 10 kDa<br>62 kDa, 10 kDa, 32 kDa<br>(Matsushita et al., 1993) | ND |
| *Methylobacterium nodulans* | 60 kDa, 6.5 kDa (Kuznetsova et al., 2012) | ND |
| *Candidatus* Methylomirabilis oxyfera | Not purified | 67 kDa, 11 kDa (Wu et al., 2015) |

ND: not defined

### *I.4.1. Mxa-methanol dehydrogenase (Mxa-MDH)*

The Mxa-MDH form catalyzes the oxidation of methanol to formaldehyde most effectively with the highest affinity to methanol in *Hyphomicrobium* WC ($K_M$ ~14 μM), followed by *Pseudomonas* W1 ($K_M$ of ~15 μM), *M. methylotrophus* ($K_M$ ~20 μM), *Methylocystis* sp. GB25 ($K_M$ ~34 μM), *Methylosinus* sp. W1 ($K_M$ ~45 μM) and *Methylobacterium nodulans* ($K_M$ ~230 μM) (Keltjens et al., 2014; Ghosh and Quayle, 1981; Kuzetsova et al., 2012). In addition to methanol, MDH oxidizes primary alcohols and aldehydes, and can use artificial electron acceptors, such as phenazine methosulfate (PMS) and phenazine ethosulfate (PES). Crystal structure analyses shows that the protein is a heterotetramer ($\alpha_2\beta_2$). While the function of the smaller subunit remains unknown, the function of the large subunit is identified to provide the $Ca^{2+}$-active site for oxido-reductive reaction with PQQ cofactor group. The $Ca^{2+}$ ion in the active site is coordinated by six bonds between an oxygen atom of Asn 261, two oxygen atoms of Glu 77, and a carbon atom of carboxylate (C7), carbonyl-O (C5) and a nitrogen atom of quinoline N (N6) of the PQQ group. The bond lengths range between 2.4 Å – 2.8 Å (Williams et al., 2005). Cysteines (Cy103 and Cys104) form a disulphide bond which interacts with the neighboring PQQ prosthetic group in a hydrophobic manner. Ghosh et al., (1995) reported that PQQ was present in semiquinone oxidation state in methanol dehydrogenase from *M. extorquens*, whereas Williams et al., (2005) report the possible presence of PQQ in the oxidized orthoquinone state due to a 40 ºC kink from the tricyclic plane of the PQQ group by the C4 carbonyl atom of orthoquinone. At a resolution of 1.2 Å, Williams et al., (2005) show that the hydrogen-bonding pattern remains consistent with previous structural analyses of quinohaemoprotein dehydrogenase (Chen et al., 2002a; Oubrie et al., 2002).

The conformation of the β-subunit is predominantly non-helical (first 34 amino acids), followed by helical conformation for the rest of the protein. The potential helical region was predicted to be able to form amphipathic helices in the C-terminal end and hydrophobic regions on the N-terminal side. This subunit has an exceptionally high proportion of lysine residues (15 out of 74 in *M. extorquens;* Nunn et al., 1989). The five lysines in the C-terminal of the protein were proposed to charge this side of the proposed amphipathic α-helix. *Paracoccus* Mxa-MDH form also was found to have four lysines while that of *A. methanolicus* had no lysines in that region, questioning the importance of lysine residues in Mxa-MDH.

In two methylotrophic strains, *Methylophaga aminisulfidivorans* MP $^{T}$ (Kim et al., 2012) and *Acetobacter methanolicus* (Matsushita et al., 1993), along with the Mxa-MDH with two (α and β) subunits, a second form of methanol dehydrogenase was also found with a third subunit. In *Acetobacter methanolicus*, the first (type I) MDH has a large 62 kDa subunit and a small 10kDa subunit with the $\alpha_2\beta_2$ conformation. The second (type II) MDH has an additional 32 kDa subunit found to be present partly in the free form or in the bound form with the $\alpha_2\beta_2$ conformation or as a complex with cytochrome $c_L$ in the periplasm. This third subunit was proposed to be the MoxJ or MxaJ protein, cotranslated with *moxFGI* in methanol oxidation systems (mox) in *Paracoccus denitrificans* and *Methylobacterium extorquens* AM1, which was never detected before and so its function remains unknown. While both MDH types showed the highest enzyme activity at alkaline pH of 9.5, required $NH_4Cl$ for activating methanol and could reduce cytochrome $c_L$, Matsushita et al., (1993) demonstrated that the type II MDH with MoxJ has a lower enzyme activity but better electron transfer activity resistance to inhibitors like NaCl or EDTA in comparison with type I MDH. Given that, it was proposed that the third subunit could function

by interacting with the $\alpha_2\beta_2$ heterodimer. Findings from Kim et al., (2012) show that the type II MDH from *Methylophaga aminisulfidivorans* MP $^T$ possesses an additional ~30 kDa subunit along with 66 kDa large and 8 kDa small subunits. This subunit was also speculated to be MxaJ, playing a critical role in MDH complex conformation and its associations with PQQ and $Ca^{2+}$ion for complete activity.

*I.4.1.a. Genetic organization of Mxa-MDH*

*Methylobacterium extorquens* AM1 serves as a well characterized model system for studying methanol oxidation. The gene expression for methanol oxidation system in *M. extorquens* AM1 includes five gene clusters, namely, *mxaFJGIRSACKLDB*, *mxbDM*, *mxcQE*, *pqqABCDE* and *pqqFG* (Zhang and Lidstrom, 2003; Springer et al., 1998).

The large (α) and small (β) subunits are encoded by *mxaF* and *mxaI*, respectively. *MxaF* gene is known to be linked to *mxaG*, *mxaI* and *mxaJ* as shown by Kim et al., (2012) where *mxaG* encodes for cytochrome $c_L$ for electron transfer, *mxaI* encodes for the smaller subunit believed to facilitate $Ca^{2+}$ insertion (Keltjens et al., 2014) and *mxaJ* is proposed to be involved in MDH activity. Van Spanning et al., (1991) propose that MxaJ might function as a chaperone in MxaFI association. The genes *mxaACKLD* are required for $Ca^{2+}$ insertion into the active site of α-subunit (Chistoserdova et al., 2003; Morris et al., 1995; Anthony et al., 1994; Richardson and Anthony, 1992). The *mxaB* gene, located last in the *mxa* gene cluster and 48 bp downstream of *mxaH*, encodes for a member of the response-regulator family with no known sensor kinase-encoding gene present in its proximity (Springer et al., 1998). There is also an element, *mxaW*, upstream of *mxaF* transcribed divergently from the methanol inducible promoter. Mutation studies of *mxaW* in *M. extorquens* AM1 showed neither differences in growth pattern nor in

enzyme activity and thus its function remains unknown (Springer et al., 1998). Also the genes, *mxaR, mxaS, mxaD, mxaE* and *mxaH* have no known function and are proposed to be involved in MDH stability (Lidstrom, 1990). Figure I.12 gives an overview of the genetic organization in *M. extorquens* AM1.

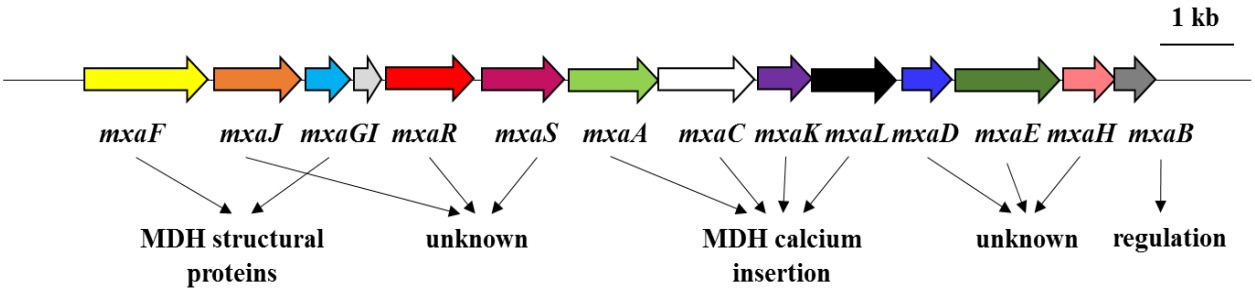


**Figure I.12** The *mxa* gene cluster and their roles in *M. extorquens* (modified from Springer et al., 1998).

In *M. extorquens* AM1, the gene clusters *mxbDM* and *mxcQE* encode for two-component regulatory system where, MxbD and MxcQ function as sensor kinases, and MxbM and MxcE function as response regulators (Springer et al., 1997, 1995; Lidstrom et al., 1994). These two different sensor kinase –response regulator pairs are known to work in concert to control methanol oxidation i.e., MxcQE controls the expression of the MxbDM, and MxbDM in turn control the expression of a number of genes involved in methanol oxidation. The *pqq* gene clusters encode for enzymes required for the biosynthesis of the methanol dehydrogenase prosthetic group, PQQ (Gliese et al., 2010; Puehringer et al., 2008; Toyama et al., 1997; Springer et al., 1996). These proteins, encoded by the five gene clusters, are preceded by an N-terminal signal peptide, indicating the presence of a complex MDH maturation system in the periplasm.

The genetic organization of Mxa-MDH in *M. trichosporium* OB3b includes a set of 14 genes, namely, *mxaFJGIRSACKLDHBY*. As compared to the gene organization in *M. extorquens* AM1, the *mxa* operon in *M. trichosporium* OB3b lacks *mxaE* but has an additional element, *mxaY*, located upstream of *mxaB* (Figure I.13). The MxaY protein is a putative methanol utilization control sensor protein probably working in concert with MxaB which is a DNA binding response regulator, belonging to LuxR family, involved in regulation of methanol oxidation.

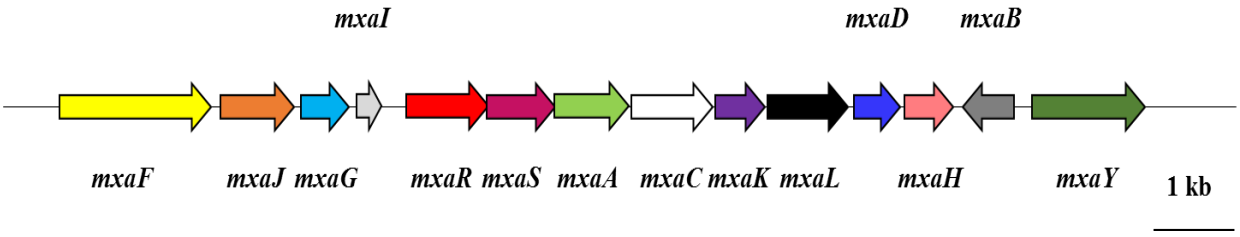


**Figure I.13** Genetic organization of Mxa-MDH in *Methylosinus trichosporium* OB3b.

### *I.4.2. Xox-methanol dehydrogenase (Xox-MDH)*

The Xox-MDH is a periplasmic PQQ-dependent MDH where the XoxF protein is a homolog of MxaF, exhibiting 50% sequence similarity with MxaF. There are five families of Xox-MDH with XoxF5-MDH being the largest, comprising of proteins from methylotrophs from *α*- and *γ*-*proteobacteria*, β-proteobacterial *Burkholderiales* and *Rhodocyclales*. The Xox-MDH system, as compared to Mxa-MDH, lacks genes encoding the small subunit, resulting in a homodimeric ($\alpha_2$) protein found in *Bradyrhizobium* sp. (Fitriyanto et al., 2011), *M. fumariolicum* SolV (Pol et al., 2014), *M. radiotolerans* (Hibi et al., 2011), and *M. extorquens* AM1 (Nakagawa et al., 2012). Alternatively, XoxF proteins have been found in association with MxaI subunits, e.g. in *Ca.* Methylomirabilis oxyfera (Wu et al., 2015). The Xox-MDH affinities for methanol is the highest

for *M. fumariolicum* SolV XoxF2 ($K_M$ ~ 0.8 μM) followed by *M. extorquens* AM1 XoxF5 ($K_M$ ~ 11 μM), *Ca.* Methylomirabilis oxyfera ($K_M$ ~ 17 μM) and *Bradyrhizobium* sp. XoxF5 ($K_M$ ~ 29 μM). This suggests better or equivalent substrate affinity for methanol as compared to Mxa-MDH.

The 1.6 Å resolution crystal structure of *M. fumariolicum* SolV (Figure I.14; Pol et al., 2014) shows that XoxF is present as a homodimer and contains a PQQ cofactor. The presence of a lanthanide at the metal active site was established by Pol et al. (2014). The PQQ cofactor coordinates a cerium atom by O5, N6 and O7. Atoms from Glu 172, Asp 301, Asp 299 and Asn 256 make seven coordinating bonds with bond lengths ranging from 2.5 Å to 2.9 Å. The arginine (Asp301) in Xox-MDH is additionally present as compared to Mxa-MDH amino acid composition. Given the larger size of lanthanides, as compared to calcium, the additional space required for insertion of lanthanide in the active site is suggested to be from glycine and threonine in Xox-MDH that replace an alanine (Ala 176) and a proline (Pro 264) from Mxa-MDH respectively.

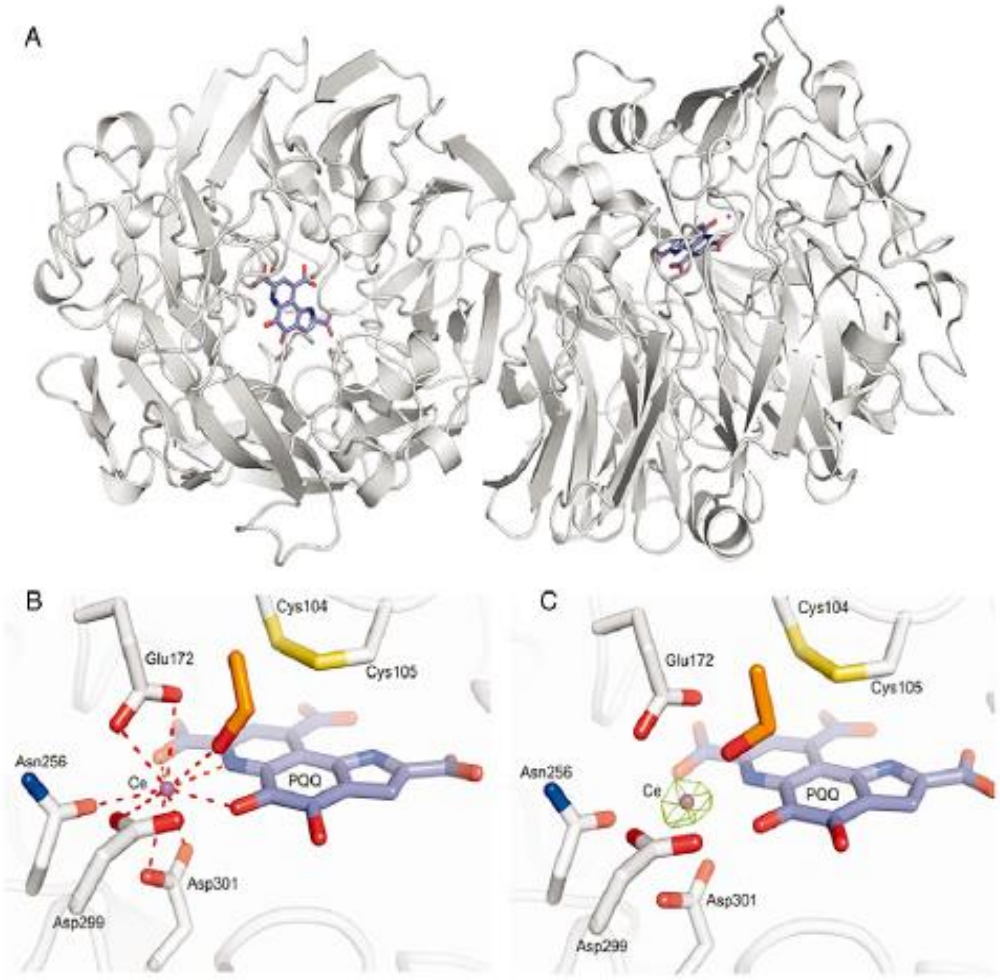


**Figure I.14** Crystal structure of *Methylacidiphilum fumariolicum* SolV showing (A) dimer structure coordinating PQQ (blue) and cerium ion (purple), (B) active site of Xox-MDH, and (C) Anomalous difference density (green mesh) supporting presence of a cerium ion at active metal center (Pol et al., 2014).

The metal active site of Xox-MDH from *M. fumariolicum* SolV was further analysed by Bogart et al. (2015) which shows the strong association of Ce ion with the substrate as compared to calcium linked Mxa-MDH. This preference was stronger when Ce is present in +3 oxidation state. Nakagawa et al., (2012) demonstrated the need for lanthanide-group rare-earth elements (REE), like cerium (III) and lanthanum (III), for growth of a *mxaF*-deletion mutant of

*Methylobacterium extorquens* on methanol. In *Methylobacterium* sp., the presence of $La^{3+}$ was shown to increase the methanol dehydrogenase activity.

Overall, several features that make Xox-MDH catalytically superior as compared to Mxa-MDH are (i) better substrate specificity for methanol, (ii) the activity for broader range of substrates including formaldehyde, (iii) highest activity at neutral cellular pH of 7, (iv) direct conversion of methanol to formate via a four-electron pathway, and (v) complete uncoupling of ammonium for activation.

*I.4.2.a. Genetic organization of Xox-MDH*

The genetic organization of Xox-MDH is simpler as compared to Mxa-MDH but has no general pattern (Figure I.15). Some commonalities with Mxa-MDH gene clusters include *xoxG* and *xoxJ* genes as homologs of *mxaG* and *mxaJ*. While genes *xoxG* and *xoxJ* are fused in the XoxF2 family of Xox-MDH, *xoxF* are not linked to other genes in the operon.

The XoxF1, XoxF3 and XoxF5 systems harbor functionally connected genes. The XoxF5 gene system is known to cluster with glutathione (GSH)-dependent formaldehyde dehydrogenase system, while *xoxF3*clusters with genes coding for cytochrome *c* oxidase (Keltjens et al., 2014). The XoxF1-MDH system of *M. oxyfera* shows that XoxF could be clustered with genes coding for putative accessory proteins like TonB which is proposed to be an uptake system for REEs from the environment.

The XoxF gene cluster in *M. trichosporium* OB3b are from XoxF1, XoxF2 and XoxF3 families (Figure I.15). The XoxF1 and XoxF2 systems show that the *xoxF* genes are linked to the cytochrome *c* coding *xoxG* genes. *XoxF*s encode for the PQQ-dependent methanol

dehydrogenase and *xoxJ1* codes for extracellular solute binding protein family 3, while *xoxJ2* codes for a putative methanol oxidation protein.

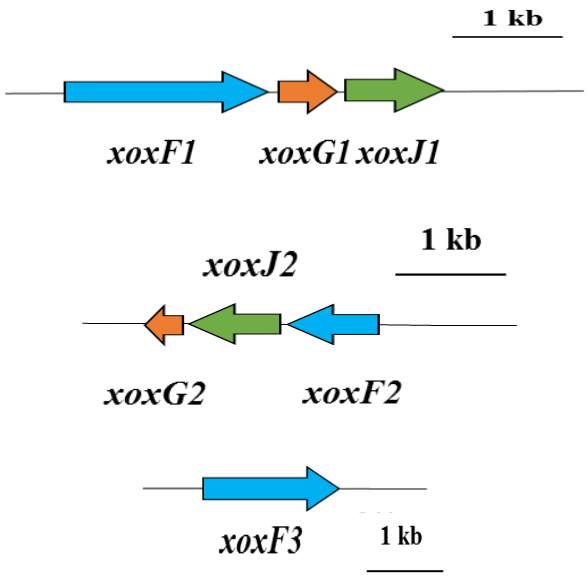


**Figure I.15** The genomic organization of Xox-MDH in *M. trichosporium* OB3b.

The XoxF3 –MDH consists of only one copy of *xoxF3* that has less than 20 % identity to *xoxF1* and *xoxF2* suggesting that it might just be an alcohol dehydrogenase and not a methanol dehydrogenase. The roles of these homologs are unknown.

### I.5. Phylogenetic classification/taxonomy

Aerobic methanotrophs were initially grouped according to their morphology, type of resting stage, intracytoplasmic membrane structure and physiological characteristics (Whittenbury et al, 1970). Subsequent 16S rDNA sequence analysis has further clarified these phylogenetic relationships and twenty seven genera of methanotrophs defined, namely *Methylococcus*, *Methylomonas*, *Methylomicrobium*, *Methylobacter*, *Methylocaldum*, *Methylosphaera*,

*Methylocystis, Methylosinus, Methlylothermus, Methylohalobius, Methylosarcina, Methlylocapsa, Methylocella, Methylosoma, Methyloglobulus, Methyloparacoccus, Methylomarinovum, Methylomarinum, Methyloferula, Candidatus Methylomirabilis, Methylacidiphilum, Methylogaea, Methylovulum, Methyloprofundus, Methylomagnum, Clonothrix* and *Crenothrix.* Table I.4 summarizes the methanotrophic genera known so far.

Most genera are divided into two distinct taxonomic groups: Type I and Type II. Type I methanotrophs assimilate formaldehyde produced from the oxidation of methane (via methanol) using the ribulose monophosphate pathway, have cellular membranes that are composed of predominantly 16-carbon fatty acids and possess bundles of intracytoplasmic membranes throughout the cell. Type II methanotrophs utilize the serine pathway for formaldehyde assimilation, have intracytoplasmic membranes arranged along the periphery of the cell and contain predominantly 18-carbon fatty acids (Hanson and Hanson, 1996). Membranes of the genus *Methylococcus* possess a combination of characteristics of both Type I and Type II methanotrophs and were initially grouped as Type X, but are now identified as subgroup of Type I methanotrophs. However, the genera *Methylocella* (Dedysh et al., 2000) and *Methylohalobius* (Heyer et al., 2005) do not fit this system of characterization very well.

Methanotrophs form coherent phylogenetic clusters that share the common physiological characteristics described above (Murrell et al. 1998). Type I methanotrophs (including *Methylococcus*) cluster in the γ-subdivision of the class *Proteobacteria*, while Type II methanotrophs are grouped within the α-subdivision of the class *Proteobacteria* based on the 16S rRNA gene analyses.

**Table I.4** A summary of methanotrophic genera and the sites of strain isolation.

| Phylum | Genera | Strains isolated from | Reference |
|---|---|---|---|
| *Gamma-Proteobacteria* | *Methylobacter* | Arctic wetland soil, Norway | Wartiainen et al., 2006b |
| | *Methylococcus* | Enrichment culture | Foster and Davis, 1966; Hazeu et al., 1980 |
| | *Methylomicrobium* | Enrichment culture | Bowman et al., 1993, 1995; Kalyuzhnaya et al., 2008 |
| | *Methylomonas* | Coastal seawater | Whittenbury and Krieg, 1984 |
| | *Methylocaldum* | Agricultural soil, underground hot spring effluent | Bodrossy et al., 1998 |
| | *Methylohalobius* | Hypersaline lakes, Ukraine | Heyer et al., 2005 |
| | *Methylothermus* | hot spring, Japan; hot aquifer, Japanese gold mine | Tsubota et al., 2005; Hirayama et al., 2011 |
| | *Methylosarcina* | Landfill, Athens; Lake Washington, Seattle | Wise et al., 2001; Kalyuzhnaya et al., 2005 |
| | *Methylosoma* | Littoral sediment of Lake Constance | Rahalkar et al., 2007 |
| | *Methylosphaera* | Sediments of Antarctic lakes, Vestfold | Bowman et al., 1997 |
| | *Clonothrix* | Artesian well | Vigliotta et al., 2007 |
| | *Crenothrix* | Water pipes of waterworks | Vigliotta et al., 2007 |
| | *Methyloglobulus* | Profundal sediment of Lake Constance | Poehlein et al., 2013 |
| | *Methylogaea* | Rice paddy field, Uruguay | Geymonat et al., 2011 |
| | *Methylovulum* | Forest soil in Japan | Iguchi et al., 2011 |
| | *Methyloparacoccus* | Pond water in South Africa and Japan | Hoefman et al., 2014 |
| | *Methylomarinum* | Marine environments, Japan | Hirayama et al., 2013 |
| | *Methylomarinovum* | Hydrothermal system in a coral reef, Japan | Hirayama et al., 2014 |
| | *Methyloprofundus* | Ocean sediment | Tavormina et al., 2015 |
| | *Methylomagnum* | Rice rhizosphere | Khalifa et al., 2015 |
| *Alpha-Proteobacteria* | *Methylocystis* | Polluted aquifer; wetland soil; *Sphagnum* peat | Dunfield et al., 2002; Wartiainen et al., 2006a; Dedysh et al., 2007 |
| | *Methylosinus* | Sites throughout eastern Australia | Whittenbury et al., 1970; Bowman et al.,1993 |
| | *Methylocella* | Acidic forest soil, Germany; *Sphagnum* peat, Russia | Dunfield et al., 2003; Dedysh et al., 2000 |
| | *Methylocapsa* | Sphagnum peat bogs, Russia; forest soil, Germany | Dedysh et al., 2002; Dunfield et al., 2010 |
| | *Methyloferula* | Sphagnum peat bogs in Russia | Vorobev et al., 2011 |
| Verrucomicrobia | *Methylacidiphilum* | Hell's Gate geothermal area, New Zealand | Khadem et al., 2011; Hou et al., 2008; Islam et al., 2008 |
| NC 10 | *Candidatus* methylomirabilis | freshwater enrichment cultures | Ettwig et al., 2010 |


**Figure I.16** Phylogenetic tree based on 16S rRNA (A) and *mxaF* (B) genes from methanotrophs based on Neighbour-Joining method and Maximum likelihood model using 500 replicates in Mega4. Bootstrap values > 50 % are displayed.

*Alphaproteobacteria* methanotrophs include two distinct families, the *Methylocystaceae* and the *Beijerinckiaceae*, while the *Gammaproteobacteria* methanotrophs are grouped into the family *Methylococcaceae* and a proposed family *Methylothermaceae* (Hirayama et al., 2014). New methanotrophic genera in *Alphaproteobacteria* since 2010 include *Methyloferula* of family

*Beijerinckiaceae*. New methanotrophic genera in *Gammaproteobacteria* since 2010 include *Methyloglobulus, Methyloparacoccus, Methylogaea, Methylovulum, Methyloprofundus* and *Methylomagnum* of family *Methylococcaeae,* and *Methylomarinovum* and *Methylomarinum* of novel family *Methylothermaceae*. The phylogenetic tree constructed based on 16S rRNA and *mxaF* genes for methanotrophic genera are shown in Figure I.16.

Until 2007, it was believed that aerobic methanotrophs belonged solely to the phylum Proteobacteria. Three novel thermoacidophilic methanotrophs were isolated later in 2007 and 2008 that were grouped into the phylum named Verrucomicrobia (Dunfield et al., 2007; Pol et al., 2007; Islam et al., 2008). Recently, bacteria in this phylum have been better understood by non-culturable means via phylogenic characterization of 16S rRNA and *pmoA* genes (Sharp et al., 2014). The Verrucomicrobia isolates are thermoacidophiles that exhibit growth at pH less than 1 and temperatures of 65 °C (Op den Camp et al., 2009). Based on high similarity of the 16S rRNA gene sequences (> 98.4 %) of the new genera *Methyloacidiphilum*, *Methylacida* and *Acidimethylosilex* (Dunfield et al., 2007; Hou et al., 2008; Islam et al., 2008; Pol et al., 2007), the three genera have been re- classified as a single genus '*Methylacidiphilum*' (Op den Camp et al., 2009). A unique feature of two of the strains, *M. infernorum* strain V4 and *M. fumariolicum* SolV is that they do not possess RuMP or the complete set of genes for serine pathway for formaldehyde assimilation for fixing carbon which is otherwise the key feature of proteobacterial methanotrophs, but do possess genes coding for ribulose-1,5-bisphosphate carboxylase/oxygenase (RuBisCO) involved in Calvin-Benson-Bassham (CBB) cycle (Hou et al., 2008; Khadem et al., 2012). Although many methanotrophs have the CBB cycle, only *M. infernorum* strain V4 and *M. fumariolicum* strain SolV have been found to use it for carbon fixation. This opens up new horizon on the prevalence of autotrophic methanotrophs.

Several studies on fresh water enrichment cultures assigned to phylum NC10 have shown presence of a dominant novel species recently named as *Candidatus* Methylomirabilis oxyfera. Genome analyses suggest that *Ca*. Methylomirabilis oxyfera, similar to Verrucomicrobia, fixes carbon using RuBisCO via CBB cycle and uses methane for energy production (Ettwig et al., 2010; Wu et al., 2011; Rasigraf et al., 2014). Apart from the autotrophic nature of this bacteria, it has been shown to have nitrite-driven anaerobic methane oxidation (Ettwig et al., 2010). The proposed new 'intra-aerobic' pathway of nitrite reduction suggest initial anaerobic nitrite reduction using nitrite reductase releasing nitric oxide that splits into di-nitrogen and oxygen by an unknown enzyme and pMMO uses this oxygen to oxidize methane carbon-dioxide. This makes *Ca*. Methylomirabilis oxyfera unique with aerobic metabolism by generating oxygen within itself while surviving in anoxic conditions. It was later investigated for the presence of bacteriohopanepolyols (BHPs) that are used as molecular biomarkers (Kool et al., 2014). The study shows the Methylomirabilis sp. enrichment culture could synthesize 3-Methyl BHPs which was previously believed to be synthesized only in aerobic environments.

There are several molecular markers proposed for identifying methanotrophs. The *pmoA* gene is a commonly used functional marker for the identification of methanotrophs from the rest of the bacterial domain in the environment due to their near-universal presence in methanotrophs and conserved nature among methanotrophs (McDonald and Murrell, 1997; Theisen et al., 2005). Initially it was assumed that all methanotrophs possess pMMO, but it is now known that species of *Methylocella* and *Methyloferula* do not have *pmoA* (Chen et al., 2010; Vorobev et al., 2011) and many Proteobacterial species do not have *mmoX* (Semrau et al., 2010). The 16S rRNA gene, although highly conserved, does not reveal methanotrophic physiology precisely. A recent work on prospective marker genes to detect all Proteobacterial methanotrophs, irrespective of the

presence or absence of the genes encoding either form of methane monooxygenase, has shown that the use of *mxaF* gene as a functional marker may be appropriate (Lau et al., 2013). *mxaF* gene sequences are highly conserved regions in methylotrophs grouped within Proteobacteria (McDonald and Murrell, 1997; Kalyuzhnaya et al., 2008). Lau et al. (2013) suggest that *mxaF* could be used as functional and phylogenetic marker to clearly differentiate between *Methylococcaceae* and *Methylocystaceae* families of α-Proteobacteria (Figure I.16).

Interestingly, while the phylogenetic tree based on 16S rRNA genes cluster the methanotrophic species according to their phylum (α-, γ- Proteobacteria, NC 10 and Verrucomicrobia), the phylogenetic tree based on *mxaF* clusters all the species as per their phylum except for one. *mxaF* gene from *Methyloglobulus morosus* belonging to γ- Proteobacteria is found to be closely related to that of *Methylacidiphilum fumariolicum* SolV belonging to Verrucomicrobia (Figure I.16). Although the functional genes are not conventionally known to cluster differently from the 16S rRNA, given the absence of the alternative methanol dehydrogenase, Xox-MDH and the alternative methane monooxygenase, sMMO, it may be possible that *Methyloglobulus morosus* obtained the *mxaF* gene by horizontal gene transfer during the event of nutrient limitation or critical growth environments.

**I.6. Methanobactin**

Copper plays a key role in the physiology of methanotrophs, because it is central to the structure and function of pMMO (Semrau et al., 2010). One way that these bacteria meet their high copper requirement is by the biosynthesis and release of high-affinity copper-binding compounds called methanobactins. Methanobactin functions as a chalkophore, similar to siderophores, by binding Cu (II) or Cu (I), then shuttling the copper into the cell. Methanobactin has an extremely high-

affinity of $10^{18}$-$10^{58}$ $M^{-1}$ for binding Cu (II) and reduces it to Cu (I) after binding (Pesch et al., 2012; El Ghazouani et al., 2011; Choi et al., 2006a). Additionally, methanobactin is known to play role in regulation of methane monooxygenase expression, protection against copper toxicity, and particulate methane monooxygenase activity (Zahn and Dispirito, 1996; Choi et al., 2005; Knapp et al., 2007).

Methanobactin from five methanotrophs has been structurally characterized so far. They are from *Methylosinus trichosporium* OB3b, *Methylocystis* strain SB2, *Methylocystis hirsuta* CSC1, *Methylocystis* strain M, and *Methylocystis rosea* $SV97^T$ with a reported molecular mass of 1154.26, 851.20, 910.20, 825.13 and 914.13 Da respectively (Krentz et al., 2010; El Ghazouani et al., 2011). The primary structure of the methanobactin was characterized by mass spectrometry, nuclear magnetic resonance and crystallography. Figure I.17 shows the primary structure of methanobactin from these methanotrophs. The common features of methanobactins known so far are (i) a peptide backbone with two heterocyclic rings, one of which is oxazolone ring and the other is either an oxazolone, imidazolone, or pyrazinedione ring, and (ii) binding copper via the two nitrogens from the heterocyclic rings and two sulfurs from the adjacent thioamides (Kim et al., 2004; Behling et al., 2008; Krentz et al., 2010; El Ghazouani et al., 2011, 2012; Bandow et al., 2012).

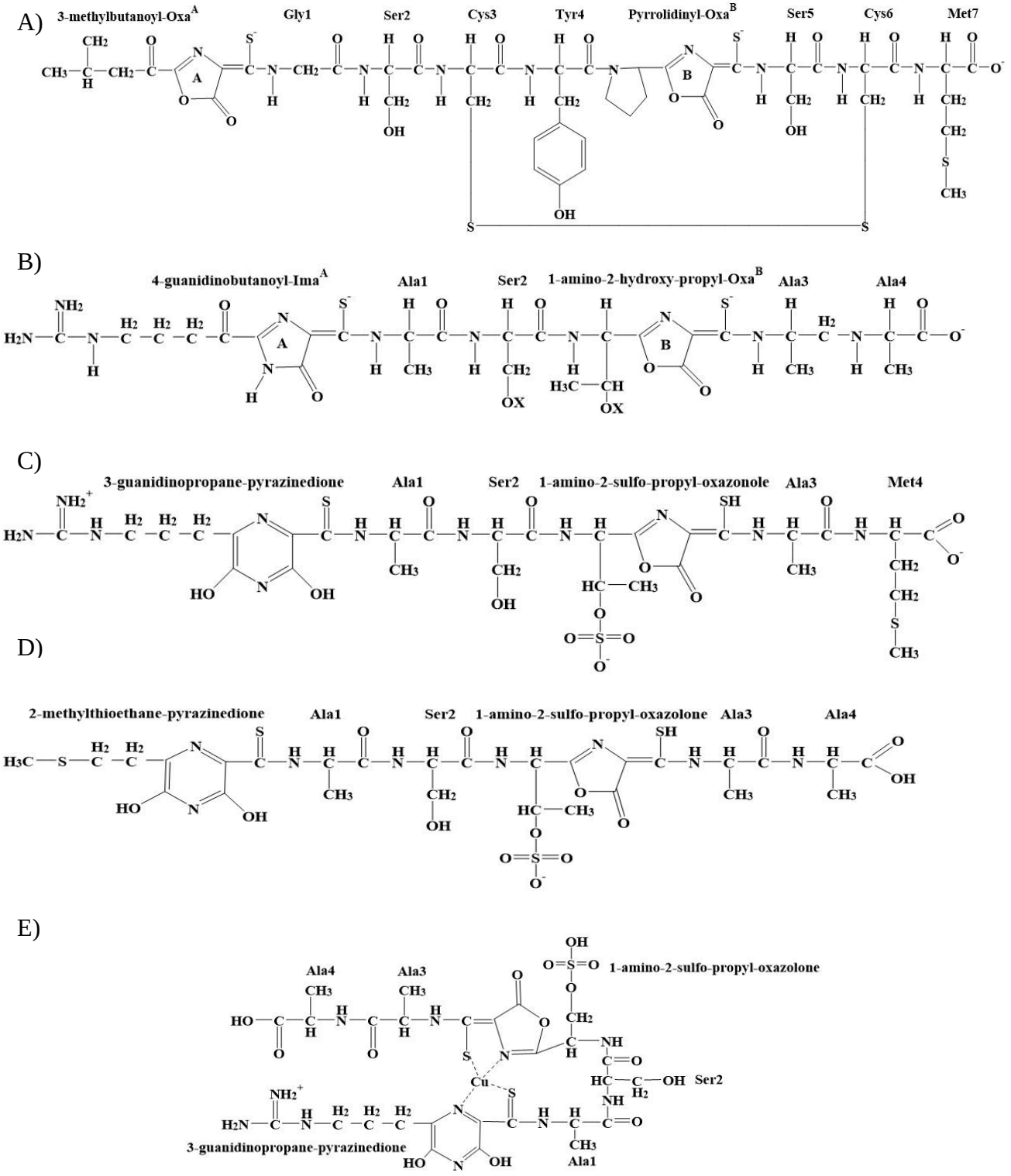


**Figure I.17** Primary structure of methanobactin from aerobic methanotrophs, A) *M. trichosporium* OB3b, B) *Methylocystis* Strain SB2, C) *Methylocystis* Strain M, D) *Methylocystis hirsuta* CSC1, and E) *Methylocystis rosea.* ImiA, and OxaA and OxaB are the imidazolone and oxazolone rings respectively (modified from Krentz et al., 2010; El Ghazouani, et al., 2012).

The two forms of methanobactin from *M. trichosporium* OB3b shows structural similarity of the Cu (I) sites even after the loss of Met residue (Figure I.18). The full length methanobactin from *M. trichosporium* OB3b has the amino acid sequence of 1-(N-[mercapto-{5-oxo-2- (3-methylbutanoyl)oxazol-(Z)-4-ylidene}methyl]-$Gly^1$-L-$Ser^2$-L-$Cys^3$-L-$Tyr^4$)-pyrrolidin-2-yl-(mercapto-[5-oxo-oxazol-(Z)-4- ylidene]methyl)-L-$Ser^5$-$Cys^6$-L-$Met^7$ (Behling et al., 2008). The two modified amino acids are believed to be alkylidene oxazolone rings. The crystal structure of OB3b-Mb reveals a pyramid-like shape with a disulfide bond between the two Cys residues. A single copper ion is bound at the base of the pyramid by a $N_2S_2$ ligand set derived from the modified amino acids. OB3b-Mb binds to copper ion by the first oxazolone ring rapidly with an initial binding rate > 640 $s^{-1}$ and 121 $s^{-1}$ by the second oxazolone ring (Choi et al., 2006a). In case of SB2-Mb that has a relatively lower affinity to copper (>$10^{20.1}$; Bandow et al., 2012), copper is bound even more rapidly by both the rings with a binding rate of 2000 $s^{-1}$. A recent finding from Bandow et al., (2012) suggests that both SB2-Mb and OB3b-Mb have similar binding constants since SB2-Mb could not displace the copper from OB3b-Mb-Cu complex and similarly OB3b-Mb could not displace copper from SB2-Mb-Cu complex.

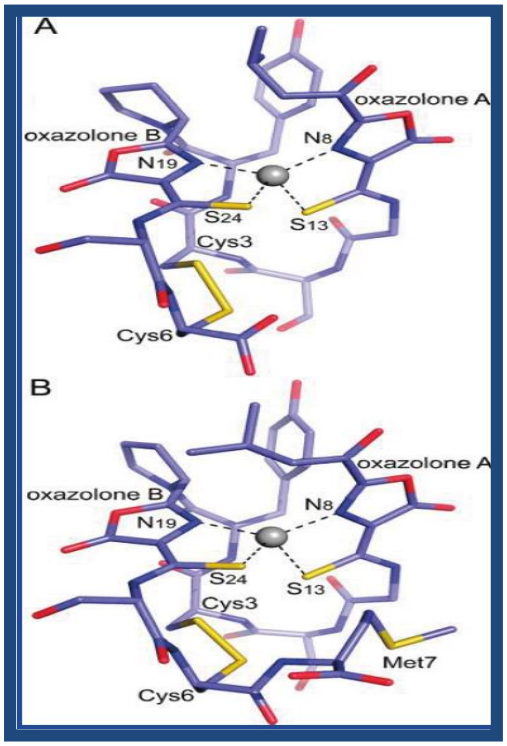


**Figure I.18** The structure of Cu (I) site from A) Met-mb, the fully functional methanobactin that lacks the C-terminal Met from the full-length form (FL-mb) and B) FL-mb from *M. trichosporium* OB3b (El Ghazouani et al., 2011).

OB3b-Mb was found to bind other metals like Fe (III), Au (III), Hg(II), Cd (II), Co (II), Mn (II), U (VI), Zn (II) in the absence of Cu (II) or Cu (I), but with a lower affinity as compared to that with Cu (II) (Choi et al., 2006b). Based on the spectral properties of metal binding to OB3b-Mb, Choi et al., (2006b) categorized the metals as Group A and Group B metals proposing a model for metal binding (Figure I.19).

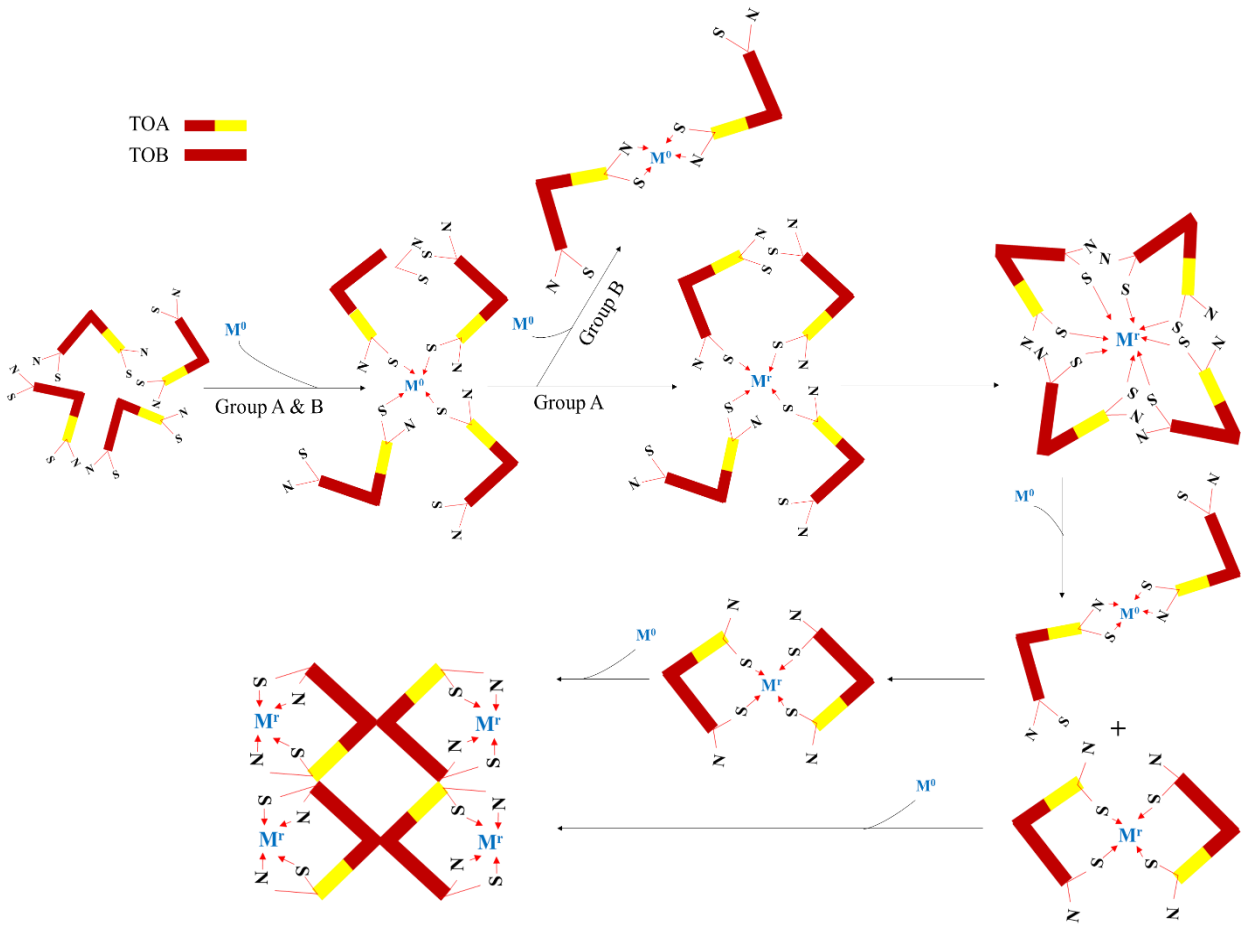


**Figure I.19** Proposed model for the binding of metals categorized as group A: Ag (I), Au (III), Cu (II), Hg (II), Pb (II) and U (VI) and group B: Cd (II), Co (II), Fe (III), Ni (II), and Zn (II) by methanobactin from *M. trichosporium* OB3b. Methanobactin is represented as two bars ending in the N atom of each oxazolone and the S atom from the thiocarbonyl group on 3-methylbutanoyl-oxazolone ring A (TOA; yellow and red bar) and on pyrrolidinyl-oxazolone ring B (TOB; red bar). Abbreviations: $M^o$, oxidized metal added to methanobactin solutions, and $M^r$, reduced metal (Modified from Choi et al., 2006b).

Group A metals are metals that showed a final coordination via 4-thiocarbonyl-5-hydroxy oxazolate A (TOA), 4-thiocarbonyl-5-hydroxy oxazolate B (TOB) and possibly Tyr. OB3b-Mb reduced these metals without the addition of an external reductant. Lastly, depending on the metal concentration, OB3b-Mb coordinated Group A metals as either a tetramer, dimer, or monomer. Apart from Cu, Group A metals include Ag (I) and Au (III), Hg (II), Pb (II) and possibly U (VI).

Group B metals consist of the transition metals Cd (II), Co (II) Fe (III), Mn (II), Ni (II), and Zn (II). Group B metals are metals that showed a final coordination to TOA and without reducing the bound metal. Depending on the concentration of group B metal, OB3b-Mb coordinated group B metals as either a tetramer or dimer, but not as a monomer. Thus, even in the presence of excess metals, OB3b-Mb coordinates group B metals as a dimer. It was found that non-copper group A metals once bound to methanobactin could not be displaced by copper, whereas group B metals could be replaced by copper (Choi et al., 2006b).

The binding affinities of OB3b-Mb to Group A and Group B metals were measured by isothermal calorimetry by Choi et al. (2006b) and are summarized in Table I.5. It was observed that, next to Cu, Ag and Hg have the highest binding affinities to OB3b-Mb whereas Au has the least binding affinity among all the other metals listed. No matter how low the affinity is, it should be noted that many metals were reduced after binding OB3b-Mb.

**Table I.5** Metal binding affinities to methanobactin from *M. trichosporium* OB3b (Choi et al., 2006b)

| Metal | Initial/Final charge | Binding affinity ($M^{-1}$) |
|---|---|---|
| Cu | +2/+1 | ~$10^{18}$-$10^{58}$ |
| Ag | +1/0 | $2.6\times10^{7}$ |
| Au | +3/0 | $1.0\times10^{5}$ |
| Cd | +2/ND | $1.3\times10^{6}$ |
| Co | +2/ND | $1.1\times10^{6}$ |
| Cr | +6/ND | ND |
| Fe | +3/+3 | $9.7\times10^{5}$ |
| Hg | +2/0 | $9.9\times10^{6}$ |
| Mn | +2/ND | $7.7\times10^{5}$ |
| Ni | +1/ND | $4.9\times10^{5}$ |
| Zn | +2/ND | $6.8\times10^{5}$ |
| Ce | +3/ND | $4.4\times10^{3}$ |

ND: not determined

### *I.6.1. Genetic organization of methanobactin*

Krentz et al., (2010) suggested that these methanobactins are encoded genetically and produced ribosomally. By genome analysis, the open reading frame with the putative polypeptide precursor region was found to be MTVKIAQKKVLPVIGRAAA**LCGSCYPCSCM** (bold letters indicate the precursor polypeptide region). Subsequently, the gene encoding this peptide precursor, *mbnA*, was found to be part of an operon (Figure I.20). Transcriptional data analysis by Semrau et al., (2013) shows that *mbnA* is a part of the operon that contains two other genes, *mbnB* and *mbnC*.

The *mbn* gene cluster from *M. trichosporium* OB3b includes a set of 10 genes, *mbnIRTABCMNPH* and the gene cluster from *Methylocystis* sp. strain SB2 contains 9 genes, *mbnHPIABCMFS* (Figure I.20).The analyses of the gene cluster shows the presence of two genes, *mbnB* and *mbnC* in the immediate vicinity of *mbnA* with the three genes transcribed polycistronically.

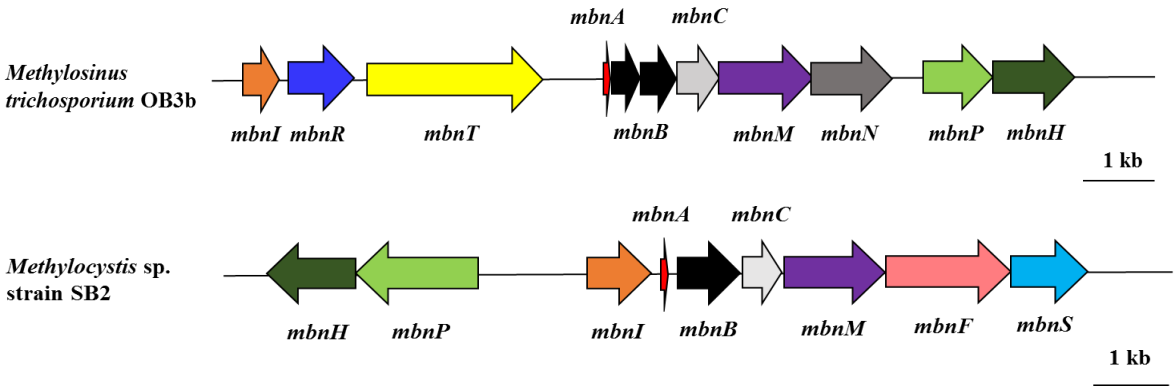


**Figure I.20** Methanobactin producing operons from *M. trichosporium* OB3b and *Methylocystis* sp. strain SB2.

Both the species considered here harbour the three key genes, *mbnA*, *mbnB*, and *mbnC*, that are speculated to code for methanobactin biosynthesis. Table I.6 highlights the functions of the *mbn* gene products from *M. trichosporium* OB3b and *Methylocystis* sp. strain SB2.

**Table I.6** Gene products of the methanobactin operon from *M. trichosporium* OB3b and *Methylocystis* sp. strain SB2.

| Genes | Product |
|---|---|
| *mbnI* | RNA polymerase sigma-70 like domain |
| *mbnA* | Methanobactin peptide precursor |
| *mbnB* | Methanobactin biosynthesis cassette protein MbnB |
| *mbnC* | Methanobactin biosynthesis cassette protein MbnC |
| *mbnM* | MATE efflux pump |
| *mbnN* | Putative aminotransferase |
| *mbnP* | Conserved exported protein of unknown function |
| *mbnH* | Putative di-haem cytochrome c peroxidase |
| *mbnR* | Putative membrane sensor, sigma factor activator |
| *mbnT* | Putative TonB-dependent receptor |
| *mbnF* | Putative FAD-dependent oxidoreductase |
| *mbnS* | Putative sulfotransferase |

*mbnB* and *mbnC* are predicted to encode for peroxidase or dehydrogenase activity required for biosynthesis of methanobactin by forming the oxazolone ring structure from ribosomally encoded amino acids. In *M. trichosporium* OB3b, the upstream elements includes *mbnT,* that encodes for a putative Ton-B receptor and the downstream elements, *mbnM*, *mbnN*, *mbnP* and *mbnH,* have no known function but are believed to encode for multi-drug antimicrobial protein, aminotransferase and possibly for alternative copper uptake system.

## I.7. Copper-mediated gene regulation models

Since the discovery of the two forms of methane monooxygenase, it is known that expression of sMMO genes is induced during copper starvation, while pMMO gene expression increases with copper (Stanley et al., 1983). Nielsen et al., (1997) suggested the existence of a common regulatory pathway for regulating the sMMO and pMMO gene expression. The inception began with the finding that copper ions activated *pmo* transcription whereas the presence of copper ions lead to down-regulation of sMMO genes. Copper-mediated transcriptional regulation of sMMO and pMMO genes was first explained by a model proposed by Nielsen et al. (1997) (Figure I.21).

The model proposes binding of a regulator protein R to the *pmo* operator repressing transcription of *pmo* genes in the absence of copper. Whereas, the regulator R or a similar regulator binds to an upstream activator sequence (UAS) of the *mmo* promoter and induces conformational changes to make contact with the RNA polymerase (RNAPol), resulting in transcription of *mmo* genes. In 'copper-containing' cells, when copper ions bind to the regulator, the regulator protein is inactivated making it impossible for binding to RNA polymerase for *mmo* operon transcription. In the absence of active regulator, the *pmo* genes are transcribed.

On the same lines, Gilbert et al. (2000), proposed that the unique metabolic switch mediated by copper ions consists of hypothetical repressor molecule (R), which normally binds to the $\sigma^{70}$ promoter of the pMMO operon, repressing it. Gilbert and colleagues suggested the presence of a hypothetical copper-binding regulator (CBR) and a hypothetical activator, which bind upstream to $\sigma^{54}$ promoter, aiding in transcription of sMMO operon (Figure I.22).

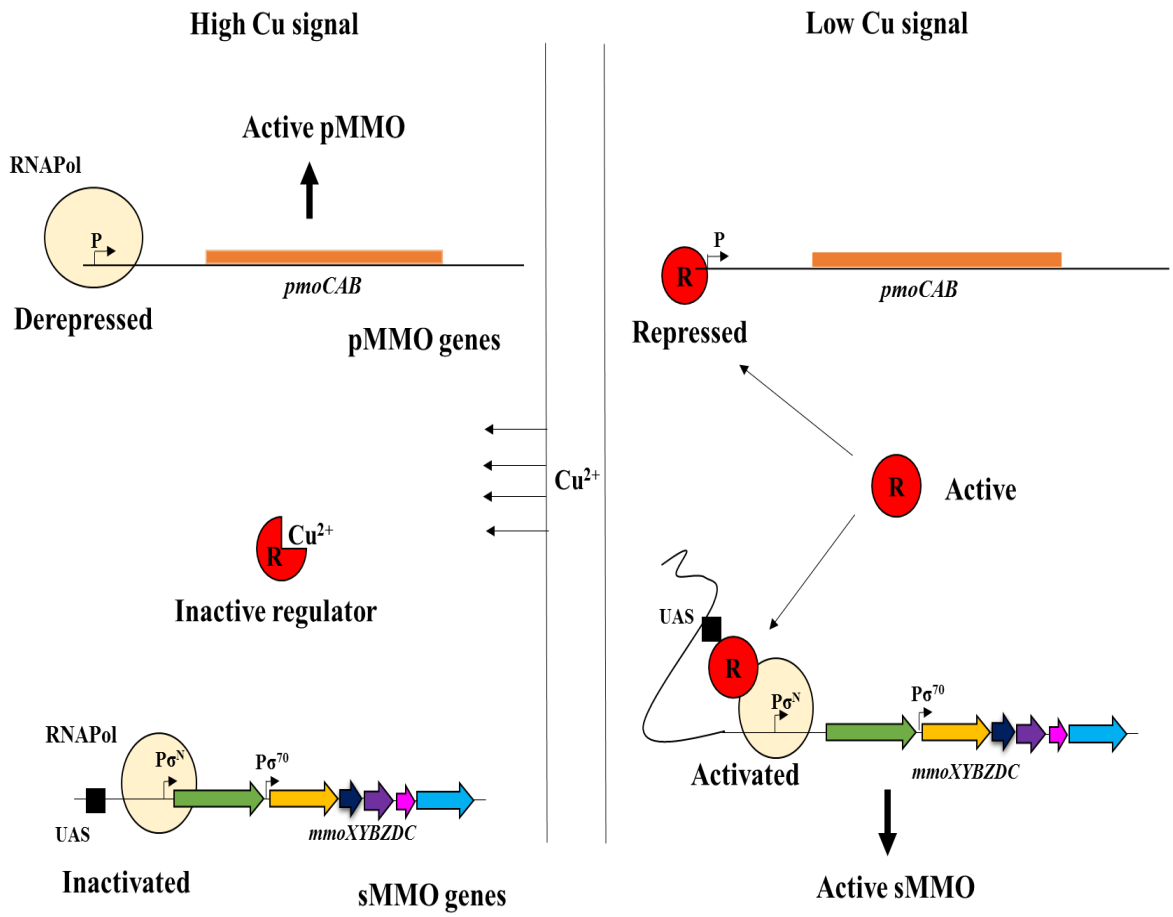


**Figure I.21** A hypothetical model for the copper-dependent transcriptional regulation of *pmo*/*mmo* genes. *pmo*, pMMO gene operon; *mmo*, sMMO gene operon; RNAPol, RNA polymerase; UAS, upstream activator sequence (modified from Nielsen et al., 1997).

In cells growing under high copper:biomass ratios, pMMO is de-repressed when the hypothetical repressor molecule (R) is bound by the hypothetical copper-binding regulator (CBR). This CBR–Cu complex also binds to the hypothetical activator. Under low copper:biomass conditions, CBR does not bind copper and thus, R is free to bind to $\sigma^{70}$ promoter of pMMO operon, repressing the transcription of the *pmo* operon.

The free activator protein (A) can then bind to the upstream activating sequence (UAS) of *mmoX*, enabling RNA polymerase to form an open complex and transcribe the sMMO-encoding genes.

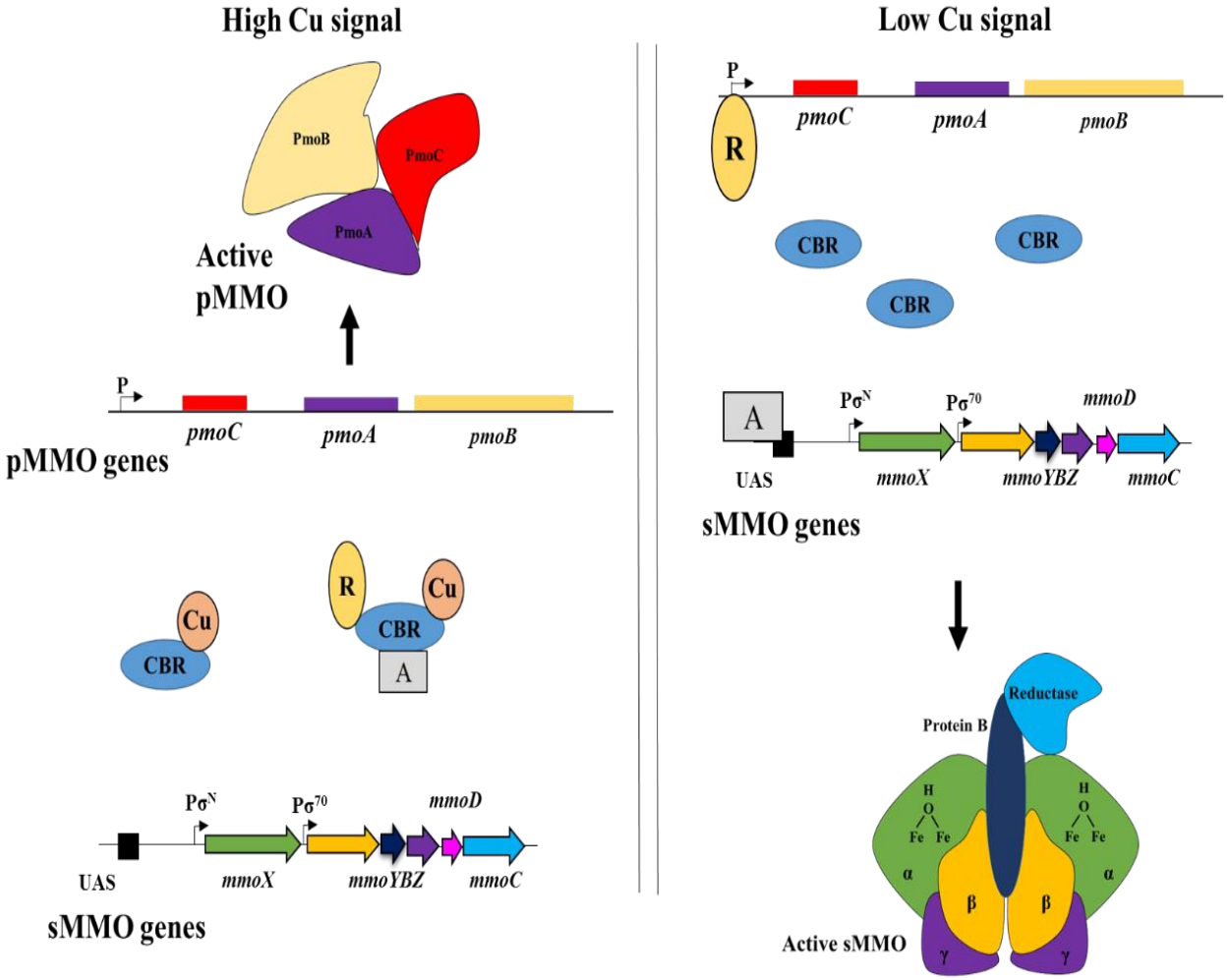


**Figure I.22** Proposed model for reciprocal expression of pMMO and sMMO genes (adapted from Gilbert et al., 2000).

Stafford et al., (2003) proposed an extended model for *mmo* gene regulation by copper ions (Figure I.23). This model links low copper conditions in *M. trichosporium* OB3b to expression of the regulatory genes *mmoR* and *mmoG*, found upstream of the structural genes for the sMMO.

When there is low copper signal, the assembly of a functional sMMO complex requires functional MmoR and MmoG for initiating the transcription of sMMO genes that is $\sigma^N$-dependent. However, the *mmoR* and *mmoG* genes are transcribed independent of a $\sigma^N$-promoter, implying the transcription of regulatory genes under all copper conditions. On addition of copper, it is proposed that a signal is relayed to inactivate MmoR and thus hinder the transcription of downstream sMMO genes. At this point, how the bacterial cell senses the intracellular copper concentration is unknown.

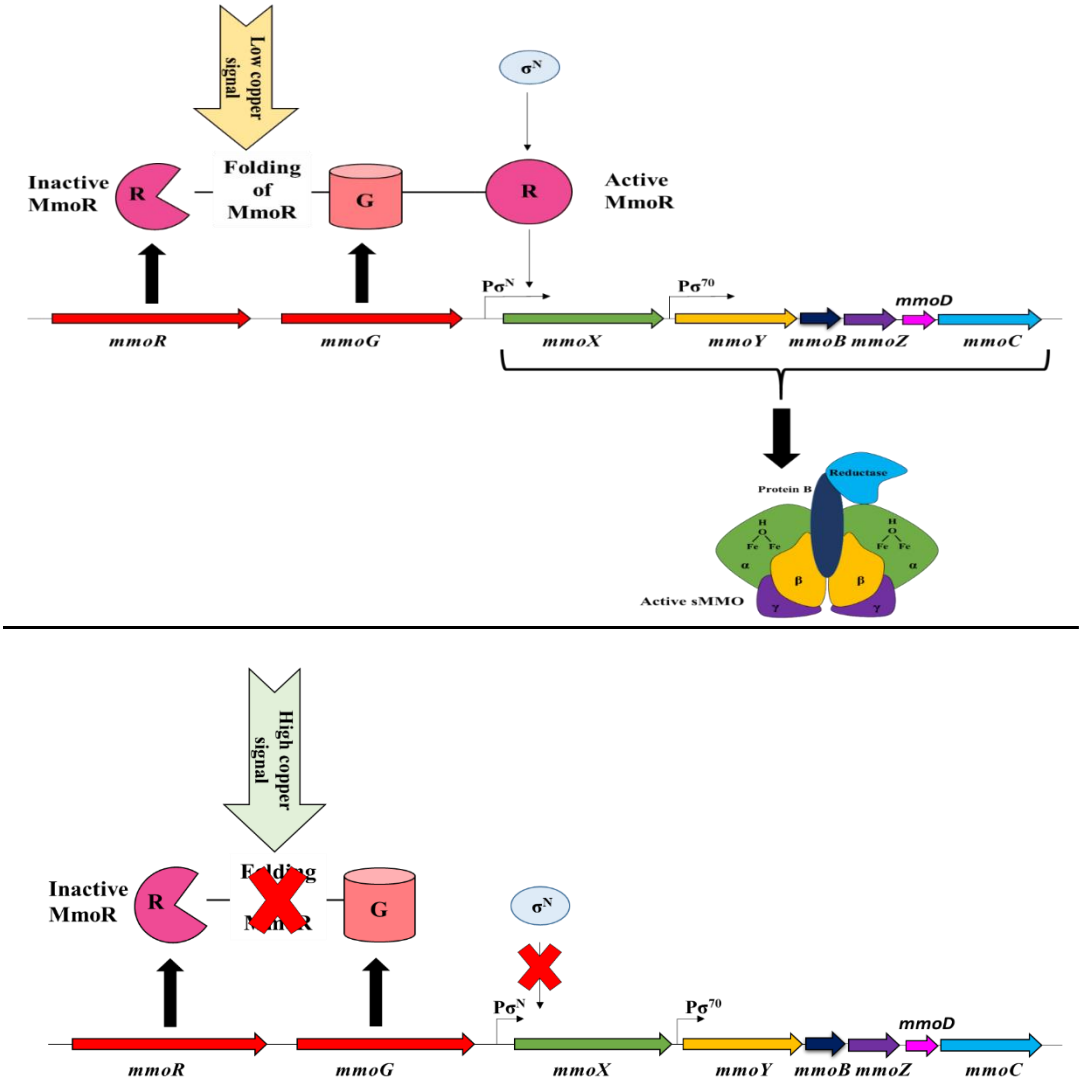


**Figure I.23** Proposed model for the regulation of sMMO genes in *M. trichosporium* OB3b (adapted from Stafford et al., 2003).

The most recent study by Semrau et al., (2013) on the copper switch mechanism in *M. trichosporium* OB3b elucidates the role of MmoD and methanobactin in understanding the reciprocal expression pattern of pMMO and sMMO genes. The model (Figure I.24) suggests that at low copper: biomass ratios, the MmoD protein downregulates *pmo* genes while upregulating *mmo* and *mbn* operons.

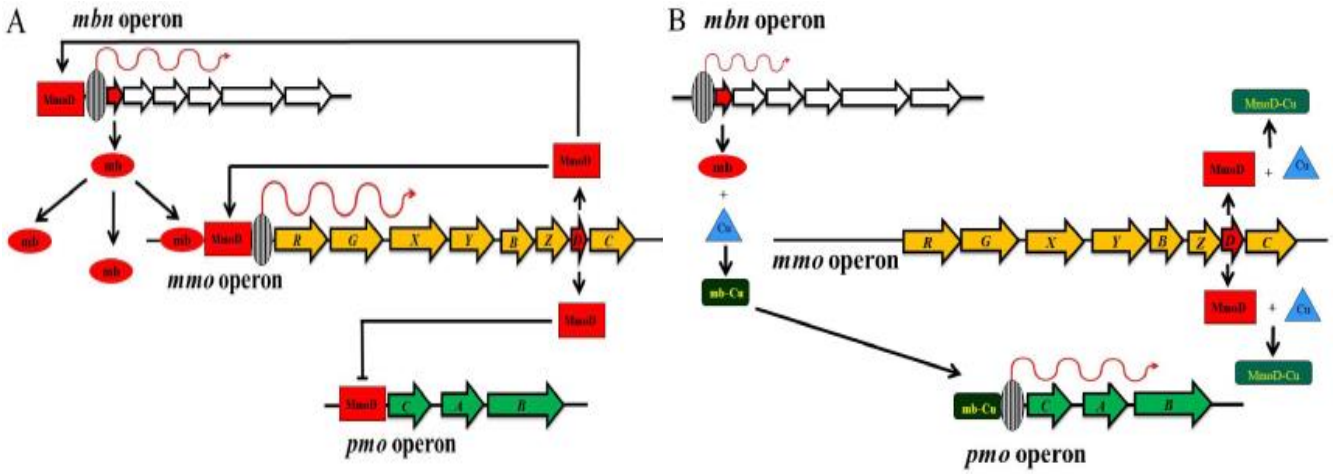


**Figure I.24** Proposed model for the copper mediated regulation of *mmo*, *pmo* and *mbn* operons in *M. trichosporium* OB3b: A) low copper:biomass ratio; B) high copper:biomass ratio (Semrau et al., 2013).

Subsequent increase in intracellular methanobactin concentration is suggested to enhance the expression of *mmo* operon. In the case with high copper: biomass ratios, copper binds to methanobactin reducing the *mmo* expression. Copper also binds to MmoD thereby disabling MmoD binding to *pmo* operon and thus induces expression of *pmo* genes.

Although much is known regarding copper uptake and gene expression, topics that need more attention are: (1) How do metals other than copper impact gene expression? (2) Does methanobactin play a role in gene regulation? These issues form the basis of this thesis.

# CHAPTER II: MATERIALS AND METHODS

## II.1. Bacterial strain and growth conditions

*Methylosinus trichosporium* OB3b was grown on nitrate mineral salt (NMS) medium (Whittenbury et al., 1970) at 30 °C in 250-ml sidearm Erlenmeyer flasks shaken at 200 rpm in the dark either with no added copper (creating a background copper concentration of 0.03 ± 0.01 μM) or with varying copper concentrations of 1 μM, 2 μM and 10 μM added as $CuCl_2$. Varying concentration of gold, cerium, and methanobactin from *M. trichosporium* OB3b and *Methylocystis* sp. strain SB2 were added for different experimental conditions discussed in detail below. The stock solutions of metals and methanobactin solutions used for the study were filter sterilized using 0.2 μm polyethersulfone membranes.

To screen for the effect of competing metal binding to methanobactin on gene expression, *M. trichosporium* OB3b was grown with 2 μM copper and various concentrations of Ag as $AgNO_3$, Hg as $HgCl_2$, Au as $HAuCl_4$, Zn as $ZnSO_4 \cdot 7H_2O$, Mn as $MnCl_2 \cdot 4H_2O$, Mo as $Na_2MoO_4 \cdot 2H_2O$, Ni as $NiCl_2 \cdot 6H_2O$, and Co as $CoCl_2 \cdot 6H_2O$. Subsequently, *M. trichosporium* OB3b was grown in

the presence of 0 and 5 µM gold along with 2 µM copper for quantifying gene expression under these conditions. Methanobactin from *M. trichosporium* OB3b (5 µM) as a complex with copper was also added in the presence of 2 µM copper and 5 µM gold. Methanobactin used in the study was isolated and purified as described in Section *II.1.1* and preparation of the copper-methanobactin complex is elaborated in Section *II.1.2*.

For studying the regulation of the two forms of methanol dehydrogenase by cerium, *M. trichosporium* OB3b grown with either no copper or 10 µM copper was supplemented with 0 µM and 25 µM cerium added as $CeCl_3$. All chemicals were of American Chemical Society grade or better. Glass side-arm flasks (250 ml; each with 50 ml of NMS medium) for each condition were capped with butyl rubber stoppers. Methane was added at a methane-to-air ratio of 1:2. Cultures were grown at 30 °C and shaken at 200 rpm for 3 days until the late exponential phase was reached. The optical density at 600 nm ($OD_{600}$) was measured in a Genesys 20 Visible spectrophotometer (Spectronic Unicam, Waltham, MA) at 3- to 6-h intervals until the late exponential phase was reached. All conditions had at least duplicate biological samples and most commonly triplicate samples.

### *II.1.1. Isolation of methanobactin*

*M. trichosporium* OB3b was cultured for methanobactin in 0.2 or 1.0 µM $CuSO_4$ amended NMS medium in sequential batch reactors. Similarly, for studying the effect of methanobactin from *Methylocystis* SB2 on gene regulation in *M. trichosporium* OB3b, methanobactin from *Methylocystis* sp. strain SB2 (SB2-Mb) was isolated using procedures outlined by Bandow et al. (2011). The purity of methanobactin was determined to be 98.2 % ± 0.3 % by high-performance liquid chromatography (HPLC) as described earlier (Krentz et al., 2010).

### *II.1.2. Preparation of copper-methanobactin complexes*

The copper-methanobactin complex was prepared by adding equimolar amounts of $CuCl_2$ and methanobactin to create a 5 mM stock solution. Methanobactin from *M. trichosporium* OB3b was used for studying metal competition for binding to methanobactin and that from *Methylocystis* sp. strain SB2 for studying the effect of methanobactin on gene expression in *M. trichosporium* OB3b. Copper-methanobactin was freshly prepared at 30 °C under constant mixing at 200 rpm in the dark for 1 h before use. Copper-methanobactin was then added to some cultures at a concentration of 5 µM and 50 µM. The concentration of copper not bound to methanobactin (free copper) in the Cu-methanobactin solutions was tested by monitoring the copper concentration in the flowthrough fraction of samples passed through Sep-Pak cartridges (Bandow et al., 2011). Copper concentrations in the flowthrough fractions were then determined by atomic absorption spectroscopy (Kalidass et al., 2015). The concentration of free copper in the flowthrough was below detection limit, i.e., <1 nM. The stability of Cu-methanobactin complex at 30 °C in NMS medium was monitored by changes in the UV-visible light absorption spectra and by the presence of unbound copper. Following a 3-day incubation period, 0.30 % ± 0.01 % sample loss was observed.

## II.2. Protein measurements

The procedure outlined by Semrau et al. (2013) was used to quantify protein concentrations. Briefly, protein was measured using the Bradford assay (Bio-Rad Laboratories) after concentration of 5 ml of the culture to 1 ml and digestion in 2M NaOH (0.4 ml 5M NaOH per 1.0 ml of culture) at 98 °C for 15 min. A plot of protein concentrations of cultures of *M. trichosporium* OB3b cells at different optical densities at 600 nm ($OD_{600}$) yielded a linear

regression of an OD595 value of 1.0, equal to 850 µg of protein per ml, with a coefficient of determination value ($R^2$) of 0.995. This correlation was used to calculate protein concentration for all cultures.

### II.3. Metal measurements

Cultures were centrifuged at 5,000 × g for 10 min at 4 °C. Supernatant samples were stored at –80 °C and cell pellets resuspended in 1 ml of fresh NMS medium before storage at – 80 °C. Supernatant samples were then diluted in NMS medium with 5 % (vol/ vol) $HNO_3$ to achieve a final concentration of 2 % (vol/vol) $HNO_3$. Cell suspensions were acidified in 1 ml of 70 % (vol/vol) $HNO_3$ and incubated for 2 h at 95 °C (Vorobev et al., 2013). The acidified cell suspensions were mixed by inverting the tubes every 30 min. Copper and gold associated with biomass and supernatant were analyzed using an inductively coupled plasma mass spectrometry (ICP-MS) instrument (PerkinElmer, Waltham, MA). Duplicate biological samples were used for each experimental condition, with each replicate measured five times.

### II.4. Prediction of metal speciation

Copper speciation in NMS medium amended with either copper or copper and gold or copper with cerium was predicted using Visual Minteq version 3.0 (http://vminteq.lwr.kth.se/) using the assumption of equilibrium. pH and temperature were set at 6.8 and 30°C, respectively, to simulate growth conditions. The model parameter and interface model were set to the default hydrous ferric oxide model (Dzombak and Morel, 1990) and a 2-site protonation model (Lützenkirchen, 1988), respectively.

### II.5. Naphthalene assay for sMMO activity

sMMO activity in *M. trichosporium* OB3b was assayed using a modified version of the naphthalene assay (Brusseau et al., 1990; Morton et al., 2000). Briefly, growth was monitored by measuring the optical density at 600 nm ($OD_{600}$) using a Milton Roy Spectronic 20D spectrophotometer (Milton Roy Company, Warminster, PA). Cultures were grown to an optical density of between 0.3 and 0.4, and triplicate samples of 3 ml each were put in 10-ml serum vials with several flakes of naphthalene, capped with Teflon-coated butyl rubber stoppers, and sealed. Cultures were incubated for 2 h at 200 rpm and 30 °C. The cell suspension was then centrifuged for 5 min at 6,300×g. A total of 130 μl of freshly prepared 4.21 mM tetrazotized o-dianisidine was then placed in a 1.5-ml cuvette with 1.3 ml of the culture supernatant, and the absorbance at 528 nm was monitored immediately using a Genesys 20 Visible spectrophotometer (Spectronic Unicam, Waltham, MA).

### II.6. Nucleic acid extraction and reverse transcriptase –quantitative PCR (RT-qPCR)

RNA was extracted from *M. trichosporium* OB3b grown in 250-ml sidearm flasks as follows. Briefly, 2.5 ml of stop solution (5% Tris equilibrated phenol [pH 7.3] in ethanol) was added to individual cultures (22.5 ml each) to stop any new mRNA synthesis. Cell pellets were then collected by centrifugation at 5,000 × g for 10 min at 4°C and resuspended in 0.75 ml of extraction buffer (0.2 M $NaH_2PO_4$-$Na_2HPO_4$ buffer [pH 7.5] and 5% cetyltrimethylammonium bromide [CTAB] in 2.4 M NaCl). The above mix was subjected to bead beating using 0.5 g of 0.1-mm zirconia-silica beads (Biospec Products), 35 μl of 20% SDS, 35 μl of 20% laurylsarcosine, and 750 μl of phenol-chloroform-isoamylic alcohol (25:24:1) for 1 min at 4,800

rpm in 2-ml plastic tubes. The samples were then centrifuged at 14,000 rpm for 5 min at 4 °C to separate the organic and aqueous phase. The supernatant containing the aqueous phase was transferred to a fresh 2-ml plastic tube, mixed with an equal volume of chloroform-isoamylic alcohol (24:1) and centrifuged at 14,000 rpm for 5 min at 4 °C. The total RNA was precipitated by adding $MgCl_2$ (final concentration, 2.5 mM), 0.1 volumes of 3 M sodium acetate, and 0.7 volumes of isopropanol and incubating the mixture overnight at – 80 ºC. Total RNA was then recovered by centrifugation at 14,000 rpm for 30 min at 4 °C. RNA was then subjected to RNasefree DNase treatment until free of DNA contamination. RNA was checked for any DNA contamination via PCR amplification of the 16S rRNA gene, and the concentration of purified RNA was determined spectrophotometrically (NanoDrop ND1000; NanoDrop Technologies, Inc., Wilmington, DE). RNA samples were stored at – 80 °C and used for cDNA synthesis within 2 days of extraction. cDNA was prepared from DNA-free RNA samples (500 ng each) by reverse transcription using Superscript III reverse transcriptase (Invitrogen, Carlsbad, CA) according to the manufacturer's instructions. Relative gene expression in *M. trichosporium* OB3b was quantified by RT-qPCR by comparative $C_T$ method as described below. The specificities of these primers were verified by gel electrophoresis and sequencing of PCR products. Gene specific primers were used for the RT-qPCR (Table II.1) analyses of *pmoA*, *mmoX*, *mbnA*, 16S rRNA, *mxaF*, *mxaI*, *xoxF1* and *xoxF2* in *M. trichosporium* OB3b.

Quantitative PCR (qPCR) amplifications were performed in 96-well reaction PCR plates using Mx3000P qPCR systems (Stratagene, La Jolla, CA). The final reaction volume (20 µl) contained 0.8 µl of cDNA, 1×Brilliant III SYBR green qPCR Mastermix (Agilent Technologies, Santa Clara, CA), 15 nM 6-carboxy-X-rhodamine (ROX) dye, 0.5 µM (each) forward and reverse primer, and sterile water (Ambion Life Technologies, Grand Island, NY). The Mx3000P PCR

program involved 40 cycles of denaturation (95 °C for 30 s), annealing (58 °C for 20 s), and extension (68 °C for 30 s) after an initial denaturation at 95 °C for 10 min. After the qPCR cycles, samples were subjected to melting curve analysis with temperatures ranging from 55 °C to 95 °C to confirm the specificity of qPCR products.

**Table II.1** RT-qPCR primer sets used in this study

| Primer | Targeted gene | Sequence (5'-3') | Reference |
|---|---|---|---|
| qpmoA_FO | *pmoA* | TTCTGGGGCTGGACCTAYTTC | Semrau et al., 2013 |
| qpmoA_RO | | CCGACAGCAGCAGGATGATG | |
| qmmoX_FO | *mmoX* | TCAACACCGATCTSAACAACG | Semrau et al., 2013 |
| qmmoX_RO | | TCCAGATTCCRCCCCAATCC | |
| qmbnA_FO | *mbnA* | TGGAAACTCCCTTAGGAGGAA | Semrau et al., 2013 |
| qmbnA_RO | | CTGCACGGATAGCACGAAC | |
| q 16S rRNA_FO | 16S rRNA | GCAGAACCTTACCAGCTTTTGAC | Semrau et al., 2013 |
| q 16S rRNA_RO | | CCCTTGCGGGAAGGAAGTC | |
| qmxaF_FO | *mxaF* | CTACATGACCGCCTATGACG | Farhan Ul Haque et al., 2015 |
| qmxa_RO | | ATTGGCCTTGTTGAAGTCGT | |
| qmxaI_FO | *mxaI* | TACGATCCCAAGCATGACCC | Farhan Ul Haque et al., 2015 |
| qmxaI_RO | | CGTAGATCCATTTGCCGCTC | |
| qxoxF1_FO | *xoxF1* | TCAAGGACAAGGTGTTCGTC | Farhan Ul Haque et al., 2015 |
| qxoxF1_RO | | CGAGCCGTCCTTGATGTTAT | |
| qxoxF2_FO | *xoxF2* | GCGCGAAGGATTGGGAATAT | Farhan Ul Haque et al., 2015 |
| qxoxF2_RO | | GCCTCGTAATTCATGCACAG | |

MxPro software (Stratagene, La Jolla, CA) was used to import the threshold amplification cycle values. Relative gene expression levels were calculated from these threshold cycle ($C_T$) values and the comparative $C_T$ method ($2^{-\Delta\Delta CT}$) (Schmittgen and Livak, 2008), with 16S rRNA as the

housekeeping gene (Kalidass et al., 2015). Calibration curves for examined qPCR products are shown in Figure II.1.

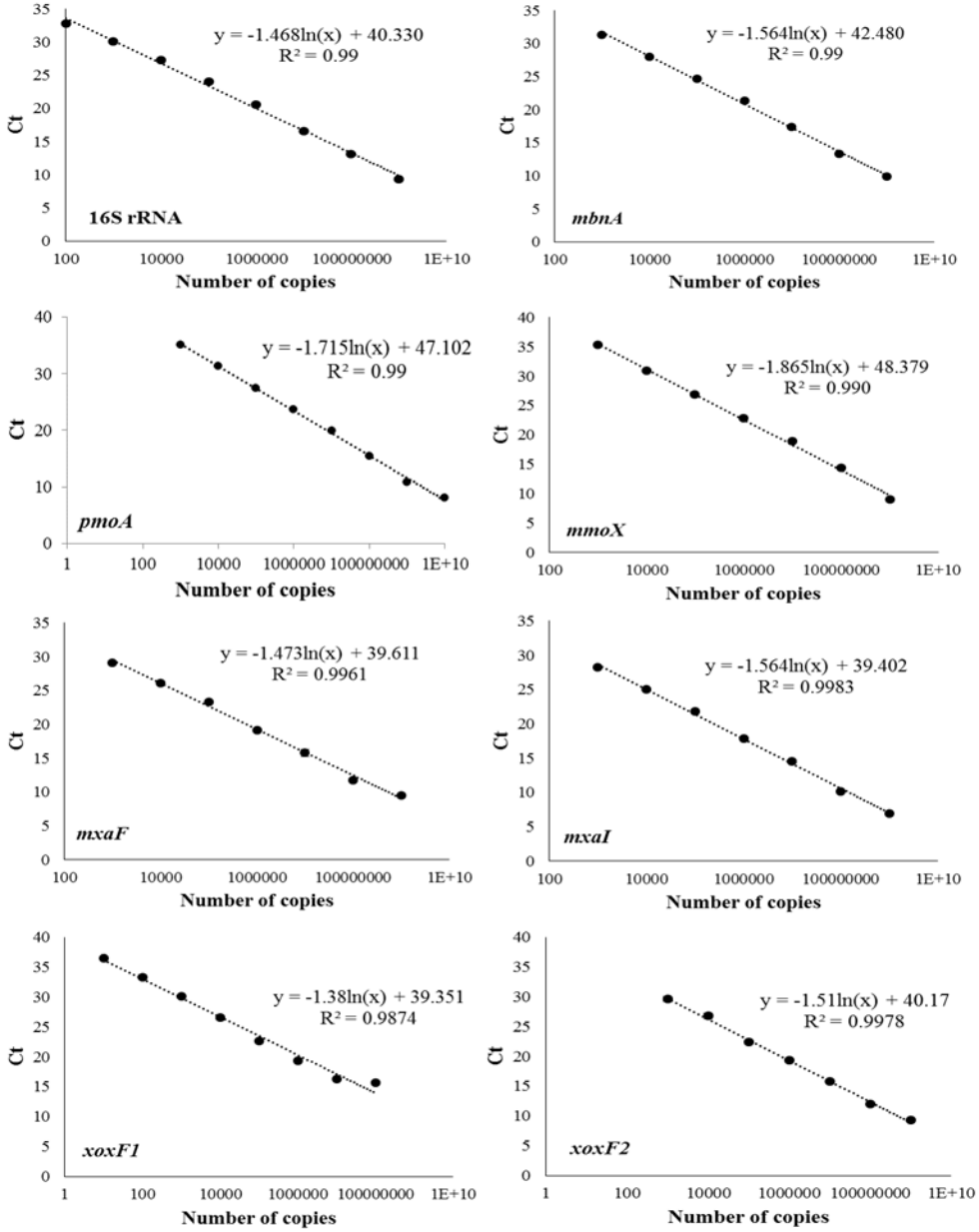


**Figure II.1** Standard curves for the qPCR of 16S, *mmoX*, *mbnA*, *pmoA*, *mxaF*, *mxaI*, *xoxF1* and *xoxF2* genes. Plasmids were prepared after ligating *mmoX*, *mbnA*, *pmoA*, *mxaF*, *mxaI*, *xoxF1* and *xoxF2* gene fragments from *M. trichosporium* OB3b individually into a cloning vector pCR2.1®-TOPO® TA (Invitrogen). Standards were prepared by tenfold dilution series of the purified plasmids and used as template for qPCR. Threshold cycle (Ct) values were plotted against the known copy numbers of the plasmid based standards. Each point represent the average of triplicate/duplicate samples with error bars showing the standard deviation.

## II.7. Statistical analyses

Data were analyzed using unpaired, two-tailed Student's t-tests assuming equal variance between groups to determine any significant differences in the response of *M. trichosporium* OB3b to different culture conditions. To determine any significant differences in the responses of *M. trichosporium* OB3b to various amounts of SB2-Mb or Cu-SB2-Mb in the presence or absence of $CuCl_2$, both one-way analyses of variance (ANOVA) and unpaired, two-tailed Student's t-tests, assuming equal variance between groups were performed when only two data sets were compared.

## II.8. Construction of expression plasmid of an MmoD fusion protein

Nested PCR was used to amplify *mmoD* (324 bp) from genomic DNA of *M. trichosporium* OB3b by using *Pfu* Ultra hotstart PCR mix (Agilent) and the nested PCR primers: 5'-CGC CAA GAG CAA ATA TGA GG-3' and 5'-AGA TTA CGC TCT GCC TCA GC-3'. The PCR product (700 bp) was then used as template DNA for amplifying *mmoD*. The PCR primers used are 5'-GGT ATT GAG GGT CGC ATG GAC CAA CAG ACG GCG-3' and 5'-AGA GGA GAG TTA GAG CCC TAA ATA TGC GCC GGC TTC G-3'. The PCR program involves 33 cycles of denaturation (94 °C for 20 s), annealing (53 °C for 20 s), and extension (72 °C for 15 s) after an initial denaturation at 94 °C for 3 min. Overhangs compatible with the LIC (Ligation-independent cloning) sites of pET Xa/LIC vector (Xa/LIC cloning kit, Novagen) were created by treating the PCR product with T4 DNA polymerase in the presence of dGTP as per manufacturer's instructions. *mmoD* with the overhangs was fused to the linearized pET32Xa vector by incubating it with the vector and T4 DNA Polymerase treated *mmoD* insert at 22 °C for

10 min in the presence of 25 mM EDTA, following manufacturer's instructions. The pET32Xa/LIC-*mmoD* vector-gene construct was transformed into NovaBlue GigaSingles competent cells (Novagen) and plated on Luria Bertani (LB; Bertani, 1951) agar plates containing 100 µg/ml ampicillin. Positive clones were identified by performing PCR using vector specific forward primer (5'-TAA TAC GAC TCA CTA TAG GG-3') and gene specific reverse primer (5'-AGA GGA GAG TTA GAG CC CTA AAT ATG CGC CGG CTT CG-3').

**II.9. Expression of recombinant MmoD fusion protein**

The expression vector-gene construct, pET32Xa/LIC-*mmoD,* was isolated from positive clones and transformed into *E. coli* BL21 (DE3) cells. Expression was performed using a modified protein expression procedure from Merkx and Lippard (2001). A 50 ml LB medium with 200 µg/ml ampicillin was inoculated with 1 ml of glycerol stock solution of BL21 (DE3)/pET32Xa/LIC-*mmoD,* and incubated at 37 °C and 200 rpm until the optical density at 600 nm ($A_{600}$) reached ~ 0.8. This 50 ml culture was later used as starter culture to inoculate 300 ml of LB medium (with 200 µg/ml ampicillin) and grown at 37 °C with shaking at 200 rpm until $A_{600}$ reached 0.6. Protein expression was induced using 0.4 mM isopropyl β-D-thiogalactopyranoside (IPTG; Invitrogen, Carlsbad, CA) and the cells were incubated for 4 hours before harvesting. The expression cell culture, *E. coli* BL21 (DE3)/pET32Xa/LIC-*mmoD,* was checked for expression of MmoD by lysing 100 µL cells at 95 °C with 100 µL Tricine SDS sample buffer (2X) (Novex, Carlsbad, CA) for 10 min and then loading in a 10 % Tris-Tricine Polyacrylamide Gel Electrophoresis (PAGE) Pre-Cast gel (Novex, Carlsbad, CA). The gel was run at 100 V for 2 hours using Tricine SDS Running Buffer (1X buffer: Tris Base – 12.1 g/L; Tricine – 17.9 g/L; SDS – 1 g/L) in an XCell *SureLock* Mini-Cell electrophoresis system

(Invitrogen, Carlsbad, CA). After confirming the expression of MmoD fusion proteins, cultures were then harvested by centrifugation at 8000 x *g* for 10 min and purified as described in the following section.

**II.10. Purification of recombinant MmoD**

The harvested cells were resuspended in 10 ml of lysis/equilibration buffer (20 mM $NaH_2PO_4$, 300 mM NaCl, 3 mM imidazole, pH 7.4). Cell lysis was performed using cell homogenizer (Avestin Inc., Ottawa, ON) for ~ 3 passes at 15,000 – 20,000 psi. The cell lysate was centrifuged at 12,000 x *g* for 15 min at 4 °C and the supernatant is collected. This removes the cell debris from the lysate. About 20 µl of the cleared cell lysate is saved for SDS-PAGE. Benzonase nuclease (3U/ ml; Sigma-Aldrich, St. Louis, MO) was added to cell lysate and incubated on ice for 15–30 min to remove nucleic acids. Meanwhile, the storage buffer from the Ni-NTA spin columns was removed by removing the bottom plug and centrifuging the column for 2 min at 890 x *g*. The column was equilibriated with two resin-bed volumes of lysis buffer and centrifuging for 2 min at 890 x *g*. Bottom plug was placed and cleared cell lysate (upto two resin-bed volumes) containing the 6X His-tagged MmoD fusion protein was loaded onto the preequilibriated column and mixed on an orbital shaker for 30 min at room temperature. The bottom plug was then removed and the column was centrifuged at 270 x *g*. The flow through was collected for SDS-PAGE to check for 6XHis-tagged protein binding efficieny. The column was washed with two resin-bed volumes of wash buffer (20 mM $NaH_2PO_4$, 300 mM NaCl, 25 mM imidazole, pH 7.4) and 20 mM β-mercaptoethanol to reduce the disulphide bonds. The column was washed two more times with wash buffer. The flow-through from these washes are saved for SDS-PAGE to check for wash stringency. Since the Factor Xa protease functions in a Factor Xa

cleavage buffer (Novagen) at pH 8.0, the column was equilibriated with one resin-bed volume of Factor Xa cleavage buffer along with two resin-bed volumes of wash buffer. The column is then incubated overnight (~14 h) with one resin-bed volume of Factor Xa cleavage buffer and 8 μg of Factor Xa protease (Novagen, > 150 IU/mg). MmoD is then eluted thrice with one-resin bed volume of wash buffer/lysis buffer by centrifuging at 890 x *g* for 2 min. SDS-PAGE is performed with the saved flow throughs and eluate fractions to check for MmoD purity.

**II. 11 Synthesis of DNA oligonucleotide for EMSA**

The following primer sets (Table II.2) were used to generate DNA regions upstream of genes from *mmo, pmo, mxa, xox* and *mbn* operons. PCR conditions used to generate include 30 cycles of denaturation (94 °C for 1 min), annealing (52 °C for 1 min), and extension (72 °C for 1 min) after an initial denaturation at 94 °C for 3 min. The PCR products were gel purified and confirmed by sequencing.

**Table II.2** Primers synthesized to generate DNA consensus sequence for EMSA.

| Upstream regions of genes | Primer (5'-3') | bp | $T_m$ | Product size | PCR product distance from gene |
|---|---|---|---|---|---|
| *mmoX* (F) | TCGATCAGACCTATGGAATCG | 21 | 60.04 | 484 bp | ~ 53 bp |
| *mmoX* (R) | GCGCGATACACATGTCAAAG | 20 | 60.29 | | |
| *pmo1* (F) | AAGTGAGCAGCCTCCCCTA | 19 | 59.96 | 441 bp | 9 bp upstream |
| *pmo1* (R) | CCTAAGTGCTCCCAGGGATT | 20 | 60.46 | | |
| *mmoY* (F) | ATCCCCTATCAGTGGCTCCT | 20 | 59.92 | 483 bp | ~ 8 bp |
| *mmoY* (R) | AGGATTTTTGGTGCTTCGTG | 20 | 60.11 | | |
| *mmoD* (F) | AGAAGCTCTCGGTGCTGAAG | 20 | 59.89 | 422 bp | 16 bp overlap |
| *mmoD* (R) | CCGTCTGTTGGTCCATTTTC | 20 | 60.35 | | |
| *mbnA* (F) | GGAGGACCAAAAATGAAACG | 20 | 59.41 | 493 bp | ~ 70 bp |
| *mbnA* (R) | GCATCTGCAACTCCAAACAG | 20 | 59.45 | | |
| *mmoR* (F) | GGCTCTGCTCGGCTATGTC | 19 | 61.96 | 363 bp | ~ 88 bp |
| *mmoR* (R) | AGGACGGGCTTTCTCACTG | 19 | 59.39 | | |
| *xoxF1* (F) | TGTCCCTGATGGACGAAGAC | 20 | 61.08 | 443 bp | 10 bp overlap |
| *xoxF1* (R) | GCTTTTGCATGAGCTTTTCC | 20 | 59.97 | | |
| *xoxF2* (F) | CTTCAGCGCCTGTCATCTTC | 20 | 61.09 | 423 bp | 34 bp overlap |
| *xoxF2* (R) | AGTCGGATCGACGTGAAAAG | 20 | 60.25 | | |
| *mxaF* (F) | TTCGAACTTCCTCGTCTGCT | 20 | 60.13 | 366 bp | 21 bp overlap |
| *mxaF* (R) | GGAATTCAGCAGCTTCCTCA | 20 | 60.48 | | |
| *mbnI* (F) | GTTCGCGGATATCTGTCGTC | 20 | 60.63 | 500 bp | 124 bp overlap |
| *mbnI* (R) | GGAACGTCTCCTGCAATAGG | 20 | 59.69 | | |

## II.12 Electro-mobility shift assay

A positive control system was used for optimization. Epstein-Barr Nuclear Antigen (EBNA) extract (LightShift EMSA Optimization and Control kit, ThermoScientific) was checked for binding with unlabeled EBNA DNA. Binding reactions (20 µl) were performed for 20 mins using the following components at room temperature (Table II.3). MmoD and Mb were used as glycerol stock (25%) for final protein concentration of 175 ng/ µl. In the reaction mix, after addition of protein, the reaction mix was incubated for 15 min before addition of DNA, as this preincubation is known to enhance DNA:protein binding.

**Table II.3** EMSA binding reaction components

| DNA/Protein | $H_2O$ (µl) | 10X Binding buffer (µl) | 50% Glycerol (µl) | 100mM $MgCl_2$ (µl) | % NP-40 (µl) | DNA (µl) | Protein (µl) |
|---|---|---|---|---|---|---|---|
| EBNA DNA | 13 | 2 | 1 | 1 | 1 | 2 | 0 |
| EBNA protein | 13 | 2 | 1 | 1 | 1 | 0 | 2 |
| EBNA DNA:protein | 9 | 2 | 1 | 1 | 1 | 2 | 4 |
| *mmoX*/*pmo1* | 14 | 2 | 1 | 1 | 1 | 1 | 0 |
| *mmoX*/*pmo1*-MmoD | 4 | 2 | 1 | 1 | 1 | 1 | 10 |
| *mmoX/pmo1*-MmoD-Cu | 4 | 2 | 1 | 1 | 1 | 1 | 10 |
| *mmoX/pmo1*-Mb | 4 | 2 | 1 | 1 | 1 | 1 | 10 |
| *mmoX/pmo1*-Mb-Cu | 4 | 2 | 1 | 1 | 1 | 1 | 10 |
| MmoD | 5 | 2 | 1 | 1 | 1 | 0 | 10 |
| Mb | 5 | 2 | 1 | 1 | 1 | 0 | 10 |

Once the reaction is over, the reaction mix was quickly loaded in a 6% Tris Borate EDTA (TBE)-polyacrylamide gel electrophoresis gel using 5 µl of 5X EMSA loading dye provided in the EBNA optimization kit. The gel was run at 90 V for 60 min at 4 °C. After electrophoresis, the gel was first stained using 100 ml of SYBER green DNA stain for 20 mins. The gel was destained by washing in 100 ml of dd$H_2O$ and visualized under 312 nm UV-transilluminator. For protein staining, the gel was incubated overnight in 100 ml of SYPRO Ruby stain. The gel was then destained in a destain solution containing 5% methanol and 10% acetic acid for 3 h before visualizing under UV-transilluminator.

# CHAPTER III: IMPACT OF COMPETING METALS BINDING TO METHANOBACTIN ON EXPRESSION OF SOLUBLE METHANE MONOOXYGENASE IN THE PRESENCE OF COPPER

Previously published: Competition between metals for binding to methanobactin enables expression of soluble methane monooxygenase in the presence of copper. *Applied and Environmental Microbiology*, **81**(3):1024–2031. http://dx.doi.org/10.1128/AEM.03151-14.

## III.1. Introduction

Metals in complex natural systems are well-known to affect gene expression in micro-organisms (O'Halloran, 1993). In the case of methanotrophs, studies have focused on the effect of copper on *pmo* and *mmo* gene expression. It is quite possible, however, that other metals might impact gene expression in methanotrophs and the presence of other metals may also affect the uptake of copper.

Copper is bound by OB3b-Mb with very high affinity (reported affinities range from $10^{18}$ to $10^{58}$ $M^{-1}$) using nitrogen from both heterocyclic rings and the sulfur of the enethiol groups (Pesch et al., 2012; El Ghazouani et al., 2011; Choi et al., 2006a). Methanobactin, however, can bind many other metals, but generally with much lower affinities, ~ $10^5$ to $10^7$ $M^{-1}$ (Choi et al., 2006b). It

has been found that at least one metal, Hg (II), binds to OB3b-Mb rapidly, with most binding occurring in the dead time of the stopped-flow system used (1.8 ms). For the remainder, binding was observed to have a rate of 640 $s^{-1}$ (Vorobev et al., 2013). Further, mercury was found to be irreversibly bound to methanobactin, i.e., copper could not displace mercury. It is possible that in the presence of copper, sMMO expression may be possible if methanotrophs are unable to collect copper via methanobactin due to the presence of competing metals.

In the following set of experiments, the effect of uptake of a suite of metals was tested on gene expression in *M. trichosporium* OB3b in the presence of copper. The metals tested include Zn, Mn, Mo, Ni, Co, Fe that belong to Group B metals and Ag and Au belonging to Group A metals as categorized by Choi et al. (2006). In this study, sMMO activity was assayed in the presence of various Group A metals and Group B metals and in the presence of copper. Here, sMMO activity was assayed instead of pMMO, since it is known that *M. trichosporium* OB3b expresses *pmoA*, that encodes for the 26-kDa subunit of pMMO, constitutively irrespective of the presence or absence of copper (Vorobev et al., 2013). Preferential activity of sMMO, if induced by any of the metals tested in the presence of copper, could be an alternative and cost-effective strategy to induce sMMO activity in methanotrophic community *in situ*. This has broad implications in the field of pollutant biodegradation as sMMO is known to transform broader range of chemical pollutants as compared to pMMO (Semrau et al., 2010).

## III.2. Results

### *III.2.1. Growth and expression of sMMO in the presence of copper and various metals*

An initial survey of both group A and B metals was performed to determine if, in the increased presence of these metals, sMMO expression was possible in the simultaneous presence of 2 μM copper. As shown in Table III.1, *M. trichosporium* OB3b grew in the presence of many group B metals (Zn, Mn, Mo, Ni, and Co), either singly or in combination at concentrations as high as 500 μM each. In no case, however, was any sMMO activity observed via the naphthalene assay. Given these results, further study of the effect of these metals on methanotrophic activity was not pursued. Of the three tested group A metals, mercury and silver were toxic at a concentration as low as 5 μM (i.e., no growth was observed) and were also not considered further. Growth, however, occurred in the presence of 5 μM gold, and despite the presence of 2 μM copper, sMMO activity was observed via the naphthalene assay. The impact of gold on methanotrophic activity and gene expression was thus explored in more detail.

**Table III.1** Growth and sMMO activity of *M. trichosporium* OB3b in the presence of 2 μM copper and various concentrations of competing metals for binding to methanobactin

| Competing metal(s) | Metal concentration(s) (μM) | Growth of *M. trichosporium* OB3b[a] | sMMO activity[b] |
|---|---|---|---|
| None (2 μM copper only) | | Yes | No |
| Group A | | | |
| Hg | 5 | No | ND |
| Ag | 5 | No | ND |
| Au | 5 | Yes | Yes |
| Group B | | | |
| Zn | 10 | Yes | No |
| Mn | 10 | Yes | No |
| Mo | 10 | Yes | No |
| Ni | 10 | Yes | No |
| Co | 10 | Yes | No |
| Zn + Ni + Mn + Mo + Co | 25, 50, 100, 250, and 500 | Yes | No |

[a] Positive growth defined as $OD_{600}$ of > 0.2 within 3 days from an initial $OD_{600}$ of ~ 0.05.
[b] sMMO activity determined using the naphthalene assay (Brusseau et al., 1990). ND, not determined due to lack of growth.

### *III.2.2. pmoA, mmoX, and mbnA expression in M. trichosporium OB3b in the presence of copper, gold, and copper-methanobactin*

Figure III.1A shows that *pmoA* expression was constitutive in the presence of 2 μM copper regardless of the simultaneous presence of various amounts gold and copper-methanobactin, and such expression was not significantly different across all tested conditions ($P > 0.05$). As expected, in the presence of 2 μM copper, very little *mmoX* expression was observed (Figure III.1B). In the presence of 2 μM copper and 5 μM gold, however, *mmoX* expression increased over 10,000-fold (significant at a P value of $< 0.003$). In the presence of 2 μM copper, 5 μM gold, and 5 μM copper-methanobactin, very little *mmoX* expression was observed, and it was not significantly different from that observed in the presence of only 2 μM copper ($P < 0.4$).

Interestingly, *mmoX* expression was ~ 5-fold greater in the presence of 2 μM copper and 5 μM gold than when the two metals were not added ($P < 0.007$). Expression of *mbnA* also varied in response to changing growth conditions, as shown in Figure III.1C. Specifically, *mbnA* expression increased significantly in the presence of 2 μM copper and 5 μM gold compared to that in the presence of 2 μM copper alone ($P < 0.03$) and was similar to that observed when either copper nor gold was added ($P = 0.09$).

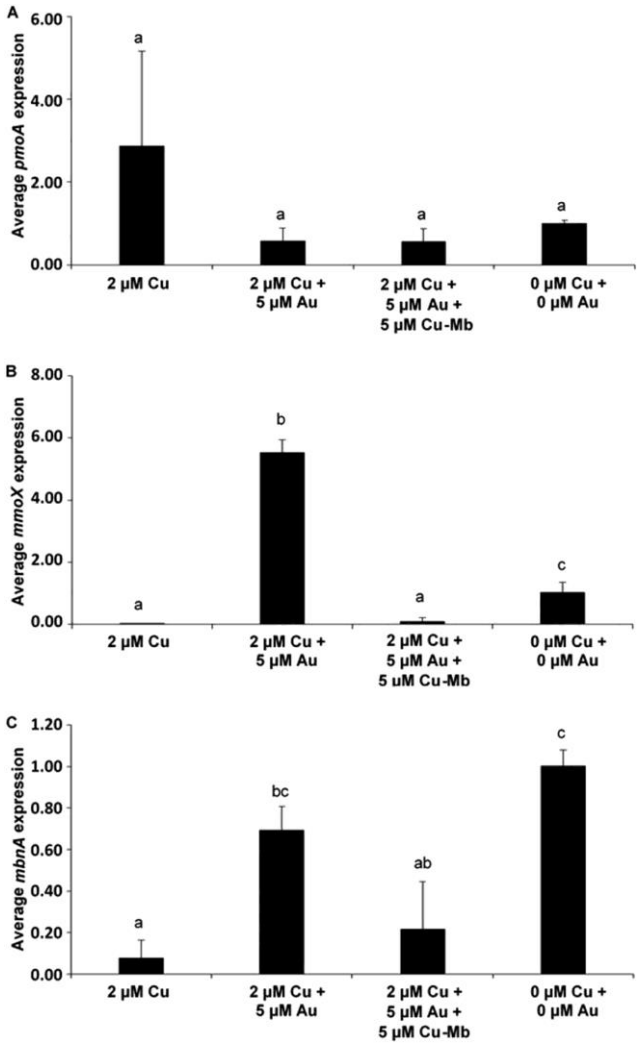


**Figure III.1** RT-qPCR of *pmoA* (A), *mmoX* (B), and *mbnA* (C) in *M. trichosporium* OB3b grown in the presence of copper (Cu), gold (Au), and copper-methanobactin (Cu-mb). Columns within each plot labeled by different letters are significantly different ($P < 0.05$). Error bars represent standard deviation (n=3).

When 5 μM copper-methanobactin was also added, expression of *mbnA* decreased but was not significantly different from the level of expression when *M. trichosporium* OB3b was grown either with 2 μM copper or with 2 μM copper and 5 μM gold (P = 0.5 and 0.12, respectively).

### *III.2.3. sMMO activity in the presence of copper, gold, and copper-methanobactin*

To determine if sMMO was active as well as its genes expressed in the presence of gold, copper, and methanobactin pre-equilibrated with copper, the naphthalene assay was used to monitor sMMO activity (Brusseau et al., 1990). As shown in Figure III.2, in the presence of 2 μM copper, no sMMO activity was observed. Clear evidence of naphthalene oxidation, however, was observed in cultures grown with no added copper, gold, or copper-methanobactin, as well as in the presence of both 2 μM copper and 5 μM gold, indicating that the genes for sMMO were expressed and active enzyme was produced under these conditions. When 5 μM copper-methanobactin was added in addition to 2 μM copper and 5 μM gold, no sMMO activity was observed, and this is in agreement with the results of RT-qPCR.

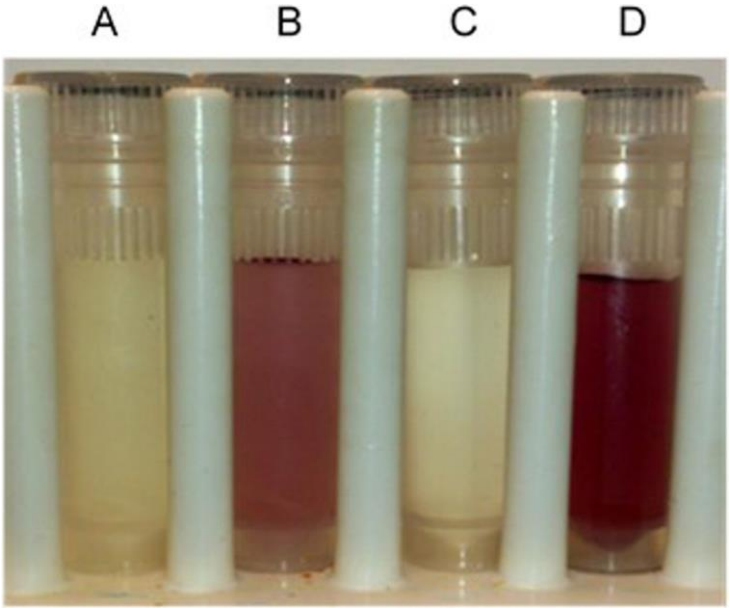


**Figure III.2** sMMO oxidation of naphthalene in *M. trichosporium* OB3b grown in the presence of various amounts of copper, gold, and copper-methanobactin, as follows: 2 μM copper (A); 2 μM copper and 5 μM gold (B); 2 μM copper, 5 μM gold, and 5 μM copper-methanobactin (C); and no added copper, gold, or copper-methanobactin (D).

### *III.2.4. Copper and gold associated with biomass*

As shown in Figure III.3, ICP-MS analyses of the biomass of *M. trichosporium* OB3b indicated that in the presence of gold, the amount of copper associated with biomass significantly decreased, ~ 2.3-fold ($P < 0.03$). When copper was also added as copper-methanobactin, copper per unit biomass increased ~ 40 % compared to that in cultures grown only in the presence of copper, but such an increase was not statistically significant ($P < 0.2$). Approximately 85 times more gold was associated with biomass than copper when both were present in the growth medium (~ 27 times more on a molar basis). In the simultaneous presence of 5 μM copper-methanobactin, the amount of gold per unit biomass was reduced by ~ 60 % (significant at a P value of < 0.03), but approximately 10 times more gold was associated with biomass than copper under these conditions (~ 3 times more on a molar basis).

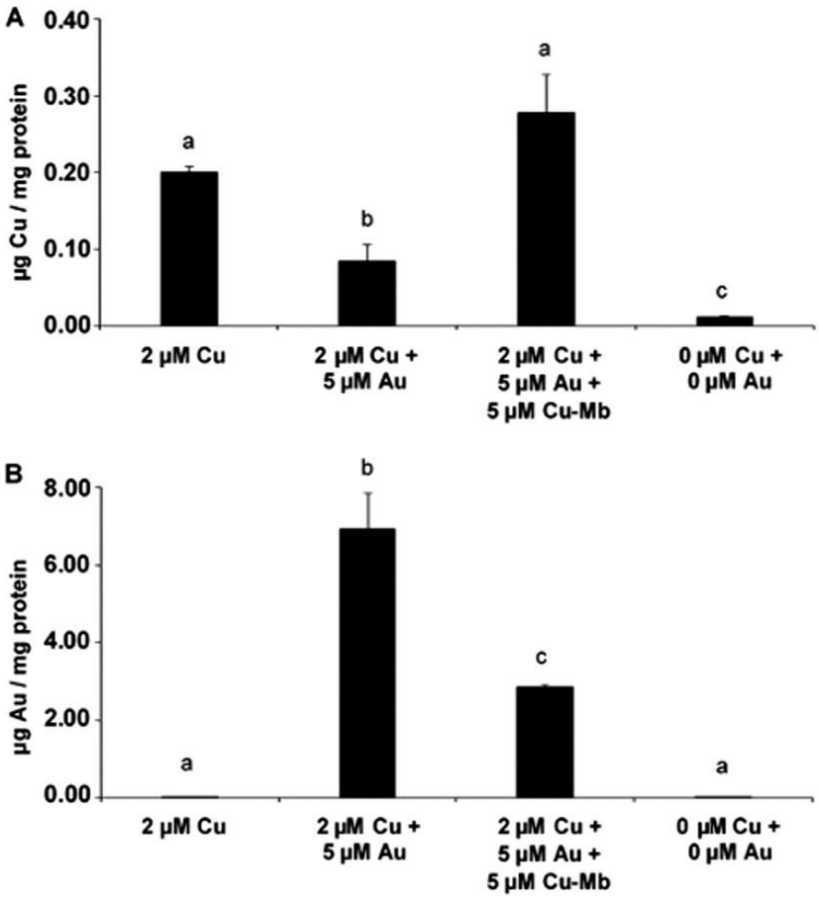


**Figure III.3** Metals associated with the biomass of *M. trichosporium* OB3b grown in the presence of copper (Cu), gold (Au), and copper-methanobactin. (A) Copper. (B) Gold. Columns in each plot labeled by different letters are significantly different ($P < 0.05$). Error bars represent standard deviation (n=3).

### *III.2.5. Metal speciation*

The MINTEQ program was run for two conditions: (i) the presence of 2 µM copper and (ii) the presence of 2 µM copper and 5 µM gold. The results (Table III. 2) show no differences in the distribution of $Cu^{2+}$ between these conditions, indicating that the observed response of *M. trichosporium* OB3b in the presence of gold and copper versus copper alone was not due to the addition of gold causing copper speciation to change.

**Table III.2** Predicted equilibrium speciation of copper in the presence and absence of gold

| | **2 µM Cu** | **2 µM Cu + 5 µM Au** |
|---|---|---|
| Species | % of total component | % of total component |
| $Cu^{+2}$ | 16 | 16 |
| $CuOH^{+}$ | 2.9 | 2.9 |
| $Cu(OH)_2$ (aq) | 0.058 | 0.058 |
| $Cu_2(OH)_2^{+2}$ | 0.074 | 0.074 |
| $CuCl^{+}$ | 0.12 | 0.12 |
| $CuSO_4$ (aq) | 2.3 | 2.3 |
| $CuNO_3^{+}$ | 0.27 | 0.27 |
| $CuHPO_4$ (aq) | 51 | 51 |
| $CuEDTA^{-2}$ | 26 | 26 |

## III.3. Discussion

It is commonly stated that for those methanotrophs that can express both forms of MMO (i.e., the "switchover" strains), sMMO is expressed only when copper concentrations are low. Such a conclusion is based on laboratory experiments that used simple culture conditions to identify the response of methanotrophs to various amounts of copper (Choi et al., 2003; Han and Semrau, 2004). Although these experiments provided insight into the role of copper in methanotrophic physiology, the natural environments are intrinsically much more complex, with the geochemistry of many environments poorly understood. It should also be stressed that there are very few reported examples of sMMO expression in nature (Bao et al., 2014; Liebner and Svenning, 2013; Hazen et al., 2009), raising the question, "Under what conditions do methanotrophs express sMMO *in situ*?"

To answer this question, one must consider not only the geochemistry of various natural environments, i.e., whether copper is present or not, but also the mechanism(s) by which methanotrophs collect copper, i.e., methanobactin. This chalkophore is well known to have a very high affinity for copper ($10^{18}$-$10^{58}$ $M^{-1}$), but it has also been recently found that methanobactin from *M. trichosporium* OB3b can bind other metals (e.g., group A metals such as mercury and gold) and that copper cannot displace these after they are bound to methanobactin (Choi et al., 2006b). Further, at least for mercury, binding to methanobactin is very rapid, and as a result, substantial mercury binding can occur even in the presence of copper (Vorobev et al., 2013). With this in mind, we chose to rephrase the question above to instead ask, "What happens to copper uptake and resulting MMO expression in methanotrophs when other metals are present along with copper?" From the data presented here, it is obvious that group B metals (those that bind to only one of the oxazolone rings of methanobactin from *M. trichosporium* OB3b and are displaced if copper is subsequently added) have no effect on expression of sMMO in *M. trichosporium* OB3b. Although it was not measured, it appears that the presence of these metals had little impact on the ability of *M. trichosporium* OB3b to sequester copper (based on the lack of sMMO expression when these metals were added in excess). However, at least one group A metal, gold, can limit copper uptake by *M. trichosporium* OB3b. It appears that binding of gold by both oxazolone rings of methanobactin of *M. trichosporium* OB3b prevents copper from displacing gold once bound and, as a result, allows for sMMO expression and activity in the presence of copper. Further, substantially more gold than copper was found to be associated with biomass when both were added (Figure III.3).

Such a finding can be explained by considering the mixed metal binding studies that was performed in conjunction to this study. It was found that in the presence of equimolar amounts of copper, gold, and methanobactin, more gold was associated with methanobactin than copper (Kalidass et al., 2014). This is surprising, as the affinity of methanobactin for gold is reported to be many orders of magnitude lower than that measured for copper (Choi et al., 2006). It appears, as was found for mercury (Vorobev et al., 2013), that the kinetics of gold binding are rapid (Kalidass et al., 2014) and possibly irreversible, and this may allow for the binding of gold in the presence of copper.

Thus, it should be stressed that it is inaccurate to predict, based on measurement of copper concentration alone, if sMMO will be expressed. Rather, it is expressed when methanotrophs are limited in their ability to sequester copper, e.g., through competition between metals for binding to methanobactin. This is supported by the finding that if methanobactin was preloaded with copper and added at a concentration of 5 μM, along with 2 μM copper and 5 μM gold, *mmoX* expression decreased significantly compared to expression in the presence of 2 μM copper and 5 μM gold (Figure III.1), and no sMMO activity was apparent (Figure III.2). Further, the amount of copper associated with biomass increased significantly (Figure III.3). It appears that under these conditions, *M. trichosporium* OB3b was able to sequester copper and, by doing so, to prevent sMMO expression and activity. It is interesting, however, that a substantial amount of gold was still associated with the biomass. It appears that the endogenous methanobactin produced by *M. trichosporium* OB3b bound gold under these conditions, but the uptake of gold itself did not allow for sMMO expression. Rather, it appears that the absence of copper-methanobactin complexes when only gold and copper were present enabled sMMO expression in

the presence of copper. It is also interesting that not only did *mmoX* expression increase in the presence of gold, but also expression of the gene encoding the precursor polypeptide of methanobactin, *mbnA*, increased, and such expression was not significantly different from that in cultures grown in the absence of copper and gold (Figure III.1C). It appears that *M. trichosporium* OB3b responded to the inability to collect copper in the presence of gold by increasing the production of methanobactin. Figure III.4 shows a proposed pathway by which copper and gold affect gene expression in *M. trichosporium* OB3b.

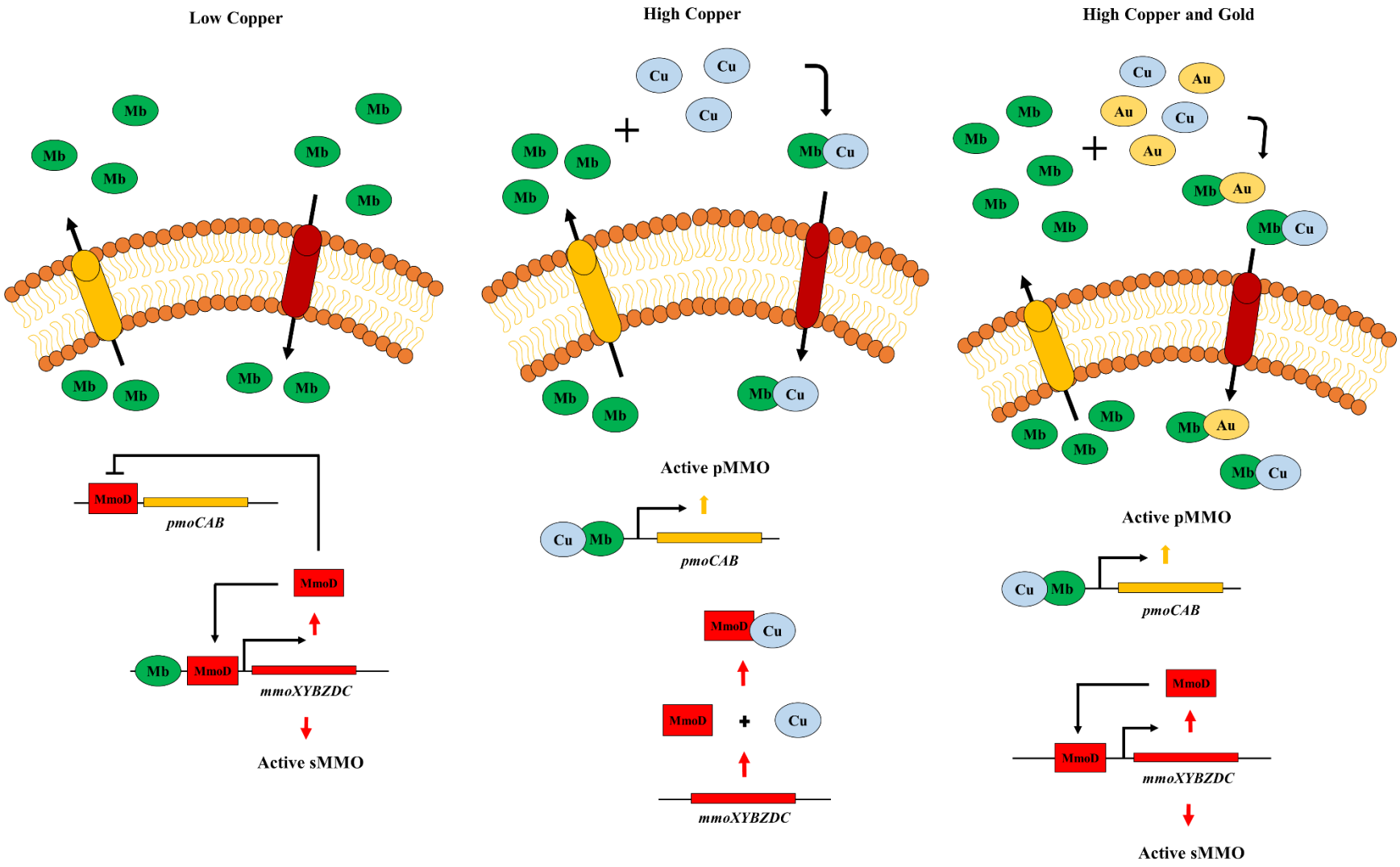


**Figure III.4** Proposed regulatory pathway of *pmo* and *mmo* operons by copper, gold and methanobactin.

The addition of gold, although it clearly affected the expression and activity of sMMO as well expression of *mbnA*, had no discernible effect on the expression of *pmoA* in *M. trichosporium* OB3b. It is clear, then, that genes for both forms of MMO were expressed simultaneously in the presence of copper and gold, and it may be that both MMOs were active when *M. trichosporium* OB3b was grown in the presence of gold and copper. It is interesting that polypeptides of both sMMO and pMMO from the bacterial group of *Methylocystaceae* were found in the same sample of microbial communities as associated with the roots of field-grown rice (Bao et al., 2014). It may be that in many environments, both forms of MMO are simultaneously expressed, either by the same or by different members of the methanotrophic community. The data presented here suggest that such expression may be due in part to the presence of copper and other group A metals.

The finding that the presence of at least one group A metal, gold, can allow for expression and activity of sMMO in the presence of copper also suggests new strategies to manipulate methanotrophic activity in both natural and engineered environments. It may be desirable to have sMMO expressed due to its faster turnover rate, but inducing sMMO expression may be challenging if copper is present. It is difficult, if not practically impossible, to remove copper from a large complex environment. It may be much easier, however, to reduce copper uptake by adding a group A metal such that methanobactin binding of copper is limited. Certainly the use of gold for such a purpose is not feasible given its high cost. It may be that other group A metals, either singly or in combination, that provide an inexpensive means to selectively force methanotrophic communities to express sMMO can be identified. It is recommended that further field work be done integrating molecular and biochemical assays for detection of the expression

and activity of both forms of MMO with more detailed geochemical characterization of metal speciation and concentration. Such work will help determine if there is any correlation between the presence of other metals that can compete with copper for binding to methanobactin and sMMO expression and activity. Finally, it should be kept in mind that it is unclear how widespread this phenomenon may be; i.e., do all switchover methanotrophs express sMMO in the presence of metals that compete for binding to methanobactin, thereby limiting copper uptake? Do all forms of methanobactin exhibit the same ability to bind gold or other group A metals? Given the significant functional similarity between the known forms of methanobactin (El Ghazouani et al., 2012; Krentz et al., 2010; Behling et al., 2008), it is plausible to presume that they would all bind gold to some degree, but the resultant impact on MMO expression is less clear. For example, some non-switchover methanotrophs, i.e., those that can express only pMMO, are known to produce methanobactin (El Ghazouani et al., 2012; Krentz et al., 2010). If these strains are challenged with gold, it may be that their growth and activity may be inhibited, as they cannot express sMMO and are unable to take up sufficient copper to allow for optimal pMMO activity. Therefore, the presence of competing metals may serve to stimulate the survival of switchover methanotrophs *in situ.*

# CHAPTER IV: REGULATION OF ALTERNATIVE METHANOL DEHYDROGENASES IN *METHYLOSINUS TRICHOSPORIUM* OB3B

Previously published: Cerium regulates expression of alternative methanol dehydrogenases in *Methylosinus trichosporium* OB3b. *Applied and Environmental Microbiology*, **81**(21): 7546–7552. doi:10.1128/AEM.02542-15.

## IV.1. Introduction

Copper is required for the expression and activity of pMMO. Extensive studies have been performed on understanding how copper regulates the two forms of methane monooxygenase, i.e., the "copper-switch" (Semrau et al., 2013; Stafford et al., 2003; Nielsen et al., 1997; Stanley et al., 1983). Little is known how metals might regulate the expression of other genes, particularly those encoding for subsequent steps in the central pathway of methane monooxygenase. For example, methanol dehydrogenase, the enzyme catalyzing the conversion of methanol to formaldehyde, has been known widely as the pyrroloquinoline quinone (PQQ)-dependent heterotetrameric protein ($\alpha_2\beta_2$) composed of two large (α, MxaF) and two small (β, MxaI) subunits containing a calcium in its active site. It was initially believed that this enzyme was critical for methylotrophic growth on methanol since no methanol dehydrogenase activity

was observed in mutants defective in the production of this protein (Nunn et al., 1986). Subsequently, however, much later after the discovery of XoxF, a homolog of MxaF, thought to encode for the larger subunit of an alternative PQQ-linked dehydrogenase (Chistoserdova and Lidstrom, 1997), Schmidt et al., (2010) purified and functionally characterized Xox-MDH from *M. extorquens* AM1. It was found that XoxF, with 50 % sequence identity to MxaF (Wu et al., 2015; Skovran et al., 2011), also encodes a PQQ-dependent methanol dehydrogenase that is associated with the periplasm (Wu et al., 2015; Harms et al., 1996) but appears to be composed only of a single subunit with a predicted mass of 65 kDa (Schmidt et al., 2010) or associated with the small subunit of MxaI (Wu et al., 2015), depending on the microbe. Further, it is often observed that multiple homologs of XoxF are found in the genome of a variety of methylotrophs and methanotrophs (Wu et al., 2015; Lapidus et al., 2011; Skovran et al., 2011).

Xox-MDH, however, appears to have a rare earth element in its active site. Studies in *Methylobacterium radiotolerans* and *Methylobacterium extorquens* AM1 showed that cerium and lanthanum both increased methanol oxidation by Xox-MDH (Nakagawa et al., 2012; Hibi et al., 2011). Such increase was not due to increased expression of *xoxF* but was more likely due to posttranslational activation (Nakagawa et al., 2012). Further, simple yet elegant studies showed that growth and overall MDH activity of a *M. extorquens* AM1 mutant in which *mxaF* was disrupted was severely limited in the absence of lanthanum but growth recovered in its presence, regardless of whether calcium was simultaneously present or not (Nakagawa et al., 2012). Such results indicate that lanthanum was required for the activity of Xox-MDH. Subsequent studies supported these findings, i.e., it was found that growth of *Methylacidiphilum fumariolicum* SolV was enhanced in the presence of multiple rare earth elements (e.g., cerium, lanthanum,

praseodymium, and neodymium [Pol et al., 2014]). Purification of the active MDH from *M. fumariolicum* SolV and subsequent crystallization of this MDH revealed it to be encoded by *xoxF* and that rare earth metals were in the crystal structure (Pol et al., 2014).

Given these findings, it was speculated that under selective growth conditions, differential expression of not only genes encoding polypeptides of sMMO and pMMO would vary but also genes encoding the two alternative forms of MDH. Here, we report on the effect of various amounts of copper and cerium on gene expression and the growth of *Methylosinus trichosporium* OB3b.

## IV.2. Results

### *IV.2.1. Metal speciation*

Two conditions were analyzed by MINTEQ program: (i) the presence of 10 µM copper, (ii) the presence of 10 µM copper and 25 µM cerium (Table IV.1). While the $Cu^{+1}$ ion concentration reduce by ~ 10 % in the presence of cerium and copper as compared to the condition with only copper, the other copper species showed no difference regardless of the presence or absence of cerium.

**Table IV.1** Predicted equilibrium speciation of copper and cerium in the presence and absence of cerium

| | **10 µM Cu** | **10 µM Cu + 25 µM Ce** |
|---|---|---|
| Species | % of total component | % of total component |
| $Cu^{+1}$ | 3.9 | 3.5 |
| $CuCl_2^{-1}$ | 66 | 68 |
| $CuCl_3^{-2}$ | 0.23 | 0.25 |
| CuCl (aq) | 29 | 28 |
| $Ce^{+3}$ | | 1.3 |
| $CeOH^{+2}$ | | 0.01 |
| $CeCl^{+2}$ | | 0.01 |
| $Ce(SO_4)_2^{-1}$ | | 0.07 |
| $CeSO_4^{+1}$ | | 1.2 |
| $CeNO_3^{+2}$ | | 0.03 |
| $CeH_2PO_4^{+2}$ | | 0.11 |
| $CePO_4$ (aq) | | 97 |
| Total | 100 | 100 |

### *IV.2.2. Growth as a function of copper*

In the presence of various amounts of copper and cerium, little difference of the growth of *M. trichosporium* OB3b was observed (Figure IV.1).

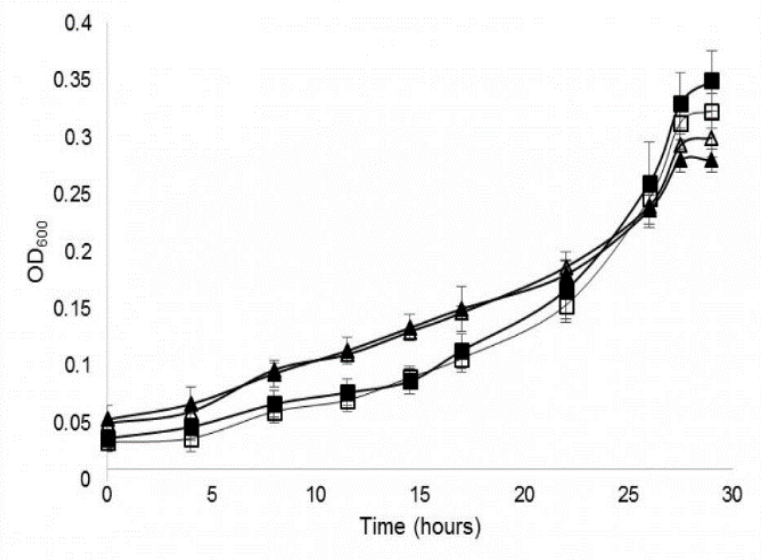


**Figure IV.1** Growth of *M. trichosporium* OB3b on methane with 0 µM Cu and 10 µM Cu.△, 0 µM Cu plus 0 µM Ce; ▲, 0 µM Cu plus 25 µM Ce; □, 10 µM Cu plus 0 µM Ce; ■, 10 µM Cu plus 25 µM Ce. All data are means of triplicates. Error bars represent standard deviations (n=3). When error bars are not visible, they are smaller than the size of the symbols.

### *IV.2.3. Copper and cerium associated with biomass*

Copper associated with biomass significantly increased (approximately three orders of magnitude; $P < 6 \times 10^{-3}$) with the addition of copper (Figure IV.2A). Interestingly, as cerium was added, the amount of cerium associated with biomass also increased significantly (by 3 to 4 orders of magnitude; $P < 1.1 \times 10^{-4}$; Figure IV.2B), and in fact, most of the added cerium (> 98 %) was cell associated. The mass balance performed for copper and cerium distributed in different fractions of the liquid culture is shown in Table IV. 2.

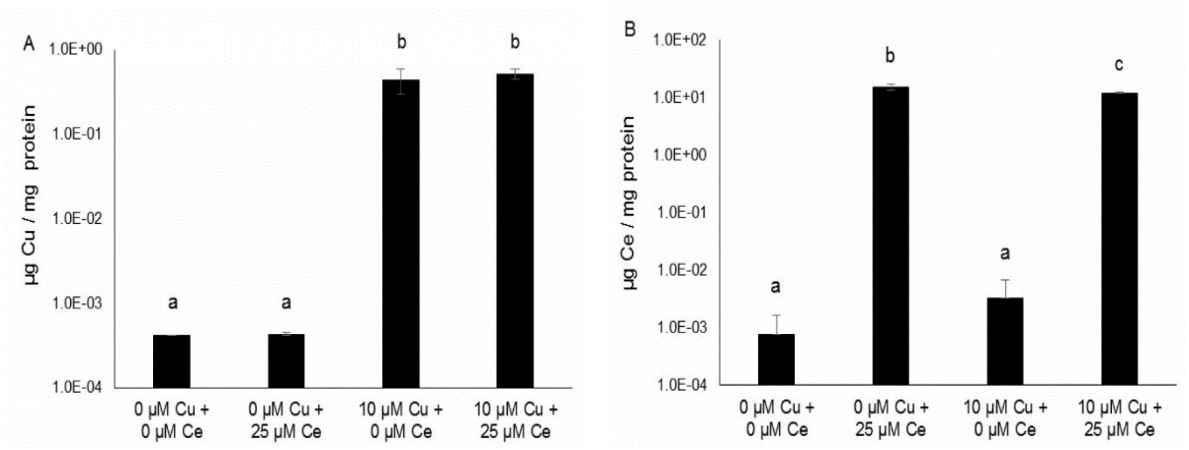


**Figure IV.2** Metals associated with the biomass of *M. trichosporium* OB3b grown in the presence of copper (Cu) and cerium (Ce). (A) Copper. (B) Cerium. Columns in each plot labeled by different letters are significantly different ($P < 0.05$). Error bars represent standard deviation (n=3).

**Table IV.2** Mass balance for copper and cerium in different fractions of the liquid culture of *M. trichosporium* OB3b grown under varying conditions of copper and cerium.

| **Copper mass balance** | | | | | | | |
|---|---|---|---|---|---|---|---|
| Cu-Ce | Supernatant (S) | Biomass (B) | Total (S+B) | Total added | error % | Concentration | |
| (μM-μM) | (μg) | (μg) | (μg) | (μg) | | S (μg /ml) | B (μg/mg protein) |
| 0-0 | 5.9E-4 | 0.6 | 0.6 | 0 | 0 | 5.9E-5 | 0.2 |
| 0-0 | 2.4E-3 | 1.0E-3 | 2.4E-3 | 0 | 0 | 2.4E-4 | 4.1E-4 |
| 0-0 | 2.3E-2 | 1.0E-3 | 2.3E-2 | 0 | 0 | 2.3E-3 | 4.1E-4 |
| 0-25 | 1.8E-2 | 1.0E-3 | 1.8E-2 | 0 | 0 | 1.8E-3 | 4.3E-4 |
| 0-25 | 6.2E-3 | 1.0E-3 | 6.2E-3 | 0 | 0 | 6.2E-4 | 4.4E-4 |
| 0-25 | 9.1E-3 | 1.0E-3 | 9.1E-3 | 0 | 0 | 9.1E-4 | 4.1E-4 |
| 10-0 | 5.2 | 1.1 | 6.4 | 6.4 | 0.6 | 0.5 | 0.4 |
| 10-0 | 5.0 | 1.7 | 6.7 | 6.4 | 5.2 | 0.5 | 0.6 |
| 10-0 | 5.4 | 8.0E-1 | 6.2 | 6.4 | 2.1 | 0.5 | 0.3 |
| 10-25 | 4.7 | 1.6 | 6.3 | 6.4 | 1.1 | 0.5 | 0.5 |
| 10-25 | 4.8 | 1.3 | 6.1 | 6.4 | 4.1 | 0.5 | 0.4 |
| 10-25 | 4.9 | 1.6 | 6.5 | 6.4 | 2.3 | 0.5 | 0.6 |
| **Cerium mass balance** | | | | | | | |
| Cu-Ce | Supernatant (S) | Biomass (B) | Total (S+B) | Total added | error% | Concentration | |
| (μM-μM) | μg | μg | μg | (μg) | | S (μg g/ml) | B(μg/mg protein) |
| 0-0 | 8.04E-3 | 5.7E-4 | 5.7E-4 | 0 | 0 | 8.0E-4 | 2.1E-4 |
| 0-0 | 0 | 4.3E-3 | 4.3E-3 | 0 | 0 | 0 | 1.8E-3 |
| 0-0 | 0 | 7.2E-4 | 7.2E-4 | 0 | 0 | 0 | 3.0E-4 |
| 0-25 | 0.2 | 31 | 31 | 35 | 10 | 2.4E-2 | 13 |
| 0-25 | 0.2 | 37 | 38 | 35 | 7.4 | 1.6E-4 | 17 |
| 0-25 | 0.5 | 37 | 37 | 35 | 6.8 | 4.6E-2 | 15 |
| 10-0 | 0 | 1.9E-3 | 1.9E-3 | 0 | 0 | 0 | 7.1E-4 |
| 10-0 | 0 | 5.5E-3 | 5.5E-3 | 0 | 0 | 0 | 2.0E-3 |
| 10-0 | 0 | 1.9E-2 | 1.9E-2 | 0 | 0 | 0 | 7.3E-3 |
| 10-25 | 0.2 | 35 | 36 | 35 | 1.6 | 1.7E-2 | 11 |
| 10-25 | 0.9 | 36 | 37 | 35 | 4.4 | 9.0E-2 | 12 |
| 10-25 | 0.1 | 31 | 32 | 35 | 9.8 | 1.0E-2 | 12 |

Further, the spectral changes in methanobactin were minor following cerium addition and suggested that the association is only to the enethiol groups and not to the oxazolone rings of methanobactin (Figure IV.3). The binding of cerium by methanobactin, $K_{Ce} = 4.35 \times 10^3\ M^{-1}$ was orders of magnitude lower than that found earlier for copper, $K_{Cu} = 10^{18}$ to $10^{58}\ M^{-1}$ (Pesch et al., 2012; El Ghazouani et al., 2011; Choi et al., 2006a) and copper displaced cerium associated with methanobactin (Farhan Ul Haque et al., 2015).

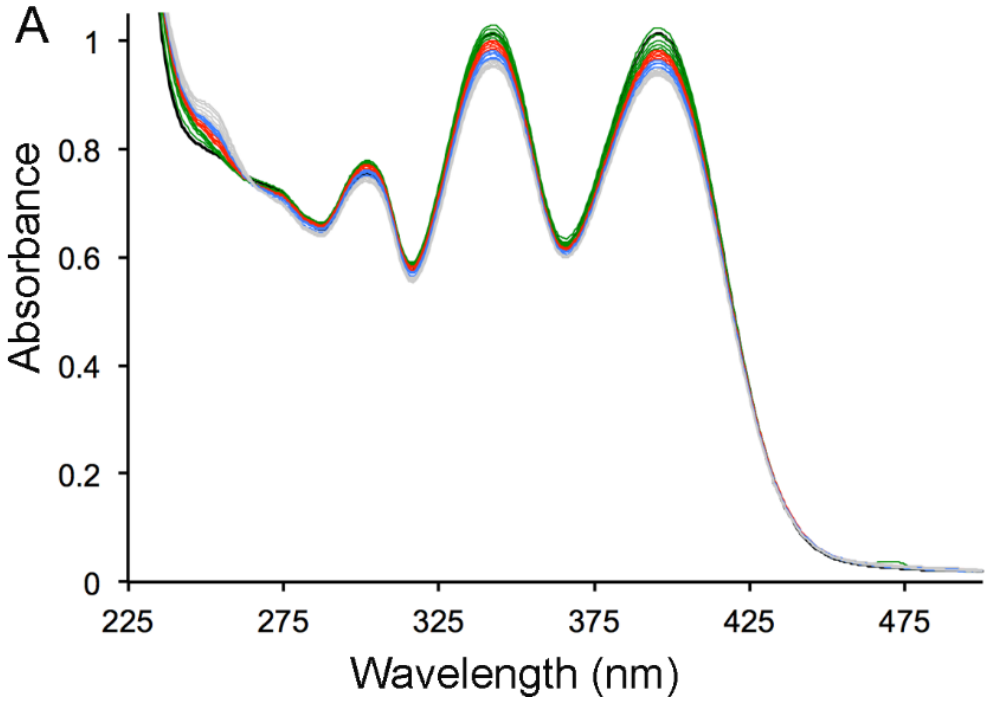


**Figure IV.3** UV-visible absorption spectra of methanobactin on addition of 0.1 M cerium. Black traces, methanobactin as isolated; green traces, $CeCl_3$ additions between 0.1 and 0.5; red traces, $CeCl_3$ additions between 0.6 and 1; blue traces, $CeCl_3$ additions between 1.1 and 1.5; and gray traces, $CeCl_3$ additions between 1.6 and 2.0.

### *IV.2.4. Gene expression in M. trichosporium OB3b in the presence of copper and cerium*

Quantitative PCR (qPCR) of cDNA was then performed to determine whether various amounts of copper and cerium affected expression of the various forms of both methane monooxygenase and methanol dehydrogenase. As found previously (Farhan Ul Haque et al., 2015; Kalidass et al., 2014; Semrau et al., 2013), the addition of copper reduced *mmoX* expression by 4 orders of magnitude (Figure IV.4A), while *pmoA* expression increased 54-fold (Figure IV.4B), with both changes significant ($P = 0.03$ and $7.6 \times 10^{-3}$, respectively). The addition of cerium, however, did not significantly affect either *mmoX* or *pmoA* expression in either the presence or absence of copper.

The expression of *mxaF* and *mxaI*, however, did respond to the addition of copper or cerium (Figure IV.4C and IV.4D). When 25 μM cerium was added in the absence of copper, both *mxaF* and *mxaI* expression decreased > 50-fold compared to no added cerium and copper ($P = 6.3 \times 10^{-3}$ and $1.9 \times 10^{-3}$, respectively). In the presence of 10 μM copper, the simultaneous addition of 25 μM cerium caused *mxaF* and *mxaI* expression to be reduced by > 2.5- fold each compared to when no cerium was added in the presence of copper ($P = 7.6 \times 10^{-3}$ and $8.4 \times 10^{-3}$, respectively). Further, *mxaF* expression increased 2-fold in the presence of 10 μM copper compared to no added copper ($P = 0.038$), whereas *mxaI* expression also increased 2.4-fold ($P = 0.05$). The expression of *mxaF* and *mxaI* in the presence of both copper and cerium, however, was similar to that found in the absence of both metals ($P = 0.4$ and 0.5, respectively).

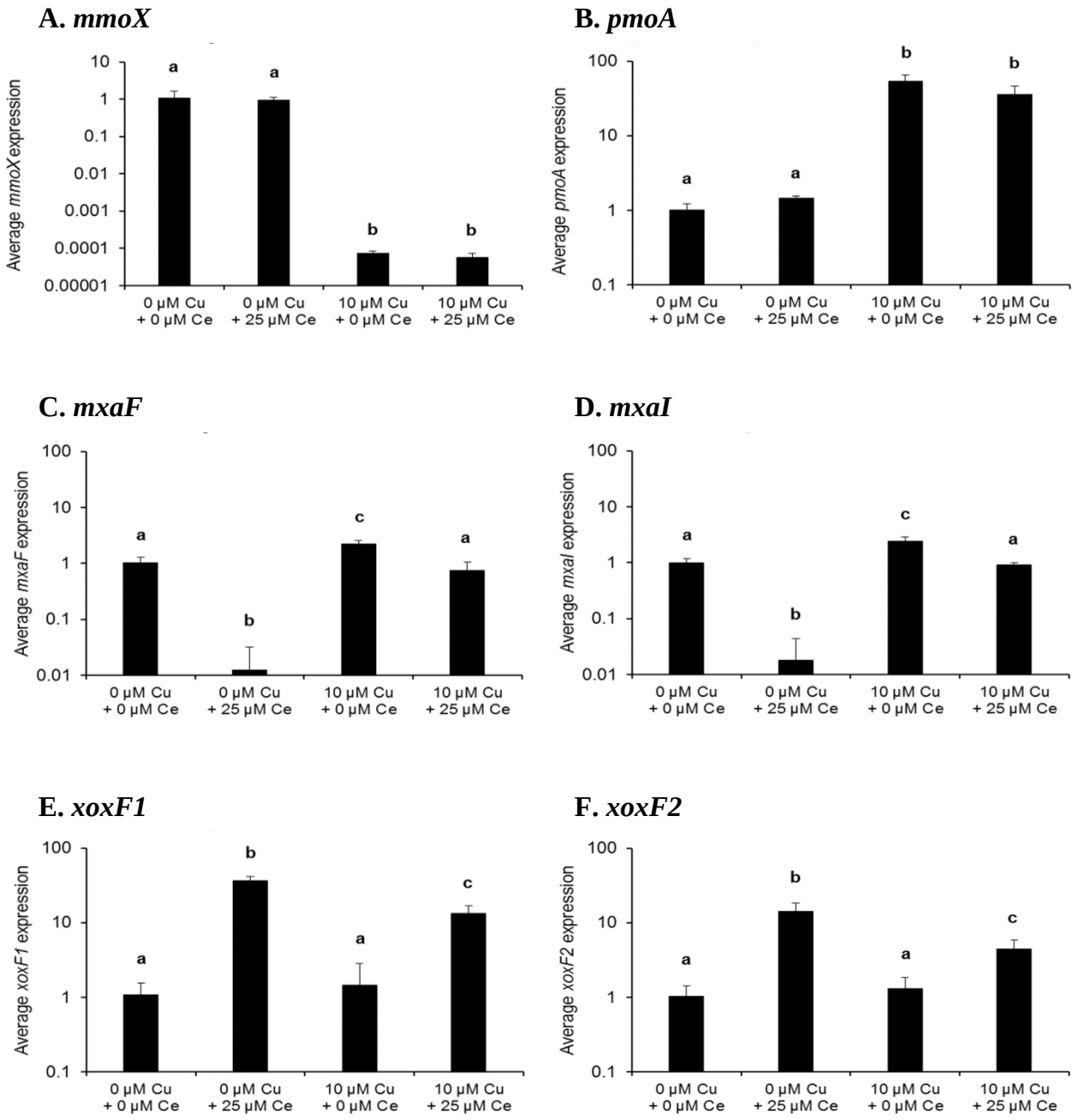


**Figure IV.4** RT-qPCR of *mmoX* (A), *pmoA* (B), *mxaF* (C), *mxaI* (D), *xoxF1* (E), and *xoxF2* (F) genes in *M. trichosporium* OB3b grown in the presence of varying amounts of copper and cerium. Errors bars represent the standard deviation of triplicate samples. Columns in each plot labeled by different letters are significantly different ($P < 0.05$).

The expression of both *xoxF1* and *xoxF2* (Figure IV.4E and IV.4F) increased more than an order of magnitude when cerium was added compared to when both metals were absent ($P = 3.3 \times 10^{-4}$ and $4.7 \times 10^{-3}$, respectively). In the presence of 10 μM copper, the expression of both *xoxF1* and *xoxF2* was not significantly different from that observed in the absence of both metals (P = 0.7 and 0.6, respectively). With the simultaneous addition of 25 μM cerium, however, *xoxF1* and *xoxF2* expression increased by approximately 9- and 3.5-fold, respectively, and again such increases were significant ($P = 7.0 \times 10^{-3}$ and 0.02, respectively).

Given the response of *mxaF*, *xoxF1*, and *xoxF2* expression to the presence of cerium in the absence of copper, it appears that under some conditions, i.e., sMMO-expressing conditions, that Xox-methanol dehydrogenase could replace the Mxa-methanol dehydrogenase.

This was examined more closely for protein expressions through SDS-polyacrylamide gel electrophoresis. Given the similar sizes of XoxF1/F2 and MxaF (65 and 66 kDa, respectively [Schmidt et al., 2010; Kalyuzhnaya et al., 2008; Williams et al., 2005]), the presence of the small subunit of Mxa-methanol dehydrogenase, MxaI (8.5 kDa [Williams et al., 2005]), was tracked. A band at 8.5 kDa was observed in the cell extract of *M. trichosporium* OB3b in the absence of copper and cerium, and also in the presence of copper regardless of the presence or absence of cerium (Figure IV.5; lanes 1, 3, 4). The band was absent when 25 μM cerium was added in the absence of copper (Figure IV.5; lane 2). All identified amino acids (10 of the first 11, with one unidentified residue) from the N-terminal sequence aligned with the predicted amino acid sequence of MxaI from *M. trichosporium* OB3b (Figure IV.6).

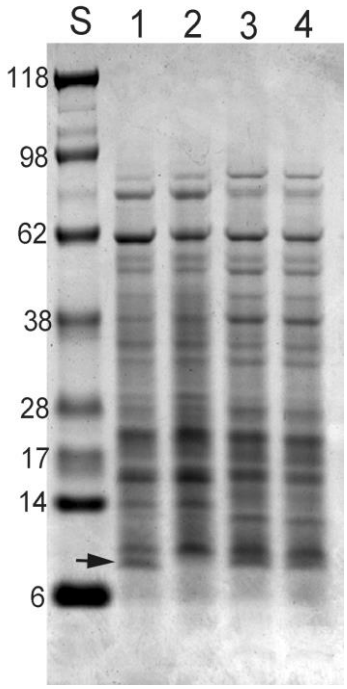


**Figure IV.5** SDS-polyacrylamide gel electrophoresis of cell-free extracts of *M. trichosporium* OB3b grown with varying amounts of copper and cerium. S: molecular weight standards, 1: *M. trichosporium* OB3b grown with 0 µM copper plus 0 µM cerium; 2: *M. trichosporium* OB3b grown with 0 µM copper plus 25 µM cerium; 3: *M. trichosporium* OB3b grown with 10 µM copper plus 0 µM cerium; 4: *M. trichosporium* OB3b grown with 10 µM copper plus 25 µM cerium.

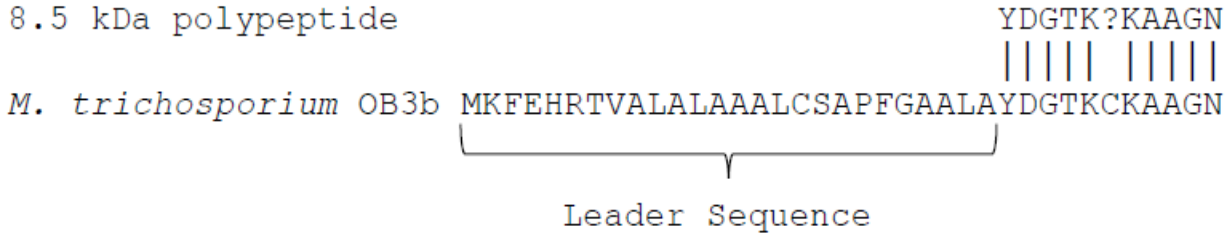


**Figure IV.6** Alignment of N-terminal sequence of the variably expressed 8.5 kDa polypeptide vs. the predicted amino acid sequence of MxaI from *M. trichosporium* OB3b. Lines indicate identical residues and question mark indicates unidentified amino acid.

## IV.3. Discussion

We show here that multiple metals affect gene expression in *M. trichosporium* OB3b. That is, in addition to the canonical "copper-switch" that is well known to control expression of the two forms of MMO (Semrau et al., 2010), cerium also appears to regulate expression of multiple methanol dehydrogenases found in this methanotroph. Specifically, the expression of *mxaF* and *mxaI* decreased significantly in the presence of cerium but with no added copper compared to the absence of both metals, whereas *xoxF1* and *xoxF2* increased. These findings suggest that Xox-MDH could replace Mxa-MDH when *M. trichosporium* OB3b was expressing sMMO. Cerium, however, had little effect on *mxaF* or *mxaI* expression under pMMO-expressing conditions, i.e., when 10 μM copper was present. Such findings support earlier conclusions that the pMMO forms a supercomplex with the Mxa-MDH (Culpepper and Rosenzweig, 2014; Myronova et al., 2006) and that this complex is critical for the oxidation of methane in methanotrophs under pMMO-expressing conditions, i.e., in the presence of copper. Figure IV.7 and IV.8 depicts a proposed regulatory scheme by which copper and cerium control expression of *mxa* and *xox* operons. It should be stressed, however, that this is highly speculative. Our findings suggest, however, that Mxa-MDH is not essential in sMMO-expressing conditions; rather, Xox-MDH is sufficient for the further oxidation of methanol. Further, SDS-PAGE data and subsequent N-terminal sequencing show that in the absence of copper but the presence of cerium, the MxaI polypeptide was not evident, suggesting that, as found for methylotrophs, Xox-MDH is active in *M. trichosporium* OB3b and requires only XoxF and not MxaI (Schmidt et al., 2010).

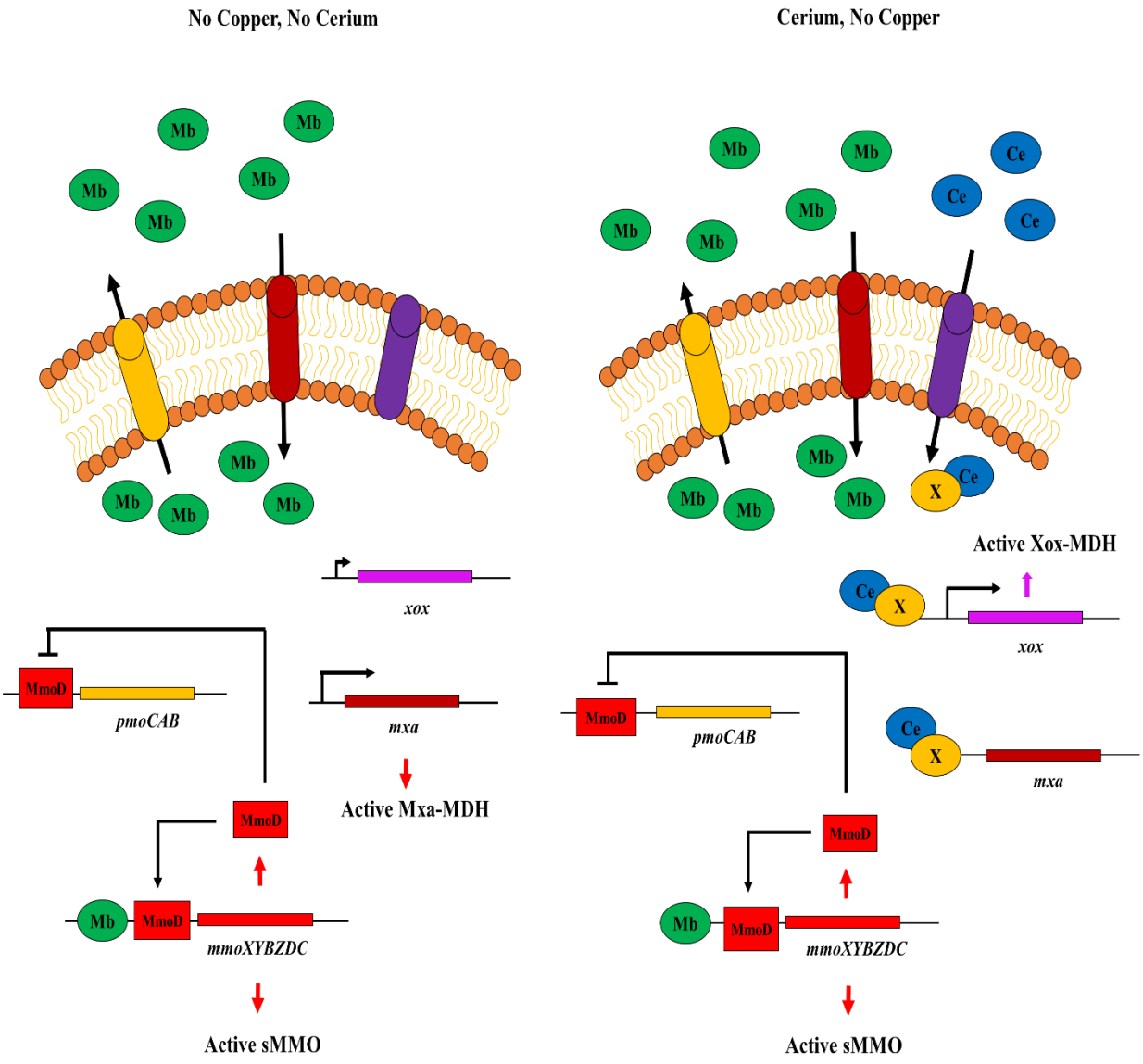


**Figure IV.7** Regulation of *mxa* and *xox* operons by copper and cerium in the absence of copper. X is an unknown protein proposed to bind cerium and impact gene expression.

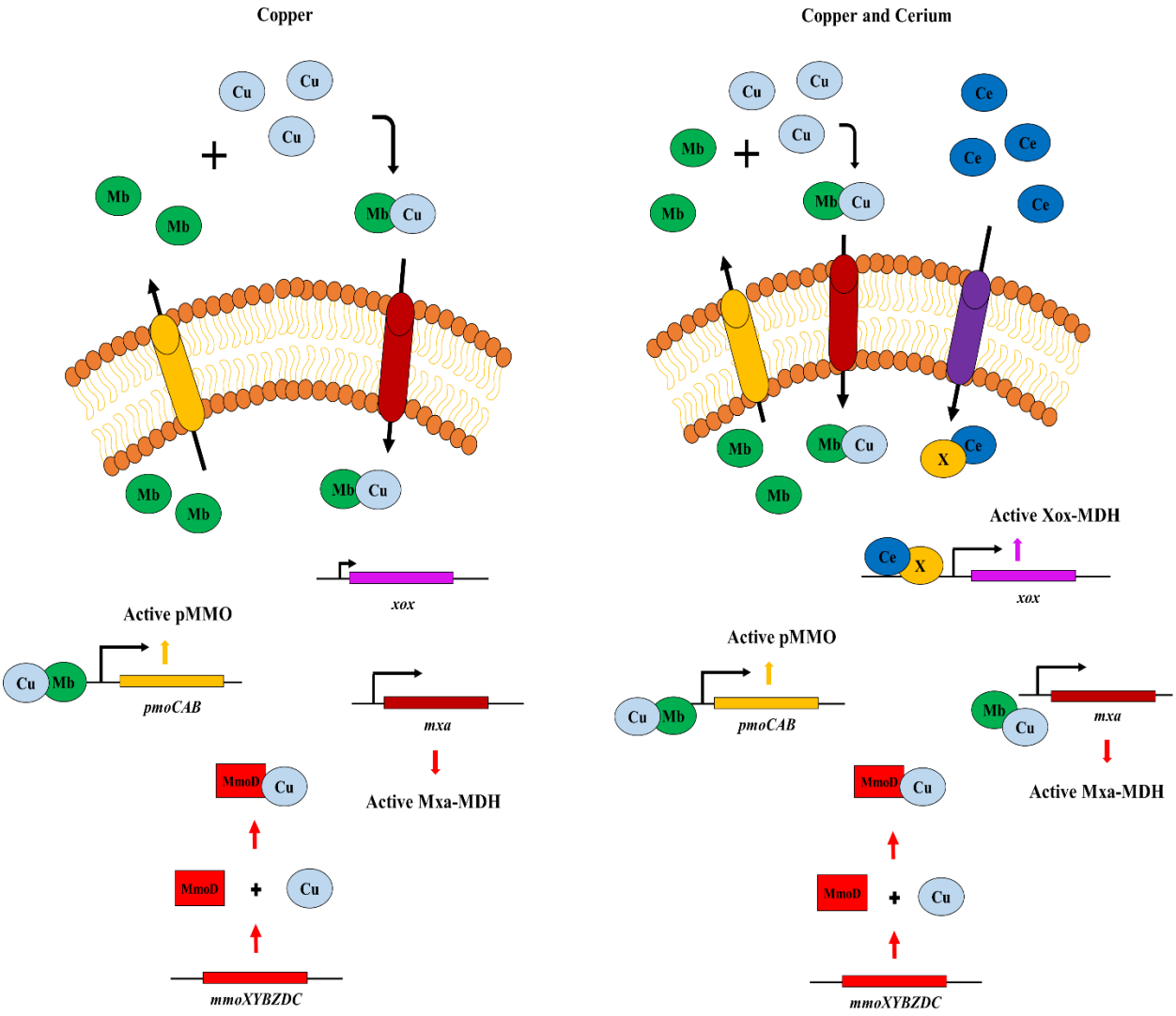


**Figure IV.8** Regulation of *mxa* and *xox* operons by copper and cerium in the presence of copper. X is an unknown protein proposed to bind cerium and impact gene expression.

The finding that multiple metals affect gene expression in *M. trichosporium* OB3b is intriguing. It suggests that this microbe has multiple mechanisms to sense and collect both copper and cerium and that these mechanisms may play a role in controlling the relative expression of Mxa- and Xox-methanol dehydrogenases. It has been shown that copper uptake in *M. trichosporium* OB3b is regulated by the chalkophore, methanobactin, and a regulatory model has been proposed whereby methanobactin serves to enhance the magnitude of the "copper-switch" but is not the

basis of the switch (Semrau et al., 2013). By analogy, there appears to be a separate mechanism by which cerium is sensed by *M. trichosporium* OB3b, but it should be stressed that this mechanism is still unknown. It does not appear that methanobactin is the mechanism for cerium uptake since it was only loosely bound to methanobactin and copper displaced cerium from methanobactin, and yet most of the added cerium was found to be cell associated. This is intriguing, for although cerium is considered a rare earth element, as noted elsewhere (Pol et al., 2014), such metals are not actually "rare" since they are a significant fraction of the earth's crust. Rather, they are considered "rare" given that most species of these elements are sparingly soluble. From the data presented here, it is tempting to speculate that systems for the uptake of rare earth elements exist and that the availability of and competition for these metals may have a significant effect on overall methanotrophic community composition and activity. Finally, it may be that rare earth elements affect methanotrophic community composition as well as specific gene expression and that simple strategies whereby the presence of rare earth elements is controlled can enhance the utility of methanotrophs for a variety of environmental and industrial applications.

# CHAPTER V: ROLE OF METHANOBACTIN IN REGULATING GENE EXPRESSION

Previously published: Methanobactin from *Methylocystis* sp. Strain SB2 affects gene expression and methane monooxygenase activity in *Methylosinus trichosporium* OB3b. *Applied and Environmental Microbiology*, **81**(7): 2466–2473. http://dx.doi.org/10.1128/AEM.03981-14.

## V.1. Introduction

The unique properties of methanobactin has expanded the use of methanotrophy in applications ranging from copper extraction processes (Kulczycki et al., 2007, treatment for Wilson's disease (Summer et al., 2011) to production of gold nanoparticles (Choi et al., 2006b) and reducing mercury toxicity (Vorobev et al., 2013). However, its role in gene regulation in methanotrophic community is not well understood. Recent studies have shown that methanobactin influences expression of the two forms of MMO; i.e., it forms part of the "copper switch." Specifically, if purified methanobactin from *M. trichosporium* OB3b is added to cultures of *M. trichosporium* OB3b, increased expression of *mmoX*, encoding the α-subunit of the hydroxylase component of sMMO, is observed (Semrau et al., 2013; Vorobev et al., 2013). Further, the earlier findings by Farhan Ul Haque et al., (2015) and Kalidass et al., (2014) suggest that metals other than copper

can affect gene expression in methanotrophs. While gold and cerium regulate gene expression in *M. trichosporium* OB3b, it was suspected that methanobactin, which facilitates bioavailability of gold and copper, could also have a significant role in gene regulation.

Thus, it was hypothesized that as methanobactin is secreted into the surrounding growth environment and as the known forms of methanobactin have significant structural similarity, methanobactin from one methanotroph may alter gene expression in another. To that end, the effect of the addition of methanobactin from *Methylocystis* sp. strain SB2 (SB2-Mb) to *M. trichosporium* OB3b on the expression of genes encoding for pMMO, sMMO and methanobactin was investigated. That is, we wished to determine whether methanobactins act as signaling molecules in methanotrophs to regulate gene expression.

## V.2. Results

### *V.2.1. Growth and gene expression in M. trichosporium OB3b incubated with various concentrations of copper, methanobactin, and copper-methanobactin from Methylocystis sp. strain SB2 (SB2-Mb)*

In the absence of $CuCl_2$, no significant trend in *mmoX* expression (encoding the α-subunit of the hydroxylase component of sMMO) was observed when various amounts of SB2-Mb were added (Figure V.1A) (ANOVA, $P = 0.36$). If 1 μM $CuCl_2$ was provided, *mmoX* expression significantly decreased by more than 4 orders of magnitude compared to values when no $CuCl_2$ was added (Student's t-test, $P = 2.3 \times 10^{-5}$). Expression of *mmoX*, however, increased by more than 3 orders of magnitude with increasing amounts of SB2-Mb (ANOVA, $P = 2 \times 10^{-6}$). A different response was observed when SB2-Mb preincubated with copper (Cu-SB2-Mb) was added to cultures of

*M. trichosporium* OB3b. In the absence of $CuCl_2$, when Cu-SB2-Mb was added, *mmoX* expression dropped by approximately 4 orders of magnitude compared to when no Cu-SB2-Mb was added (Figure V.1B) (ANOVA, $P = 7 \times 10^{-7}$). Expression of *mmoX* in the presence of 1 μM $CuCl_2$ was consistently low and did not change significantly with the addition of Cu-SB2-Mb (ANOVA, P = 0.33).

The addition of SB2-Mb had some effect on *pmoA* expression (encoding the 26-kDa subunit of pMMO) in the absence of $CuCl_2$, with overall expression increasing ~ 60 % as SB2-Mb was increased (Figure V.2A; ANOVA, P = 0.019). Further, expression of *pmoA* was ~ 2.7-fold greater in the presence of $CuCl_2$ than in its absence (Student's t-test, $P = 5.6 \times 10^{-6}$), but *pmoA* expression did not change significantly in the presence of $CuCl_2$ with the simultaneous addition of SB2-Mb (ANOVA, P = 0.08). *pmoA* expression was less dependent on the presence of Cu-SB2-Mb. A ~ 1.5- to 2-fold increase in *pmoA* expression was found in the absence of any $CuCl_2$ when Cu-SB2-Mb was also added, but such a change was not significant (Figure V.2B) (ANOVA, P = 0.29). In the presence of 1 μM $CuCl_2$, *pmoA* expression decreased by ~ 3-fold when Cu-SB2-Mb was increased to 50 μM (ANOVA, $P = 2 \times 10^{-3}$).

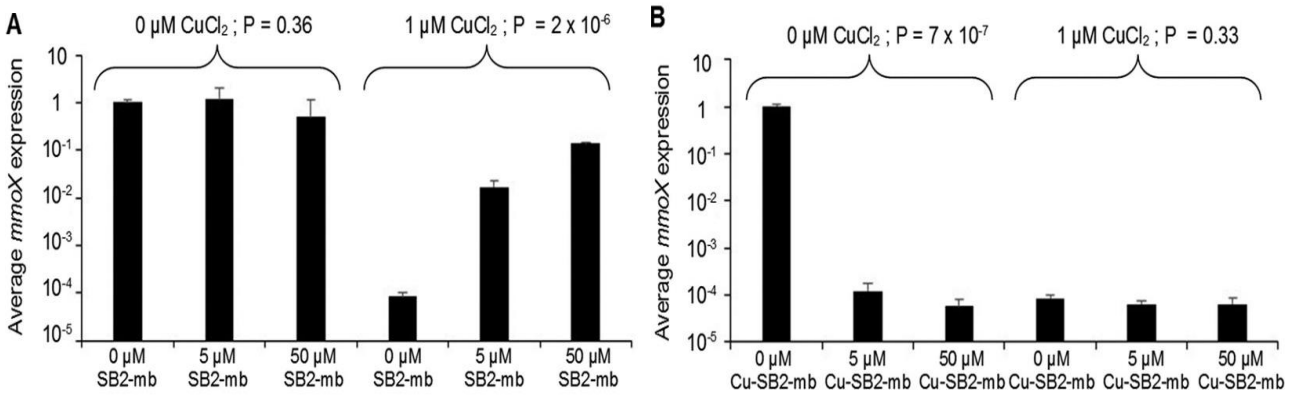


**Figure V.1** RT-qPCR of *mmoX* in *M. trichosporium* OB3b grown in either the absence or presence of 1 μM $CuCl_2$ and various amounts of methanobactin from *Methylocystis* sp. strain SB2 (A) or copper-SB2 methanobactin complexes (B). Indicated P values are from ANOVA. Error bars represent standard deviation (n=3).

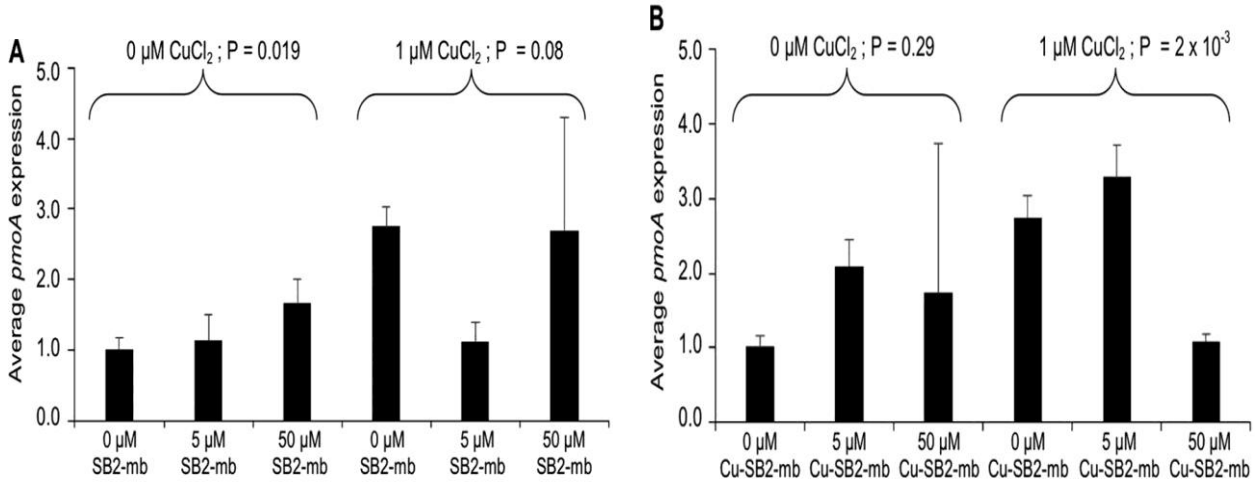


**Figure V.2** RT-qPCR of *pmoA* in *M. trichosporium* OB3b grown in either the absence or presence of 1 μM $CuCl_2$ and various amounts of methanobactin from *Methylocystis* sp. strain SB2 (A) or copper-SB2 methanobactin complexes (B). Indicated P values are from ANOVA. Error bars represent standard deviation (n=3).

Finally, expression of *mbnA* (encoding the polypeptide precursor of methanobactin) in *M. trichosporium* OB3b was not found to vary significantly in the absence of $CuCl_2$ in response to the addition of SB2-Mb (Figure V.3A) (ANOVA, P = 0.22). Further, the addition of 1 μM $CuCl_2$ reduced *mbnA* expression ~ 5-fold compared to the level in the absence of $CuCl_2$ (Student's t-

test, $P = 2 \times 10^{-3}$). No significant change in *mbnA* expression was observed in response to various amounts of SB2-Mb when it was added in conjunction with 1 μM $CuCl_2$ (ANOVA, P = 0.60). Expression of *mbnA* was affected by the addition of Cu-SB2-Mb in both the presence and absence of $CuCl_2$ (Figure V.3B). In the absence of $CuCl_2$, *mbnA* expression decreased by ~ 20- or 700-fold when either 5 or 50 μM Cu-SB2-Mb was added, respectively (ANOVA, $P = 7.9 \times 10^{-5}$). In the presence of 1 μM $CuCl_2$, *mbnA* expression decreased only when 50 μM Cu-SB2-Mb was added (by ~ 100-fold), and overall the addition of Cu-SB2-Mb in the presence of 1 μM $CuCl_2$ had a significant effect (ANOVA, $P = 5 \times 10^{-3}$).

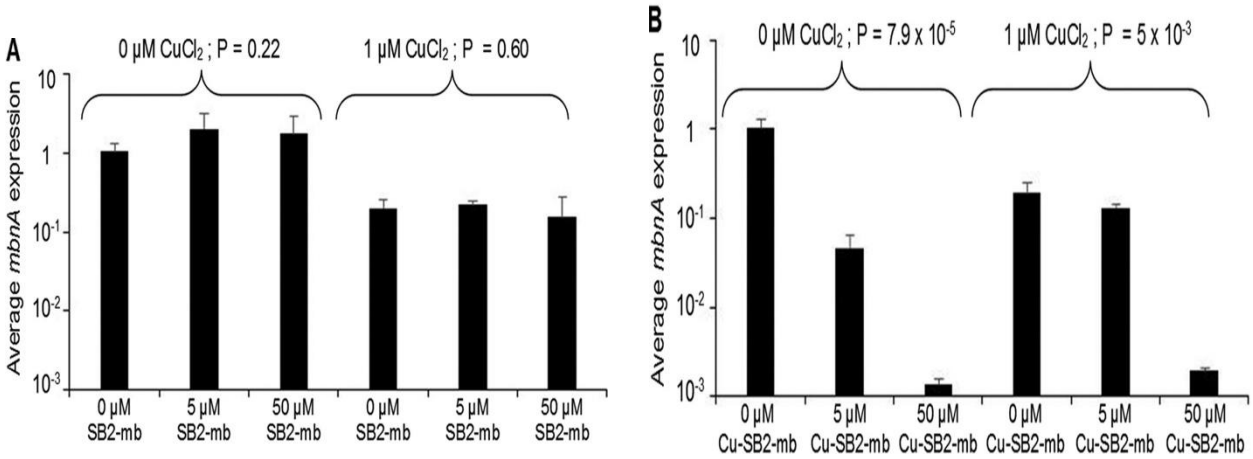


**Figure V.3** RT-qPCR of *mbnA* in *M. trichosporium* OB3b grown in either the absence or presence of 1 μM $CuCl_2$ and various amounts of methanobactin from *Methylocystis* sp. strain SB2 (A) or copper-SB2 methanobactin complexes (B). Indicated P values are from ANOVA. Error bars represent standard deviations (n=3).

### *V.2.2. Impact of various amounts of copper, methanobactin, and copper-methanobactin from Methylocystis sp. strain SB2 on sMMO activity in M. trichosporium OB3b.*

Figure V.4 summarizes the effect of SB2-Mb on sMMO activity in *M. trichosporium* OB3b, as determined using a naphthalene assay (Morton et al., 2000; Brusseau et al., 1990). The addition of up to 50 μM SB2-Mb to *M. trichosporium* OB3b grown in the absence of $CuCl_2$ had no

apparent effect on sMMO activity (ANOVA, P = 0.4). If SB2-Mb was added in the presence of 1 μM $CuCl_2$, naphthalene oxidation significantly increased ~ 6-fold (ANOVA, P = 2.1 × 10-6). When Cu-SB2-Mb was added to cultures of *M. trichosporium* OB3b grown in the absence of $CuCl_2$, naphthalene oxidation decreased ~ 20-fold, (ANOVA, P = 4.9 × 10-5). In the presence of copper, little sMMO activity was observed, and there was no significant effect of Cu-SB2-Mb on sMMO activity in *M. trichosporium* OB3b when Cu-SB2-Mb was added in conjunction with 1 μM $CuCl_2$ (ANOVA, P = 0.12).

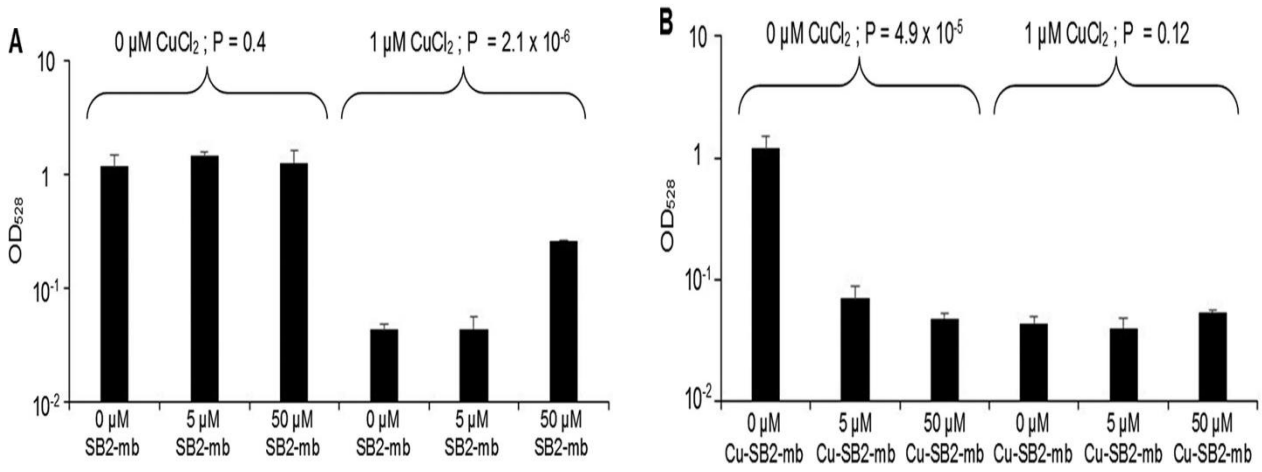


**Figure V.4** sMMO oxidation of naphthalene as indicated by changes in the $OD_{528}$ in *M. trichosporium* OB3b grown in either the absence or presence of 1 μM $CuCl_2$ and various amounts of methanobactin from *Methylocystis* sp. strain SB2 (A) or copper-SB2 methanobactin complexes (B). Indicated P values are from ANOVA.

### *2.3. Uptake of copper by M. trichosporium OB3b in the presence of methanobactin and copper-methanobactin from Methylocystis sp. strain SB2.*

To determine any effect of the addition of SB2-Mb on the ability of *M. trichosporium* OB3b to sequester copper, biomass-associated copper was also measured. The addition of SB2-Mb to *M. trichosporium* OB3b grown in the absence of $CuCl_2$ increased copper by ~ 2.2-fold, from 0.01 μg of copper · mg protein$^{-1}$ to 0.025 μg of copper · mg protein$^{-1}$ (Figure V.5A) (ANOVA, P = 0.01). More copper was associated with biomass when 1 μM $CuCl_2$ was added, i.e., 0.08 μg of copper · mg protein$^{-1}$, and such an increase was significant compared to copper measured when $CuCl_2$ was not added (Student's t-test, $P = 2.7 \times 10^{-4}$). The addition of SB2-Mb, however, did not alter the amount of copper associated with *M. trichosporium* OB3b cultures grown in the presence of $CuCl_2$ (ANOVA, P = 0.38).

Cell-associated copper, however, significantly increased with increasing amounts of Cu-SB2-Mb in both the presence and absence of $CuCl_2$ (Figure V.5B) (ANOVA, $P = 1.7 \times 10^{-11}$ and $P = 1.4 \times 10^{-3}$ for *M. trichosporium* OB3b grown in the absence and presence of $CuCl_2$, respectively). It is also interesting that approximately the same amount of cell-associated copper was found when either 5 or 50 μM Cu-SB2-Mb was added in absence or presence of $CuCl_2$. It was found earlier that *M. trichosporium* OB3b methanobactin cannot remove copper already bound to SB2-Mb and vice versa (Bandow et al., 2012). Given this and the findings reported here (e.g., copper associated with biomass increased and *mmoX* and *mbnA* expression decreased with increasing amounts of Cu-SB2-Mb), it appears that *M. trichosporium* OB3b was able to take up Cu-SB2-Mb complexes and that such uptake then caused changes in the expression of specific genes.

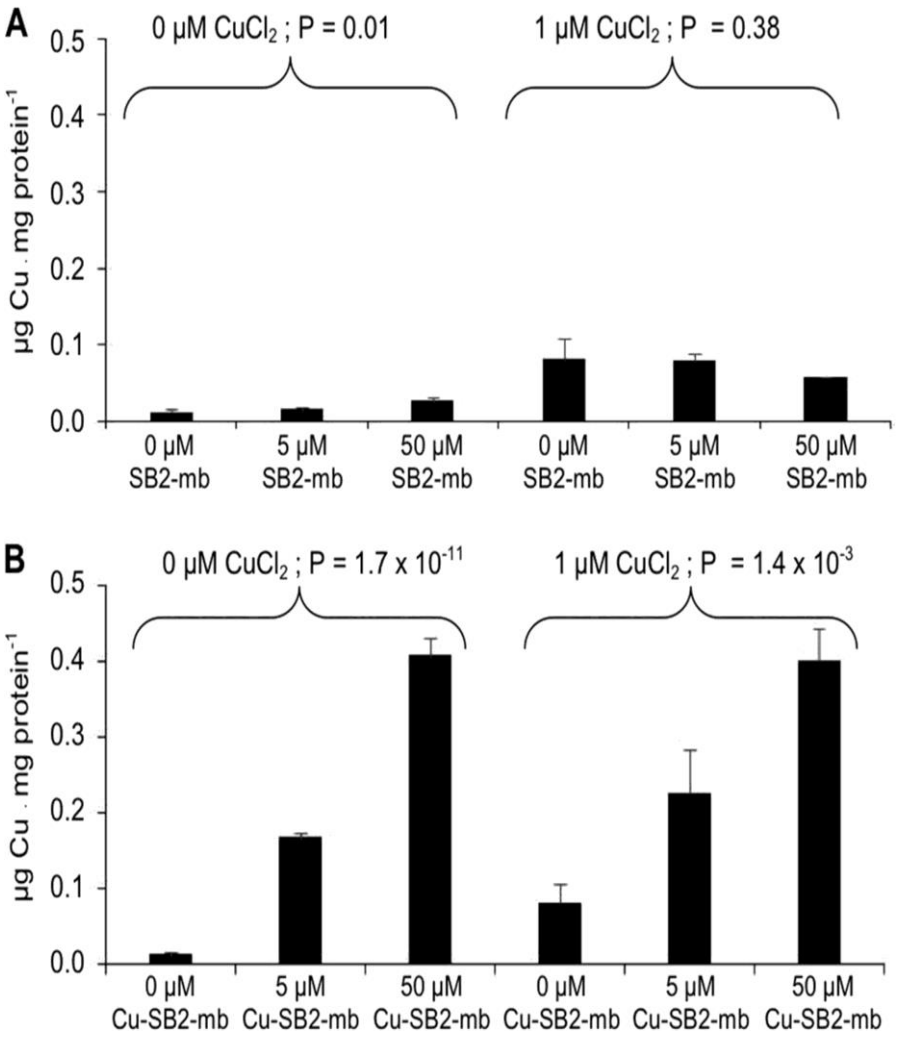


**Figure V.5** Copper associated with the biomass of *M. trichosporium* OB3b grown in either the absence or presence of 1 µM $CuCl_2$ and various amounts of methanobactin from *Methylocystis* sp. strain SB2 (A) or copper-SB2 methanobactin complexes (B). Indicated P values are from ANOVA.

## V.3. Discussion

It is well-known that methanotrophic metabolism is strongly affected by copper and that methanotrophs utilize multiple mechanisms for copper uptake (El Ghazouani et al., 2012; Ve et al., 2012; Krentz et al., 2010; Semrau et al., 2010; Behling et al., 2008; Helland et al., 2008; Kim et al., 2005; Kim et al., 2004; Karlsen et al., 2003). Further, it has been shown that in *M. trichosporium* OB3b, methanobactin plays a significant role in controlling gene expression. Specifically, in both the *M. trichosporium* OB3b wild type and an *M. trichosporium* OB3b mutant where the *mbnA* gene was disrupted, the exogenous addition of methanobactin from *M. trichosporium* OB3b increased expression of *mmoX* encoding the α-subunit of the hydroxylase component of the soluble methane monooxygenase (Semrau et al., 2012; Vorobev et al., 2013). Given the significant structural similarity between the known forms of methanobactin, the role of methanobactin in controlling gene expression in at least one methanotroph, and the observation that methanobactin is secreted into the growth environment, it was hypothesized that methanobactin may also act as a signaling molecule.

The addition of SB2-Mb increased both *mmoX* expression and whole-cell activity of sMMO in the presence of 1 μM $CuCl_2$ (Figure V.1A and V.4A). SB2-Mb, however, had a much lower impact on either *pmoA* or *mbnA* expression in the absence or presence of $CuCl_2$ (Figure V.2A and V.3A), suggesting that methanobactin selectively controls gene expression in *M. trichosporium* OB3b. Figure V.6 shows a cartoon depicting the effect of SB2-Mb on gene expression in *M. trichosporium* OB3b. It should be stressed, however, that copper-methanobactin complexes appear to more broadly regulate gene expression in *M. trichosporium* OB3b. When Cu-SB2-Mb was added, *mmoX* expression was consistently low both in the presence and absence

of $CuCl_2$, indicating that Cu-SB2-Mb complexes could control expression of the *mmo* operon. Further, *mbnA* expression was found to be dependent on the presence of Cu-SB2-Mb; i.e., *mbnA* expression decreased with increasing amounts of Cu-SB2-Mb, suggesting that copper-methanobactin complexes can control methanobactin expression, possibly through a FecIRA-like system, as speculated earlier (Kenney and Rosenzweig, 2013). Finally, Cu-SB2-Mb appeared to have relatively little effect on *pmoA* expression, suggesting that the control of MMO expression by methanobactin primarily targets regulation of the *mmo* operon. Figure V.6 and V.7 depict a proposed regulatory pathway for selective control of *mmoX* by SB2-Mb.

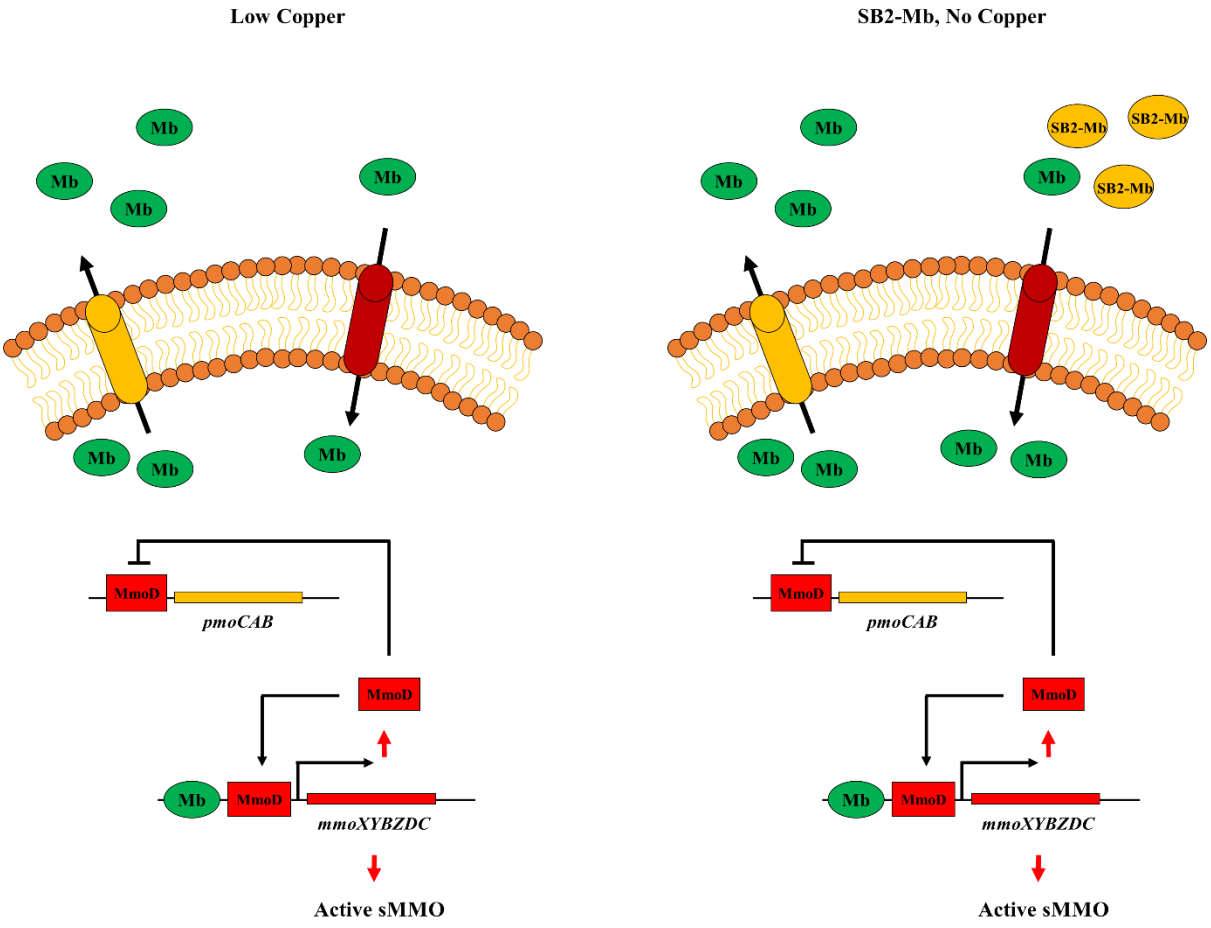


**Figure V.6** Proposed regulatory pathway depicting regulation of *mmo* and *pmo* operons by copper and SB2-Mb in the absence of copper.

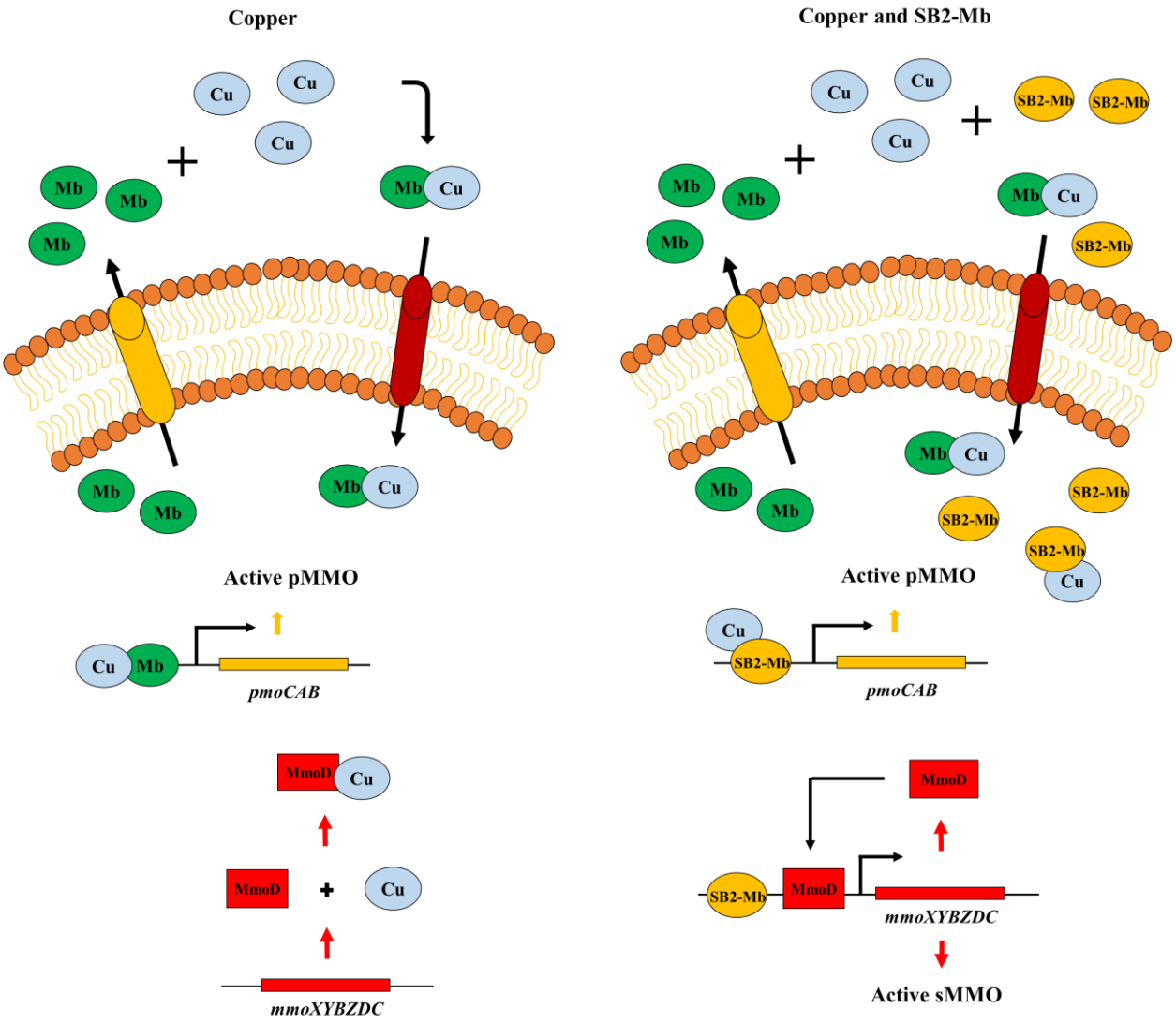


**Figure V.7** Proposed regulatory pathway for explaining the the selective control of SB2-Mb on *mmoX* expression in *M. trichosporium* OB3b in the presence of copper.

The data presented here thus indicate that methanobactin caused differential gene expression in a methanotroph that did not produce it, and therefore methanobactin appears to be a signaling molecule. Signaling molecules are defined as substances used to either monitor cell density (i.e., quorum sensing) or the particular environmental niche a microbe inhabits to then induce specific changes in gene expression throughout the population (Ryan and Dow, 2008). It should be noted,

however, that a signaling molecule must satisfy four criteria (Winzer et al., 2002): (i) the production of the signaling molecule must occur either during specific stages of growth, under definitive physiological conditions, or in response to environmental changes; (ii) the signaling molecule must accumulate extracellularly and be recognized by a specific receptor; (iii) after accumulation, the signaling molecule must induce a concerted response after some threshold concentration is reached; and (iv) the response must be more than changes required to metabolize or detoxify the signaling molecule. Methanobactin meets these requirements as follows: (i) methanobactin synthesis is tightly controlled by the availability of copper (1); (ii) methanobactin is secreted into the growth medium (El Ghazouani et al., 2012; Bandow et al., 2011; Krentz et al., 2010; Kim et al., 2005; Kim et al., 2004; DiSpirito et al., 1998), and although the specific receptor by which methanobactin is recognized has yet to be definitively determined, it is speculated that methanobactin is recognized by a TonB-dependent transporter that is encoded upstream of the gene encoding the precursor polypeptide of methanobactin (Kenney and Rosenzweig, 2013; Semrau et al., 2013); (iii) as shown here and in previous work (Semrau et al., 2013; Vorobev et al., 2013), after accumulation, methanobactin induced significant changes in expression of genes encoding sMMO polypeptides; and (iv) these genes are not the basis by which methanobactin is metabolized or detoxified [it should be noted that the biotic mechanism(s) by which methanobactin is degraded is still unknown].

To date, at least 11 general families of signaling molecules in bacteria have been identified (Yajima, 2014; Lee et al., 2013b; Ryan and Dow, 2008; Chant et al., 2007; Koldkin-Gal et al., 2007; Xavier et al., 2007; Okada et al., 2006; Takano, 2006; Chen et al., 2002b; Pesci et al., 1999): (i) the N-acylhomoserine lactone family that is used in Gram-negative bacteria; (ii) the

autoinducer oligopeptide family that is found typically in Gram-positive bacteria and also in some Gram-negative bacteria; (iii) the autoinducer-2 group, which is formed from the precursor compound 4,5-dihydroxy-2,3-pentanedione and is found in both Gram-negative and Gram-positive bacteria; (iv) the CAI-1 family, which is derived from -hydroxyketones and found in Gram-negative bacteria; (v) the diffusible signal factor family which is derived from fatty acids and is mainly found in Gram-negative bacteria; (vi) the diketopiperazine or cyclic dipeptide family found in Gram-negative bacteria; (vii) indole found in *Escherichia coli*; (viii) the *Pseudomonas* quinolone signal (PQS) found in *P. aeruginosa*; (ix) an integrated quorum-sensing (IQS) signal, 2-(2-hydroxyphenyl)-thiazole-4-carbaldehyde, also found in *P. aeruginosa*; (x) the γ-butyrolactone family found in Streptomyces; and (xi) the family of ComX pheromones, i.e., modified peptides found in Gram-positive bacteria. Of these general families, it appears that methanobactin is most similar to ComX pheromones, but to the best of the authors' knowledge, this is the first report of any Gram-negative bacteria utilizing a modified polypeptide as a signaling molecule.

The finding that the addition of methanobactin from *Methylocystis* sp. strain SB2 affected specific gene expression and whole-cell activity in *M. trichosporium* OB3b is remarkable. It is also noteworthy that copper associated with *M. trichosporium* OB3b cultures increased in the presence of Cu-SB2-Mb (Figure V.5B). These data suggest that methanobactin "piracy" may occur in methanotrophic communities, as speculated earlier (Vorobev et al., 2013). Although the number and diversity of functions ascribed to methanobactin may seem surprising, other metal-binding compounds have been found to have similar functions. For example, the siderophore bacillibactin has been shown to bind to specific promoter regions in *Bacillus subtilis* and amplify

expression of specific genes in this strain (Gaballa et al., 2012). Further, the siderophore pyoverdin has been shown not only to bind iron but also to regulate production of several virulence factors in *Pseudomonas aeruginosa* and act as a signaling molecule (Lamont et al., 2002). Finally, it has been well documented that many microorganisms perform siderophore piracy, where siderophores produced by one microbe are stolen by another to promote its growth (Traxler et al., 2012; D'Onofrio et al., 2010).

In conclusion, we report here that methanobactin, in addition to binding copper, also serves as an interspecies signaling molecule. At this time it is unknown if methanobactin also serves as a signaling molecule to other microorganisms (e.g., ammonia-oxidizing bacteria) or how widespread the use of modified polypeptides as signaling molecules might be in Gram-negative bacteria.

# CHAPTER VI: STUDY TO IDENTIFY HOW REGULATORY ELEMENTS WORK CONCOMITANTLY IN SENSING AND RESPONDING TO COPPER

## VI.1. Introduction

There are currently two existing models to explain the copper switch, however, both fail to explain all available data. One model predicts and proves to some extent the role of the regulatory genes *mmoR* and *mmoG*, upstream of the structural *mmo* genes in controlling the expression of genes encoding for sMMO (Stafford et al., 2003). Another model proves the involvement of *mmoD* for the copper switch and that methanobactin magnifies the switch by controlling expression of operons for both pMMO and sMMO polypeptides (Semrau et al., 2013). Although *mmoG* and *mmoR* are not believed to be the basis of the switch, they do seem to control the *mmo* expression and might work in consort with other genes e.g., *mmoD* for controlling the switch. Further, Merkx and Lippard (2002) speculated that *mmoD* might be involved in sensing copper. Subsequently, Semrau et al., (2013), using BindN, a web-based tool to predict DNA-RNA binding sites in amino acids, predicted the primary structure of MmoD can bind DNA. This information collectively pose MmoD as an activator that facilitates initiation of

transcription by enhancing binding of RNA polymerase to target promoter sequence. Preliminary data also suggest the presence of a copper-independent promoter region upstream of *mmoD* gene sequence. However, there is no experimental evidence of how *mmoD* product interacts with other regulatory elements to control gene expression. The control of gene expression in response to copper might involve components at the transcriptional and/or the translational level. Here, we attempted to integrate these findings into a central model and further elucidate the impact of MmoD on gene expression of *Methylosinus trichosporium* OB3b by performing DNA-protein binding studies between DNA regions, and MmoD and methanobactin via Electro-mobility Shift Assays (EMSA).

To perform EMSA, MmoD from *M. trichosporium* OB3b was overexpressed in the expression host, *Escherichia coli* BL21 (DE3) and purified. A suite of proposed promoter regions upstream of *pmo1*, *mmoX*, *mmoY*, *mmoD*, *mmoR*, *mbnI*, *mxaF*, *XoxF1*, *XoxF2* were generated from *M. trichosporium* OB3b genomic DNA via PCR and tested for binding to MmoD, methanobactin from *M. trichosporium* OB3b (OB3b-Mb), MmoD-Cu complex and OB3b-Mb-Cu complex.

## VI.2. Results

### *VI.2.1. Cloning, expression and purification of MmoD*

Firstly, *mmoD* (324 bp) was amplified from genomic DNA of *M. trichosporium* OB3b using nested PCR and confirmed by sequencing. Due to the absence of any assays for optimizing the ideal conditions for expressing MmoD, MmoD was expressed as a fusion protein by annealing *mmoD* insert to vector pET32Xa/LIC which encodes for thioredoxin, $His_6$ tag and factor Xa cleavage site. The thioredoxin tag is used to increase the solubility and thermal stability of a

recombinant protein in the expression host. The $His_6$ tag helps in purifying MmoD using Ni-NTA columns during the downstream processing. The Xa cleavage site is used to cleave off the vector specific regions such as the thioredoxin and $His_6$ tag from the MmoD fusion protein to obtain purified MmoD. pET32Xa/LIC-*mmoD* was successfully transformed into NovaBlue competent cells for maintaining the construct for subsequent expression studies.

On transforming the expression vector-gene construct into *E. coli* BL21 (DE3), MmoD fusion protein was highly expressed by induction of 0.4 mM of isopropyl β-D-thiogalactopyranoside. The fusion protein size was estimated to be ~ 30 kDa considering the size of MmoD to be ~12 kDa similar to that of MmoD from *Methylococcus capsulatus* (Bath) (Merkx and Lippard, 2002). SDS-polyacrylamide gel electrophoresis of cell free extracts of *E. coli* BL21 (DE3) transformed with *mmoD* from *M. trichosporium* OB3b (MmoD-OB3b) and *M. capsulatus* (Bath) (MmoD-mcBath) is shown in Figure VI.1. A bright band was observed against ~30 kDa indicating presence of heterologously expressed MmoD-OB3b fusion protein (Figure VI.1, lane 1) while MmoD-mcBath expression was relatively lower (Figure VI.1, lane 4). To confirm, the bands at ~30 kDa are the recombinant MmoD, two negative controls were used. Lane 2 (Figure VI.1) was loaded with cell free lysate from *E. coli* BL21 (DE3) transformed with only pET32Xa/LIC and no MmoD insert and lane 3 was loaded with cell free lysate from *E. coli* BL21 (DE3) with no pET32Xa/LIC. No protein band corresponding to ~30 kDa was observed in these conditions, confirming that the ~30 kDa is likely the recombinant MmoD. Further to confirm N-terminal sequencing of the protein band should be performed.

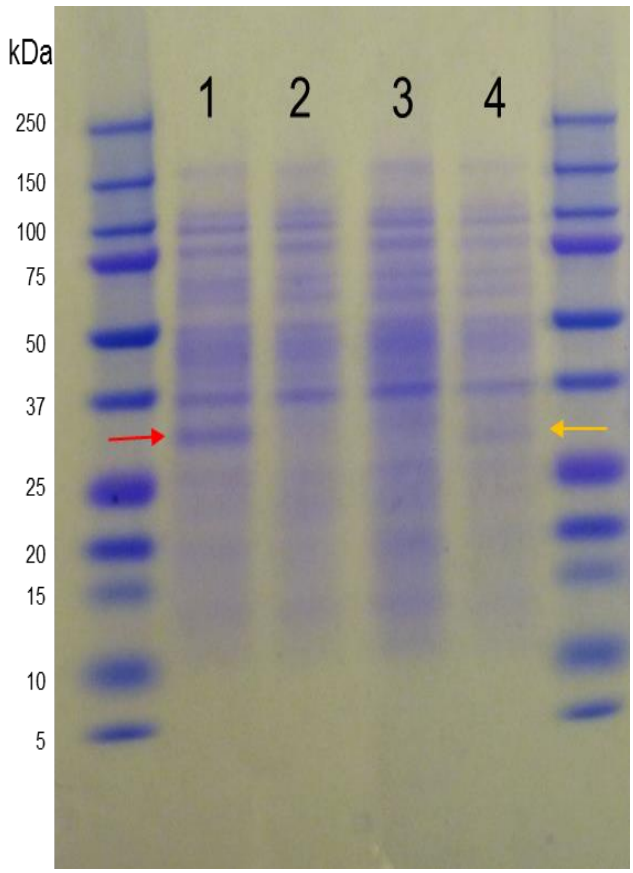


**Figure VI.1** SDS-polyacrylamide gel electrophoresis of cell free extracts from recombinant *E. coli* BL21 (DE3). Lane 1, *E. coli* BL21 (DE3) transformed with pET32Xa/LIC containing *mmoD* from *M. trichosporium* OB3b (MmoD-OB3b); lane 2, *E. coli* BL21 (DE3) transformed with only pET32Xa/LIC with no insert; lane 3, *E. coli* BL21 (DE3) with no vector; lane 4, *E. coli* BL21 (DE3) transformed with pET32Xa/LIC containing *mmoD* from *M. capsulatus* (Bath) (MmoD-mcBath). MmoD fusion protein bands are highlighted using red (MmoD-OB3b) and yellow (MmoD-mcBath) arrows.

Furthermore, the fusion protein was first purified using Ni-NTA column and subsequently purified from its vector specific tags by factor Xa enzyme treatment in the column. MmoD was then eluted in lysis buffer (20 mM $NaH_2PO_4$, 300 mM NaCl, 3 mM imidazole, pH 7.4) and wash buffer (20 mM $NaH_2PO_4$, 300 mM NaCl, 25 mM imidazole, pH 7.4) and checked for its purity.

Figure VI.2 shows multiple elution fractions from three aliquots of expression host, *E. coli* T7, that stably maintained the pET32Xa/LIC-*mmoD* construct from *M. trichosporium* OB3b.

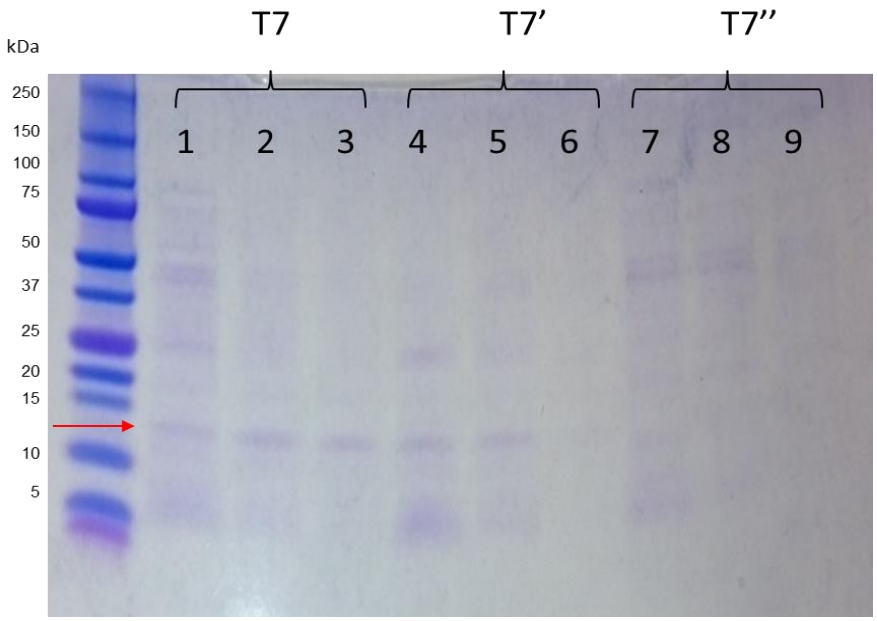


**Figure VI.2** SDS-polyacrylamide gel electrophoresis of MmoD elution fractions from *E. coli* T7 containing MmoD-OB3b after subjecting through Ni-NTA column and factor Xa treatment. T7 – MmoD eluted in wash buffer in 0.2 ml resin column; T7' – MmoD eluted in binding buffer in 0.2 ml resin column; T7'' – MMOD eluted in wash buffer in 0.4 ml resin column. Lanes 1, 4 and 7 – First elution fraction; Lanes 2, 6 and 8 – second elution fraction; Lanes 3, 7 and 9 – third elution fraction. Red arrow points at the native MmoD band

While lanes 1, 4 and 7 contained MmoD along with protein contaminants like *E. coli* specific proteins and uncleaved His-tagged MmoD, lanes 2, 3 and 5 appeared to have native MmoD with reduced impurities. MmoD concentrations as checked using Nanodrop were typically in the range of 160-350 ng/µl.

### *VI.2.2. Bioinformatic analysis of MmoD-OB3b size*

Open access online bioinformatics tools such as ExPASy translate and ExPASy ProtParam tools were used to identify and confirm the size of MmoD-OB3b. The molecular weight of MmoD-OB3b was estimated to be 12.15 kDa (Figure VI.3) as speculated earlier.

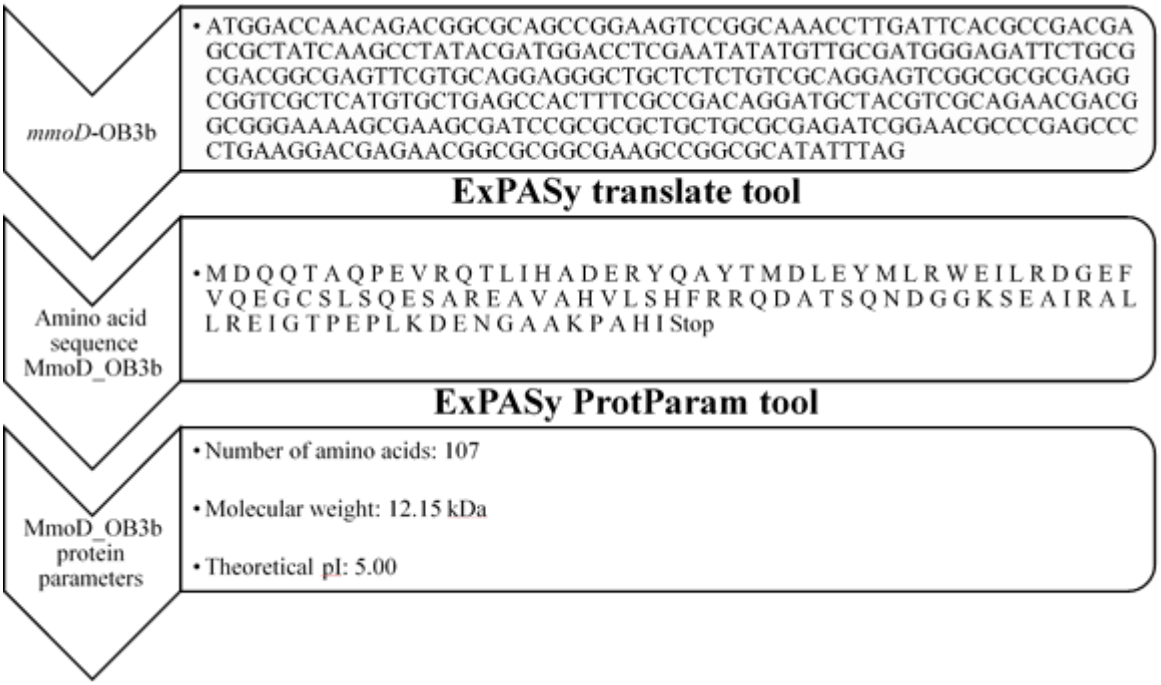


**Figure VI.3** Flowchart depicting the tools used to identify MmoD-OB3b amino acid sequence from mmoD-OB3b gene sequence and subsequently the molecular weight of MmoD-OB3b.

### *VI.2.3. Optimization of EMSA for DNA:protein binding in M. trichosporium OB3b*

EMSA can be challenging as several factors affect DNA-protein interactions. The factors optimal to keep the DNA, protein and DNA:protein complex stable include binding buffer composition, pH, salt concentration, an additive detergent like NP-40 or a protein like Bovine Serum Albumin known to help in DNA-protein binding, glycerol %, DNA:protein ratio, native PAGE components and electrophoresis conditions. A positive control Epstein Bar Nuclear

Antigen (EBNA) system was used. Here, optimization of EMSA conditions required to assist in the binding of a 60 bp EBNA consensus oligonucleotide to the EBNA protein extract was attempted. Figure VI.4 shows a TBE-polyacrylamide gel electrophoresis of the DNA:protein binding reaction mix at various DNA: protein ratios. On comparing the mobility of free DNA (lane 1) with the mobility of DNA:protein complex (lane 3, 4, 5), a DNA smear is observed at two regions, one against the size of the free DNA (Figure VI.4A, lane1) and another against the size of the protein (Figure VI.4B, lane 2, 3, 4, 5). The intensity of the DNA smear with a mobility corresponding to the mobility of protein (Figure VI.4; red arrow) appeared to increase with increase in the protein units in the reaction mix. It is ambiguous if this really is a shift in DNA or if the protein is also partly stained by the DNA stain, SYBR green. The process thus needs to be optimized further by adjusting $MgCl_2$ concentration or the amount of glycerol added to the binding reaction mix to avoid DNA smear.

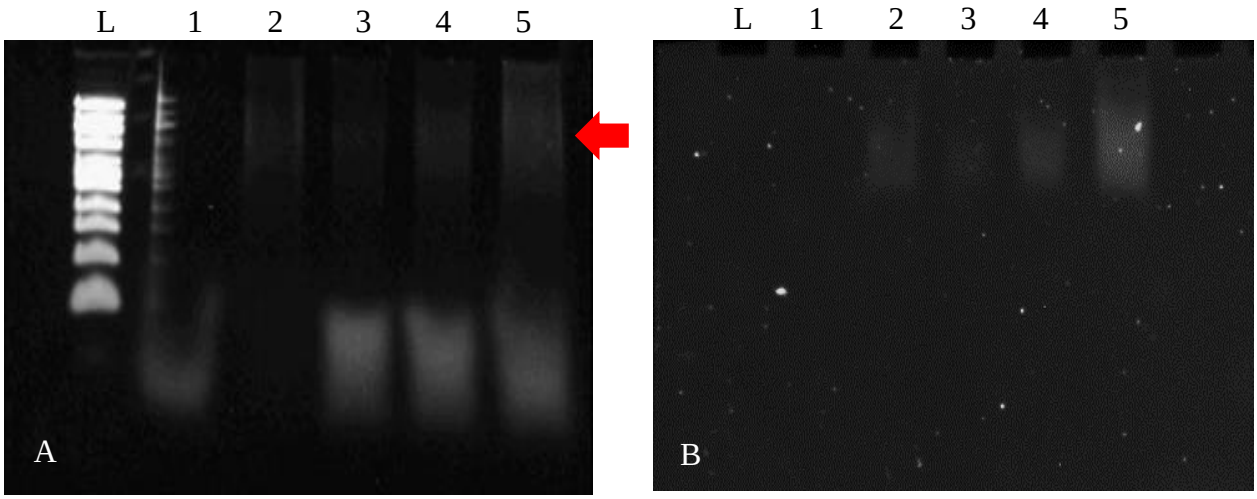


**Figure VI.4** TBE-polyacrylamide gel electrophoresis of L, DNA ladder, 1 - EBNA DNA, 2 - EBNA protein, 3 - EBNA DNA:protein (66 ng:2 Units), 4 - EBNA DNA:protein (66 ng:4 Units), 5 - EBNA DNA:protein (66 ng:8 Units) as visualized under 312 nm UV-transilluminator. A) DNA stained by SYBER green DNA stain. B) Protein stained by Sypro Ruby protein stain. Red arrow indicates the shift in DNA mobility.

It is also possible that DNA:protein complexes were not very stable while in the gel. So, the gel running conditions also has to be optimized further for confirming the presence of DNA:protein binding.

DNA:protein binding reactions were performed using *M. trichosporium* OB3b proteins, MmoD and Mb, both with and without copper. DNA regions containing proposed promoter sites of *mmo* and *pmo*, operons were amplified *de novo*. The same EMSA assay conditions were used for these samples as used for the EBNA system. Figure VI.5 shows the TBE-polyacrylamide gel electrophoresis of EMSA assay performed between DNA region upstream of *pmo1*, and proteins MmoD-OB3b and OB3b-Mb.

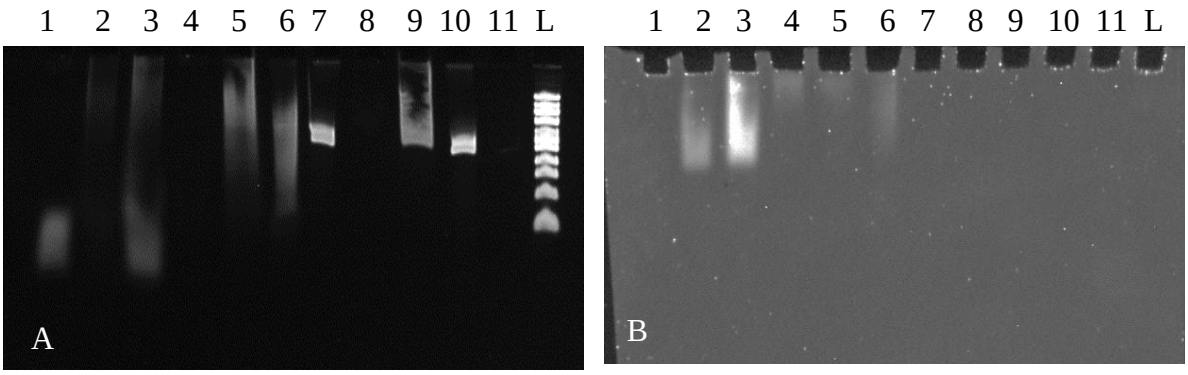


**Figure VI.5** TBE-polyacrylamide gel electrophoresis of , 1 - EBNA DNA, 2 - EBNA protein, 3 - EBNA DNA:protein (66 ng:8 Units), 4 - MmoD, 5 - *pmo1*:MmoD (100 ng: 1750 ng), 6 - *pmo1*:MmoD-Cu (100 ng: 1750 ng), 7 - *pmo1* (100 ng), 8 - Mb (1750 ng), 9 - *pmo1*:Mb (100 ng: 1750 ng), 10 - *pmo1*:Mb-Cu (100 ng: 1750 ng), 11 - empty, L - ladder as visualized under 312 nm UV-transilluminator. A) DNA stained by SYBER green DNA stain. B) Protein stained by Sypro Ruby protein stain.

From Figure VI.5, we find that the EBNA system positive control does not show a clear shift in DNA (Figure VI.5A, lanes 1 and 3). As compared to free *pmo1* (Figure VI.5A, lane 7), it is not clear if there is any shift in the presence of MmoD (Figure VI.5A, lane 5). No DNA band appeared at the top of the lane corresponding to the MmoD band under protein stain (Figure

VI.5B, lane 5). The free *pmo1* band in lane 5 (Figure VI.5A) appears as a smear with less intensity as compared to the sharp band when only *pmo1* was loaded (Figure VI.5B, lane 7). Although speculative, the DNA smear in the presence of MmoD (Figure VI.5A, lane 5) might be an unstable DNA:protein complex. When the reaction mix consisted of MmoD as a MmoD-Cu complex, clearly no shift in DNA was observed, instead the *pmo1* band was smeared with a faint band that corresponds to *pmo1* size. While no shift was observed in the presence of Mb or Mb-Cu complex (Figure VI.5A, lanes 9 and 10) as evident in the DNA stained gel, Mb could not be visualized with the protein stain (Figure VI.5B, lanes 9 and 10). The reason is not clear why a protein well characterized and purified, and loaded at a high concentration could not be visualized under the Sypro Ruby protein stain. It may be possible that since Mb is a low molecular weight protein, its mobility is much faster in the gel such that it is no longer present in the gel at the end of electrophoresis. It is thus not certain if DNA actually did not bind to Mb/Mb-Cu or Mb/Mb-Cu was available for binding.The promoter region upstream of *mmoX* was assayed for binding to proteins. Figure VI.6 shows the TBE- polyacrylamide gel electrophoresis of EMSA reaction mixtures.

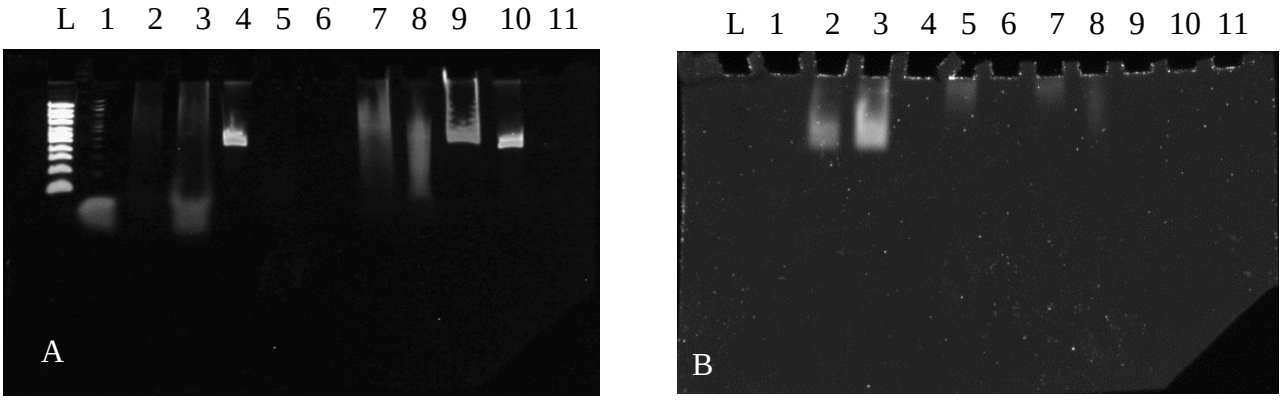


**Figure VI.6** TBE-polyacrylamide gel electrophoresis of , L - ladder, 1 - EBNA DNA, 2 - EBNA protein, 3 - EBNA DNA:protein (66 ng:8 Units), 4 - *mmoX*, 5 - MmoD (1750 ng), 6 - Mb (1750 ng), 7 - *mmoX*:MmoD (100 ng: 1750 ng), 8 - *mmoX*:MmoD-Cu (100 ng: 1750 ng), 9 - *mmoX*:Mb (100 ng: 1750 ng), 10 – *mmoX*:Mb-Cu (100 ng: 1750 ng), 11 - empty, as visualized under 312 nm UV-transilluminator. A) DNA stained by SYBER green DNA stain. B) Protein stained by Sypro Ruby protein stain.

On comparing the mobility of free DNA (Figure VI.6A, lane 4) and mobility of *mmoX* in *mmoX*:MmoD mix (Figure VI.6A, lane 7), there may be a shifted DNA band near the loading well similar to the MmoD band as seen under protein stain (Figure VI.6B, lane 7), but this is not certain due to absence of any clear DNA band. MmoD-Cu complex did not retard the mobility of *mmoX*, rather showed a smear as observed with *pmo1* in the presence of MmoD-Cu complex (Figure VI.5A, lane 6). Mb did not seem to bind to *mmoX*. Similar to EMSA with *pmo1*, since Mb was not visualized under protein stain, it is unclear if there really is no binding or if protein is available for binding.

### *VI.3. Discussion*

The Electro-mobility shift assay is a difficult assay to capture the DNA:protein binding at its stable bound form. The EMSA of the EBNA positive control system could not be achieved and requires more optimization of the factors optimal for DNA:protein binding. Similarly, it is not

certain if there is any apparent binding between MmoD and DNA upstream of *pmo* and *mmo* operon. At this point, any such binding and subsequent DNA shift is largely speculative and needs more attention towards optimization of the process itself.

# CHAPTER VII: CONCLUSIONS AND FUTURE WORK

## VII.1. Conclusions

The objective of this study was to understand how various metals and methanobactin impact gene expression in the switch-over methanotroph, *Methylosinus trichosporium* OB3b. Microbes are well known to play significant roles in biogeochemical cycling and metal transformations (Gadd, 2010). This study shows how metals in turn affect microbial, specifically methanotrophic, activities.

Firstly, the effect of competing metals from Group A and Group B, as categorized by Choi et al. (2006b), on gene expression in *M. trichosporium* OB3b was observed in the presence of copper. While Group B metals did not impact gene expression, gold (belonging to Group A) induced *mmo* expression even when copper was present. The results indicate that gold competes for uptake by OB3b-Mb, reducing copper uptake in *M. trichosporium* OB3b. Gold was observed to have its effect not only at the genetic level but also at the protein level i.e., it also induced sMMO activity despite the presence of copper. As was seen with mercury that binds OB3b-Mb irreversibly, gold also showed similar rapid irreversible binding to OB3b-Mb suggesting that

induction of *mmo* expression, and subsequently sMMO activity, could as well be performed by other prospective Group A metals that bind to methanobactin stronger and faster than copper. *M. trichosporium* OB3b was found to respond to presence of gold by over-expressing *mbnA* to increase production of methanobactin for facilitating copper uptake.

Although gold is considered a rare metal, with an average concentration of 0.005 ppm in Earth's crust, many biological agents like thermophilic bacteria and archaea, and anthropogenic mining activities make gold more bioavailable than one would expect. Plant mediated transport/ dispersion of gold has also been observed even in species as common as *Zea mays* in concentrations ranging in ppm. A recent study by Feng and van-Deventer (2011) shows that bio-organic products such as alanine, valine, histidine and glycine increase gold solubilization. These instances clearly indicate increased gold bioavailability in diverse environments, thus suggesting that the observed gold mediated sMMO activation might be a widespread phenomenon in switch-over methanotrophs *in situ*. Alternatively, binding of gold might act as a survival strategy for methanotrophic communities to evade gold toxicity in gold mines or other such acidic environments by transforming more toxic Au (III) ions to less toxic elemental Au (0) nanoparticles (Choi et al., 2006b). This strategy for exploiting gold or rather other cheaper metals that have the same impact on sMMO activity as gold could thus be used as a cost effective alternative to induce activity of either sMMO or both the MMOs for bioremediation or reducing methane emissions.

Secondly, in addition to the copper switch for the two forms of MMO, there seems to be a cerium switch for the two forms of MDH in *M. trichosporium* OB3b. Expression of Mxa-MDH decreased while expression of Xox-MDH increased in response to cerium. This is plausible since

Xox-MDHs have been shown to have a rare earth metal in their active site while Mxa-MDH possesses the more common divalent metal ion, calcium, in its active site. Interestingly, although sMMO and pMMO expressions were not affected by cerium, copper appeared to suppress the cerium switch in MDH i.e., in the presence of copper, the decrease in Mxa-MDH and increase in Xox-MDH on addition of cerium was minimal than the cerium-induced differential expression levels in MDH in the absence of copper. This suggests that Mxa-MDH is coupled to pMMO in *M. trichosporium* OB3b irrespective of cerium availability and could be uncoupled from methane oxidation by sMMO in the presence of cerium. Further, no effect on growth of *M. trichosporium* OB3b was observed in response to cerium as against studies in *Methylacidiphilum fumariolicum* SolV by Pol et al (2014). This could be attributed to the alternative MDH, Mxa-MDH that will be active even in the absence of cerium, suggesting that cerium is not indispensable for growth of *M. trichosporium* OB3b.

Further, on considering the abundance of cerium in Earth's crust, contrary to its classification under rare earth metals, cerium concentration is 60 ppm (USGS, 2001) which is about the same as environmentally studied metals like copper and zinc, and more abundant than the rarest metal, gold. Also the increasing use of rare earth metals in various applications such as electric and hybrid vehicles, car catalysts, energy-efficient lighting, wind power, digital camera, disk drives, flat panel displays, magnets, metal alloys, phosphors, contrast media for magnetic resonance imaging, treatment of renal diseases, dope for poultry fattening and fertilizers has led to increasing levels of these rare earth metals in its elemental state (Alonso et al., 2012). While some studies show rare earth metals are toxic to environment (Pagano et al., 2015), many studies have shown that rare earth elements promote growth and productivity of several crops even when

present at low concentrations (Pol et al., 2014; Zhang et al., 2013; Ge et al., 2006; Hu et al., 2004). The question is despite having low solubility in the environment, how are rare earth metals bioavailable for uptake by methanotrophs or in general, microbes and plants? In *M. trichosporium* OB3b, it was found that most of the cerium supplemented in the medium was associated to biomass and copper uptake via OB3b-Mb was not affected by cerium. This suggests an alternative uptake mechanism of cerium in *M. trichosporium* OB3b. Future work in the following section discusses the possible cerium uptake mechanism and proposed ways to identify it.

Thirdly, it was hypothesized that since metals, i.e., gold and mercury, taken up via methanobactin, regulated gene expression, methanobactin might itself have a role in gene regulation in *M. trichosporium* OB3b. Also, due to similar function roles of methanobactin from several methanotrophs, methanobactin from *Methylocystis* strain SB2 (SB2-Mb) was tested for its effects on gene regulation in *M. trichosporium* OB3b. SB2-Mb was found to selectively control gene expression in *M. trichosporium* OB3b by inducing *mmoX* expression in the presence of copper while actually increasing copper availability. Interestingly, SB2-Mb increased the whole cell activity of sMMO as well in the presence of copper. Cu-SB2-Mb complexes were also found to control expression of the *mmo* operon. Thus, methanobactin acts like a signaling molecule thereby causing differential gene expressions in methanotrophs that did not produce it.

Considering the fact that methanobactin from one species can act as a signaling molecule and impact gene expression in a completely different species, it may be possible to believe that a species-species communication or quorum sensing occurs even between methanotrophs.

However, how exactly the methanotrophs sense the signal or what is the receptor that specifically detects methanobactin is still unknown.

Another intriguing finding is that *M. trichosporium* OB3b takes up SB2-Mb that then causes the observed differential expression while *M. trichosporium* OB3b produces its very own form of methanobactin. It would be reasonable if such methanobactin piracy occurred between species that produce and do not produce methanobactin. Siderophore piracy is a similar yet widely known phenomenon among bacteria that compete for iron competition. Similarly, methanobactin piracy could be a strategy used by both methanobactin producers and non-methanobactin producers to realize a growth advantage in diverse environmental conditions like during copper limitations, copper toxicity or other heavy metal toxicity. This phenomenon thus might even have a broader impact on the microbial community structure in nature by favoring the growth of methanotrophic and non-methanotrophic bacteria that can either produce or pirate methanobactin for survival.

Fourthly, MmoD has been speculated to play a role in sensing and responding to copper by binding to DNA regions and activating transcription initiation. Electro-mobility shift assays were performed to check for binding between proposed promoter regions, and MmoD and Mb. Results from this study do not clearly indicate any binding between MmoD and DNA upstream of *pmo1* and *mmoX*. MmoD bindings occur as a free MmoD and not as a complex with copper. Future work must target at optimizing the optimal conditions required for EMSA.

## VII.2. Future work

From this study, it is evident that metals, gold and cerium, and proteins, MmoD and Mb play a key role in regulating gene expression and enzyme activities in *M. trichosporium* OB3b. As a start, the key enzymes, methane monooxygenase and methanol dehydrogenase have been the focus of this study. However, much is unknown for understanding and developing a complete central model for metals switches and methane oxidation. Therefore, here are some proposed future work.

In this study, we found that gold can induce sMMO activity in the presence of copper. However, it would not be practical to use gold *in situ* for sMMO activation since gold is a precious metal and expensive for field scale studies. While some cheaper and non-toxic metals were tested as part of this study, no metal tested could successfully impart similar effect as gold on sMMO in *M. trichosporium* OB3b. More metals could therefore be tested to have a cost effective alternative for induction of sMMO in presence of copper *in situ*. Alternatively, a microcosm study could be set up using contaminated environmental soil/water samples and gold to check if gold imparts the same effect in complex natural environment. Furthermore, since only sMMO activity was tested in this study in the presence of several competing metals with copper, pMMO activity could also be tested to check if in fact both the forms are active when gold is supplemented with copper or if there is any reduction in activity of pMMO once gold is introduced into the system. Another question is what would happen if non-switchover methanotrophs like *Methylomicrobium album* BG8 and *Methylocystis parvus* OBBP that contain only pMMO are introduced to media supplemented with gold? It is hypothesized that in such

copper limiting conditions, these strains would either not grow or have a long lag phase and stunted growth.

The expression of MDH was drastically affected by cerium in sMMO expressing conditions while its effect was suppressed in the presence of copper. To find out if the switch between the two forms of MDH is just a "cerium switch" or a broader "rare earth elements switch", the effect of other rare earth elements on expression of MDH and copper uptake should be studied. Although our study suggests that pMMO and Mxa-MDH are coupled in the presence of copper, more supporting evidence is needed to confirm this coupling effect. Future studies could target at looking for physical association between pMMO and Mxa-MDH or any chemical bonding between their amino acids or any sign of electron exchange between these two enzymes. Further, the mechanism by which cerium is taken up by *M. trichosporium* OB3b is unknown. Possible uptake pathways might either be passively through ion channels or just physical adsorption to the cell surface and inducing intracellular gene responses via a receptor at the cell surface, or via other chelating compounds like methanobactin that are specific for cerium or rare earth metals. Localization of cerium that is associated with biomass could also help in identifying if the metal enters the cells or stays associated onto the cell surface. If the metal is found to be localized inside the cells, inhibition studies that specifically inhibits either the ion channels or enzyme that provided energy for active metal uptake pathways can be used to investigate how cerium is taken up by the cells.

The transport of metals via methanobactin has been shown to have key cellular responses in gene regulation in *M. trichosporium* OB3b. However, impact of methanobactin from other methanotrophs deserves more attention. While the studies here show SB2-Mb can induce sMMO

activity in *M. trichosporium* OB3b, it will be interesting to know if SB2-Mb has the same effect on other switch-over methanotrophs. Currently, it is speculated that methanobactin uptake is facilitated by Ton-B receptor in *M. trichosporium* OB3b. Would this Ton-B receptor facilitate uptake of methanobactin from other methanotrophs? Overall, improving our understanding of environmental factors that affect the preferential induction of sMMO or pMMO in methanotrophs and the mechanism behind the processes could aid in engineering biological systems optimum for bioremediation under wide range of environments.

On trying to understand the genetic basis of copper switch, a series of electro-mobility shift assays were performed using MmoD, since data points at its probable role in copper switch. For successfully performing an EMSA, the process should be optimized for each protein used for the binding reaction. Firstly, as a positive control, purified protein such as Nuclear Factor kappa B (NFkB) p-49/p-50 should be used to check for binding with the NFkB consensus oligonucleotide. Secondly, optimization for use with MmoD and Mb can be performed by doing a titration of various DNA:protein ratios and checking the optimal binding conditions along with the gel running conditions. Once the EMSA system is optimized for MmoD and Mb, it is possible that proteins may work in concert with products of other regulatory genes such as *mmoR* and *mmoG*, a combination of different proteins from *M. trichosporium* OB3b should be performed. DNA-protein studies that check for binding of these gene products supplemented in combination should be performed. Information from this study would fill in the missing gaps in our understanding of the regulatory mechanism.

Furthermore, if any tested protein is found to bind to a region upstream of a gene, EMSA could be performed at varying concentration of the RNA polymerase (RNAP) that binds to the target

DNA to find out (i) if the protein acts as an activator i.e., if the protein induces binding of RNAP to target DNA by itself binding to the target DNA, and (ii) what downstream genes could the protein possibly control. Also, a DNA footprinting assay would help in finding out the exact DNA sequence of protein binding.

## REFERENCES


Afolabi, P. R., Mohammed, F., Amaratunga, K. & other authors (2001) Site-directed mutagenesis and X-ray crystallography of the PQQ-containing quinoprotein methanol dehydrogenase and its electron acceptor, cytochrome $c_L$. *Biochemistry* **40**: 9799–9809.

Alonso, E., Sherman, A. M., Wallington, T. J., Everson, M. P., Field, F. R., Roth, R., et al. (2012) Evaluating rare earth element availability: a case with revolutionary demand from clean technologies. *Environ Sci Technol* **46**: 3406–3414.

Anderson, B., Bartlett, K., Frolking, S., Hayhoe, K., Jenkins, J., Salas, W. (2010) Methane and nitrous oxide emissions from natural sources. Washington, DC, USA: US Environmental Protection Agency. URL http://www.epa.gov/methane/pdfs/Methane-and-Nitrous- Oxide-Emissions-From-Natural-Sources.pdf.

Anthony, C. (1986) The bacterial oxidation of methane and methanol. *Adv Microb Physiol* **27**: 113–210.

Anthony, C., Ghosh, M., Blake, C. C. (1994) The structure and function of methanol dehydrogenase and related quinoproteins containing pyrroloquinoline quinone. *Biochem J* **304**: 665–674.

Arakawa, H., Aresta, M., Armor, J. N., Barteau, M. A., Beckman, E. J., Bell, A. T., et al. (2001) Catalysis research of relevance to carbon management: progress, challenges, and opportunities. *Chem Rev* **101**: 953–996.

Balasubramanian, R., Smith, S. M., Rawat, S., Yatsunyk, L. A., Stemmler, T. L., Rosenzweig, A. C. (2010) Oxidation of methane by a biological dicopper centre. *Nature* **465**: 115–119.

Bandow, N. L., Gallagher, W. H., Behling, L., Choi, D. W., Semrau, J. D., Hartsel, S. C., et al. (2011) Isolation of methanobactin from the spent media of methane oxidizing bacteria. *Methods Enzymol* **495**: 259–269.

Bandow, N., Gilles, V. S., Freesmeier, B., Semrau, J. D., Krentz, B., Gallagher, W., et al. (2012) Spectral and copper binding properties of methanobactin from the facultative methanotroph *Methylocystis* strain SB2. *J Inorg biochem* **110**: 72–82.

Bao, Z., Okubo, T., Kubota, K., Kasahara, Y., Tsurumaru, T., Anda, M., et al. (2014) Metaproteomic identification of diazotrophic methanotrophs and their localization in root tissues of field-grown rice plants. *Appl Environ Microbiol* **80**: 5043–5052.

Beal E. J., House C. H., Orphan V. J. (2009) Manganese- and iron-dependent marine methane oxidation. *Science* **325**: 184–187.

Behling, L. A., Hartsel, S. C., Lewis, D. E., DiSpirito, A. A., Choi, D. W., Masterson, L. R., Veglia, G., Gallagher, W. H. (2008) NMR, mass spectrometry and chemical evidence reveal a different chemical structure for methanobactin that contains oxazolone rings. *J Am Chem Soc* **130**: 12604–12605.

Bertani, G. (1951) Studies on lysogenesis. I. The mode of phage liberation by lysogenic *Escherichia coli*. *J Bacteriol* **62**: 293–300.

Bloom, A. A., Palmer, P. I., Fraser, A., Reay, D. S., Frankenberg, C. (2010) Large-scale controls of methanogenesis inferred from methane and gravity spaceborne data. *Science* **327**: 322–325.

Bodrossy, L., Holmes, E. M., Holmes, A. J., Kovacs, K. L., Murrell, J. C. (1997) Analysis of 16S rRNA and methane monooxygenase gene sequences reveals a novel group of thermotolerant

and thermophilic methanotrophs, *Methylocaldum* gen. nov. *Arch Microbiol* **168**(6): 493–503.
Bogart, J. A., Lewis, A. J., Schelter, E. J. (2015) DFT study of the active site of the XoxF-type natural, cerium-dependent methanol dehydrogenase enzyme. *Chemistry* **21**(4): 1743–1748.
Bousquet, P., Ciais, P., Miller, J. B., Dlugokencky, E. J., Hauglustaine, D. A., Prigent, C., et al. (2006) Contribution of anthropogenic and natural sources to atmospheric methane variability. *Nature* **443**: 439–443.
Bowman, J. P., McCammon, S. A., Skerratt, J. H. (1997) *Methylosphaera hansonii* gen. nov., sp. nov., a psychrophilic, group I methanotroph from Antarctic marine-salinity, meromictic lakes. *Microbiology* **143**: 1451–1459.
Bowman, J. P., Sly, L. I., Nichols, P. D., Hayward, A. C. (1993) Revised taxonomy of the methanotrophs: description of *Methylobacter* gen. nov., emendation of *Methylococcus*, validation of *Methylosinus* and *Methylocystis* species, and a proposal that the family *Methylococcaceae* includes only the group I methanotrophs. *Int J Syst Bacteriol* **43**: 735–753.
Bowman, J. P., Sly, L. I., Stackebrandt, E. (1995) The phylogenetic position of the family *Methylococcaceae*. *Int J Syst Bacteriol* **45**: 182–185.
Brewer, G. J. (1999) Penicillamine should not be used as initial therapy in Wilson's disease. *Mov Disord* **14**: 551–554.
Brusseau, G. A., Tsien, H. C., Hanson, R. S., Wackett, L. P. (1990) Optimization of trichloroethylene oxidation by methanotrophs and the use of a colorimetric assay to detect soluble methane monooxygenase activity. *Biodegradation* **1**: 19–29.
Burrows, K. J., Cornish, A., Scott, D., Higgins, I. J. (1984) Substrate specificities of the soluble and particulate methane mono-oxygenases of *Methylosinus trichosporium* OB3b. *J Gen Microbiol* **130**: 3327–3333.
Castaldi, S., Costantini, M., Cenciarelli, P., Ciccioli, P., Valentini, R. (2007) The methane sink associated to soils of natural and agricultural ecosystems in Italy. *Chemosphere* **66**: 723–729.
Chan, S. I., Chen, K., Yu, S., Chen, C. L., Kuo, S. (2004) Toward delineating the structure and function of the particulate methane monooxygenase from methanotrophic bacteria. *Biochemistry* **43**: 4421–4430.
Chant, E. L., Summers, D. K. (2007) Indole signaling contributes to the stable maintenance of *Esherichia coli* multicopy plasmids. *Mol Microbiol* **63**: 35–43.
Chauhan, R., Ramanathan, A. L., Adhya, T. K. (2008) Assessment of methane and nitrous oxide flux from mangroves along Eastern coast of India. *Geofluids* **8**: 321–332.
Chen, X., Schauder, S., Potier, N., Van Dorsselaer, A., Pelczer, I., Bassler, B. L., et al. (2002b) Structural identification of a bacterial quorum-sensing signal containing boron. *Nature* **415**: 545–549.
Chen, Y., Crombie, A., Rahman, M. T., Dedysh, S. N., Liesack, W., Stott, M. B., et al. (2010) Complete genome sequence of the aerobic facultative methanotroph *Methylocella silvestris* BL2. *J bacteriol* **192**: 3840–3841.
Chen, Z.-W., Matsushita, K., Yamashita, T., Adachi, O., Beilamy, H.D., Mathews, F.S. (2002a) Structure at 1.9 Å resolution of a quinohemoprotein alcohol dehydrogenase from *Pseudomonas putida* HK5. *Structure* **10**: 837–848.

Chistoserdova, L., Chen, S. W., Lapidus, A., Lidstrom, M. E. (2003) Methylotrophy in *Methylobacterium extorquens* AM1 from a genomic point of view. *J Bacteriol* **185**: 2980–2987.

Chistoserdova, L., Lidstrom, M. E. (1997) Molecular and mutational analysis of a DNA region separating two methylotrophy gene clusters in *Methylobacterium extorquens* AM1. *Microbiology* **143**: 1729–1736.

Choi, D. W., Antholine, W. A., Do, Y. S., Semrau, J. D., Kisting, C. J., Kunz, R. C., et al. (2005) Effect of methanobactin on methane oxidation by the membrane-associated methane monooxygenase in *Methylococcus capsulatus* Bath. *Microbiology* **151**: 3417–3426.

Choi, D. W., Kunz, R. C., Boyd, E. S., Semrau, J. D., Antholine, W. E., Han, J- I., Zahn, J. A., Boyd, J. M., de la Mora, A. M., DiSpirito, A. A. (2003) The membrane-associated methane monooxygenase (pMMO) and pMMO-NADH: quinine oxidoreductase complex from *Methylococcus capsulatus* (Bath). *J Bacteriol* **185**: 5755–5764.

Choi, D. W., Zea, C. J., Do, Y. S., Semrau, J. D., Antholine, W. E., Hargrove, M. S., et al. (2006a) Spectral, kinetic, and thermodynamic properties of Cu(I)-, and Cu(II)-binding by methanobactin from *Methylosinus trichosporium* OB3b. *Biochemistry* **45**: 1442–1453.

Choi, D.-W., Do, Y.S., Zea, C.J., McEllistrem, M.T., Lee, S.-W., Semrau, J.D., et al. (2006b) Spectral and thermodynamic properties of Ag(I), Au(III), Cd(II), Co(II), Fe(III), Hg(II), Mn(II), Ni(II), Pb(II), U(IV), and Zn(II) binding by methanobactin from *Methylosinus trichosporium* OB3b. *J Inorg Biochem* **100**: 2150–2161.

Choi, J. M., Kim, H. G., Kim, J. S., Youn, H. S., Eom, S. H., Yu, S. L., et al. (2011) Purification, crystallization and preliminary X-ray crystallographic analysis of a methanol dehydrogenase from the marine bacterium *Methylophaga aminisulfidivorans* MP(T). *Acta Crystallogr Sect F: Struct Biol Cryst Commun* **67**: 513–516.

Chowdhury, T. R., Dick, R. P. (2013) Ecology of aerobic methanotrophs in controlling methane fluxes from wetlands. *Appl Soil Ecol* **65**: 8–22.

Christensen, V., Guénette, S., Heymans, J. J., Walters, C. J., Watson, R., Zeller, D., Pauly, D. (2003) Hundred year decline of North Atlantic predatory fishes. *Fish Fish* **4**: 1–124.

Clark, Jim. (2000) Explaining the reaction between methane and chlorine. URL http://www.chemguide.co.uk/mechanisms/freerad/ch4andcl2tt.html

Colby, J., Dalton, H. (1978) Resolution of the methane monooxygenase of *Methylococcus capsulatus* (Bath) into three components. Purification and properties of component C, a flavoprotein. *Biochem J* **171**: 461–468.

Colby, J., Stirling, D.I., Dalton, H. (1977) The soluble methane mono-oxygenase of *Methylococcus capsulatus* (Bath) - its ability to oxygenate n-alkanes, n-alkenes, ethers, and alicyclic aromatic and heterocyclic compounds. *Biochem J* **165**: 395–402.

Cook, S. A., Shiemke, A. K. (2002) Evidence that a type-2 NADH:Quinone oxidoreductase mediates electron transfer to particulate methane monooxygenase in *Methylococcus capsulatus* Bath. *Arch Biochem Biophys* **398**: 32–40.

Costello, A. M., Peeples, T. L., Lidstrom, M. E. (1995) Duplicate methane monooxygenase genes in methanotrophs. Poster presentation at 8th International symposium on "Microbial growth on C1 compounds". San Diego, California.

Culpepper, M. A., Rosenzweig, A. C. (2012) Architecture and active site of particulate methane monooxygenase. *Crit Rev Biochem Mol Biol* **47**(6): 483–492.

Culpepper, M. A., Rosenzweig, A. C. (2014) Structure and protein−protein interactions of methanol dehydrogenase from *Methylococcus capsulatus* (Bath). *Biochem* **53**: 6211–6219.
D'Onofrio, A., Crawford, J. M., Stewart, E. J., Witt, K., Gavrish, E., Epstein, S., et al. (2010) Siderophores from neighboring organisms promote the growth of uncultured bacteria. *Chem & Biol* **17**: 254–264.
Dedysh, S. N., Belova, S. E., Bodelier, P. L. E., Smirnova, K. V., Khmelenina, V. N., Chidthaisong, A., (2007) *Methylocystis heyeri* sp. nov., a novel type II methanotrophic bacterium possessing 'signature' fatty acids of type I methanotrophs. *Intl J Syst Evol Micr* **57**: 472–479.
Dedysh, S. N., Khmelenina, V. N., Suzina, N. E., Trotsenko, Y. A., Semrau, J. D., Liesack, W., et al. (2002) *Methylocapsa acidiphila* gen. nov., sp. nov., a novel methane-oxidizing and dinitrogen- fixing acidophilic bacterium from Sphagnum bog. *Int J Syst Evol Micr* **52**: 251–256.
Dedysh, S. N., Liesack, W., Khmelenina, V. N., Suzina, N. E., Trotsenko, Y. A., Semrau, J. D., et al. (2000) *Methylocella palustris* gen nov., a new methane-oxidizing acidophilic bacterium from peat bogs, representing a novel subtype of serine pathway methanotrophs. *Int J Syst Evol Micr* **50**: 955–969.
Dedysh, S. N., Panikov, N. S., Liesack, W., Großkopf, R., Zhou, J., Tiedje, J. M. (1998) Isolation of acidophilic methane-oxidizing bacteria from northern peat wetlands. *Science* **282**(5387): 281–284.
Dijkstra, M., Frank, J. Jr., Duine, J. A. (1989) Studies on electron transfer from methanol dehydrogenase to cytochrome $c_L$, both purified from *Hyphomicrobium* X. *Biochem J* **257**: 87–94.
DiSpirito, A. A., Zahn, J. A., Graham, D. W., Kim, H. J., Larive, C. K., Derrick, T. S., et al. (1998) Copper-binding compounds from *Methylosinus trichosporium* OB3b. *J Bacteriol* **180**: 3606–3613.
Dlugokencky, E. J., Nisbet, E. G., Fisher, R., Lowry, D. (2011) Global atmospheric methane: budget, changes and dangers. *Phil Trans R Soc A* **369**: 2058–2072.
Dominguez-Benetton, X., Srikanth, S., Satyawali, Y., Vanbroekhoven, K., Deepak, P. (2013) Enzymatic electrosynthesis: An overview on the progress in enzyme-electrodes for the production of electricity, fuels and chemicals. *J Microb Biochem Technol* **S6**: 007.
Dunfield, P. F., Belova, S. E., Vorobev, A. V., Cornish, S. L., Dedysh, S. N. (2010) *Methylocapsa aurea* sp. nov., a facultative methanotroph possessing a particulate methane monooxygenase, and emended description of the genus *Methylocapsa*. *Int J Syst Evol Micr* **60**: 2659–2664.
Dunfield, P. F., Khmelenina, V. N., Suzina, N. E., Trotsenko, Y., Dedsyh, S. N. (2003) *Methylocella silvestris* sp. nov., a novel methanotroph isolated from an acidic forest cambisol. *Int J Syst Evol Micr* **53**: 1231–1239.
Dunfield, P. F., Yimga, M. T., Dedysh, S. N., Berger, U., Liesack, W., Heyer, J. (2002) Isolation of a *Methylocystis* strain containing a novel *pmoA*-like gene. *FEMS Microbiol Ecol* **41**: 17–26.
Dunfield, P. F., Yuryev, A., Senin, P., Smirnova, A. V., Stott, M. B., Hou, S., et al. (2007) Methane oxidation by an extremely acidophilic bacterium of the phylum *Verrucomicrobia*. *Nature* **450**: 879–882.

Dzombak, D. A., Morel, F. M. M. (1990) Surface complexation modeling. Hydrous ferric oxide. John Wiley & Sons, New York.
Ehalt, D. H. (1974) The atmospheric cycle of methane. *Tellus* **26**: 58–70.
Ehalt, D. H., Schmidt, U. (1978) Sources and sinks of atmospheric methane. *Pure Appl Geophys* **116**: 452–464.
El Ghazouani, A., Basle, A., Firbank, S. J., Knapp, C. W., Gray, J., Graham, D. W., et al. (2011) Copper-binding properties and structures of methanobactins from *Methylosinus trichosporium* OB3b. *Inorg Chem* **50**: 1378–1391.
El Ghazouani, A., Basle, A., Gray, J., Graham, D. W., Firbank, S. J., Dennison, C. (2012) Variations in methanobactin structure influences copper utilization by methane-oxidizing bacteria. *Proc Nat Acad Sci USA* **109**: 8400–8404.
Elango, N. A., Radhakrishnan, R., Froland, W. A., Wallar, B. J., Earhart, C. A., Lipscomb, J. D., Ohlendorf, D. H. (1997) Crystal structure of the hydroxylase component of 136 methane monooxygenase from *Methylosinus trichosporium* OB3b. *Protein Sci* **6**: 556–568.
Ettwig, K. F., Butler, M. K., Le Paslier, D., Pelletier, E., Mangenot, S., Kuypers, M. M. M., et al. (2010) Nitrite-driven anaerobic methane oxidation by oxygenic bacteria. *Nature* **464**: 543–548.
Ettwig, K. F., Speth, D. R., Reimann, J., Wu, M. L., Jetten, M. S. M. (2012) Bacterial oxygen production in the dark. *Front Microbiol* **3**: 1–8.
Farhan Ul Haque, M., Kalidass, B., Bandow, N., Turpin, E. A., DiSpirito, A. A., Semrau, J. D. (2015) Cerium regulates expression of alternative methanol dehydrogenases in *Methylosinus trichosporium* OB3b. doi: 10.1128/AEM.02542–15.
Feely, R. A., Sabine, C. L., Lee, K., Berelson, W., Kleypas, J., Fabry, V. J., Millero, F. J. (2004) Impact of anthropogenic $CO_2$ on the $CaCO_3$ system in the oceans. *Science* **305**(5682): 362–366.
Fei, Q., Guarnieri, M.T., Tao, L., Laurens, L. M. L., Dowe, N., Pienkos, P. T. (2014) Bioconversion of natural gas to liquid fuel: opportunities and challenges. *Biotechnol Adv* 32: 596–614.
Feng, D., van-Deventer, J. S. J. (2011) The role of amino acids in the thiosulphate leaching of gold. *Miner Eng* **24**(9): 1022–1024.
Fitriyanto, N. A., Fushimi, M., Matsunaga, M., Petriwinigrum, A., Iwama, T., Kawai, K. (2011) Molecular structure and gene analysis of $Ce^{3+}$-induced methanol dehydrogenase of *Bradyrhizobium* sp. MAFF 211645. *J Biosci Bioeng* **111**: 613–617.
Foster, J. W., Davis, R. H. (1966) A methane-dependent coccus, with notes on classification and nomenclature of obligate, methane-utilizing bacteria. *J Bacteriol* **91**:1924–1931.
Fox, B. G., Froland, W. A., Dege, J. E., Lipscomb, J. D. (1989) Methane monooxygenase from *Methylosinus trichosporium* OB3b. Purification and properties of a three-component system with high specific activity from a type II methanotroph. *J Biol Chem* **264**: 10023–10033.
Friedle, S., Reisner, E., Lippard, S. J. (2010) Current challenges of modeling diiron enzyme active sites for dioxygen activation by biomimetic synthetic complexes. *Chem Soc Rev* **39**: 2768–2779.
Froland, W. A., Andersson, K. K., Lee, S. K., Liu, Y., Lipscomb, J. D. (1992) Methane monooxygenase component B and reductase alter the regioselectivity of the hydroxylase

component-catalyzed reactions. A novel role for protein-protein interactions in an oxygenase mechanism. *J Biol Chem* **267**: 17588–17597.
Fuglestvedt, J. S., Jonson, J. E., Wang, W. -C., Isaksen, I. S. A. (1995) Responses in tropospheric chemistry to changes in UV fluxes, temperatures and water vapour densities, in Atmospheric Ozone as a Climate Gas, edited by Wang, W. –C., Isaksen, I. S. A. pp. 145–162, *Springer-Verlag*, New York, USA.
Gaballa, A., MacLellan, S., Helmann, J. D. (2012) Transcription activation by the siderophore sensor Btr is mediated by ligand-dependent stimulation of promoter clearance. *Nucl Acids Res* **40**: 3585–3595.
Gadd, G. M. (2010) Metals, minerals and microbes: geomicrobiology and bioremediation. *Microbiology* **156**: 609–643.
Ge, F., Wang, X-D., Zhao, B., Wang, Y. (2006) Effects of rare earth elements on the growth of *Arnebia euchroma* cells and the biosynthesis of shikonin. *Plant Growth Regul* **48**: 283–290.
Geymonat, E., Ferrando, L., Tarlera, S. E. (2011) *Methylogaea oryzae* gen. nov., sp nov., a mesophilic methanotroph isolated from a rice paddy field. *Int J Syst Evol Micr* **61**: 2568–2572.
Ghosh, M., Anthony, C., Harlos, K., Goodwin, M. G., Blake, C. (1995) The refined structure of the quinoprotein methanol dehydrogenase from *Methylobacterium extorquens* at 1.94 Å. *Structure* **3**: 177–187.
Ghosh, R., Quayle, J. R. (1981) Purification and properties of the methanol dehydrogenase from *Methylophilus methylotrophus*. *Biochem J* **199**(1): 245–250.
Gilbert, B., McDonald, I. R., Finch, R., Stafford, G. P., Nielsen, A. K., Murrell, J. C. (2000) Molecular analysis of the *pmo* (particulate methane monooxygenase) operons from two type II methanotrophs. *Appl Environ Microbiol* **66**: 966–975.
Gliese, N., Khodaverdi, V., Görisch, H. (2010) The PQQ biosynthetic operons and their transcriptional regulation in *Pseudomonas aeruginosa*. *Arch Microbiol* **192**: 1–14.
Green, J., Dalton, H. (1985) Protein-B of soluble methane monooxygenase from *Methylococcus capsulatus* (Bath) – a novel regulatory protein of enzyme activity. *J Biol Chem* **260**: 5795–5801.
Gruber, N., Gloor, M., Fletcher, S. E. M., Doney, S. C., Dutkiewicz, s., Follows, M. J. et al. (2009) Oceanic sources, sinks, and transport of atmospheric $CO_2$. *Glob Biogeochem Cycles* **23**: GB1005.
Hakemian, A. S., Kondapalli, K. C., Telser, J., Hoffman, B. M., Stemmler, T. L., Rosenzweig, A. C. (2008) The metal centers of the particulate methane monooxygenase from *Methylosinus trichosporium* OB3b. *Biochemistry* **47**: 6793–6801.
Hallam, S. J., Putnam, N., Preston, C. M., Detter, J. C., Rokhsar, D., Richardson, P. M., et al. (2004) Reverse methanogenesis: testing the hypothesis with environmental genomics. *Science* **305**: 1457 –1462.
Han, J-I., Semrau J. D. (2004) Quantification of gene expression in methanotrophs by competitive reverse transcription-polymerase chain reaction. *Environ Microbiol* **6**:388–399.
Hanson, R.S., Hanson, T.S. (1996) Methanotrophic bacteria. *Microbiol Rev* **60**: 439–471.
Harms, N., Ras, J., Koning, S., Reijnders, W. N. M., Stouthamer, A. H., Van Spanning, R. J. M. (1996) Genetics of C1 metabolism regulation in *Paracoccus denitrificans*. In Microbial

Growth on C1 Compounds. 126–132. Edited by Lidstrom, M. E., Tabita, F. R. Dordrecht: Kluwer Academic Publishers.
Haroon, M. F., Hu, S., Shi, Y., Imelfort, M., Keller, J., Hugenholtz, P., et al. (2013) Anaerobic oxidation of methane coupled to nitrate reduction in a novel archaeal lineage. *Nature* **500**: 567–570.
Hazen, T. C., Chakraborty, R., Fleming, J. M., Gregory, I. R., Bowman, J. P., Jimenez, L., et al. (2009) Use of gene probes to assess the impact and effectiveness of aerobic in situ bioremediation of TCE. *Arch Microbiol* **191**: 221–232.
Hazeu, W., Batenburg-van der Vegte, W. H., deBruyn, J. C. (1980) Some characterizations of *Methylococcus mobilis* sp. nov. *Arch Microbiol* **124**: 211–220.
Helland, R., Fjellbirkeland, A., Karlsen, O. A., Ve, T., Lillehaug, J. R., Jensen, H. B. (2008) An oxidized tryptophan facilitates copper binding in *Methylococcus capsulatus*-secreted protein MopE. *J Biol Chem* **283**: 13897–13904.
Heyer, J., Berger, U., Hardt, M., Dunfield, P. F. (2005) *Methylohalobius crimeensis* gen. nov., sp. nov., a moderately halophilic, methanotrophic bacterium isolated from hypersaline lakes of Crimea. *Int J Syst Evol Micr* **55**: 1817–1826.
Hibi Y., Asai, K., Arafuka, H., Hamajima, M., Iwama, T., Kawai, K. (2011) Molecular structure of La (3+)-induced methanol dehydrogenase-like protein in *Methylobacterium radiotolerans*. *J Biosci Bioeng* **111**: 547–549.
Hinrichs, K-U., Boetius, A. (2002) The anaerobic oxidation of methane: New insights in microbial ecology and biogeochemistry. In Ocean Margin Systems. pp. 457–477. *Springer-Verlag*, Berlin.
Hirayama, H., Abe, M., Miyazaki, M., Nunoura, T., Furushima, Y., Yamamoto, H., et al. (2014) *Methylomarinovum caldicuralii* gen. nov., sp. nov., a moderately thermophilic methanotroph isolated from a shallow submarine hydrothermal system, and proposal of the family *Methylothermaceae* fam. nov. *Int J Syst Evol Microbiol* **64**(3): 989–999.
Hirayama, H., Fuse, H., Abe, M., Miyazaki, M., Nakamura, T., Nunoura, T., Furushima, Y., Yamamoto, H., Takai, K. (2013) *Methylomarinum vadi* gen. nov., sp. nov., a methanotroph isolated from two distinct marine environments. *Int J Syst Evol Microbiol* **63**: 1073–1082.
Hirayama, H., Suzuki, Y., Abe, M., Miyazaki, M., Makita, H., Inagaki, F., et al. (2011) *Methylothermus subterraneus* sp. nov., a moderately thermophilic methanotroph isolated from a terrestrial subsurface hot aquifer. *Int J Syst Evol Microbiol* **61**: 2646–2653.
Hoefman, S., Van der Ha, D., Iguchi, H., Yurimoto, H., Sakai, Y., Boon, N., Vandamme, P., Heylen, K., De Vos, P. (2014) *Methyloparacoccus murrellii* gen. nov., sp. nov., a methanotroph isolated from pond water. *Int J Syst Evol Microbiol* **64**: 2100–2107.
Hou, S., Makarova, K. S., Saw, J. H., Senin, P., Ly, B. V., Zhou, Z., et al. (2008) Complete genome sequence of the extremely acidophilic methanotroph isolate V4, *Methylacidiphilum infernorum*, a representative of the bacterial phylum *Verrucomicrobia*. *Biol Direct* **3**: 26.
Hu, S., Zeng, R. J., Keller, J., Lant, P. A., Yuan, Z. (2011) Effect of nitrate and nitrite on the selection of microorganisms in the denitrifying anaerobic methane oxidation process. *Environ Microbiol Rep* **3**: 315–319.
Hu, Z., Richter, H., Sparovek, G., Schnug, E. (2004): Physiological and biochemical effects of rare earth elements n plants and their agricultural significance: a review. *J Plant Nutr* **27**: 183–220.

Iguchi, H., Yurimoto, H., Sakai, Y. (2011) *Methylovulum miyakonense* gen. nov., sp. nov., a type I methanotroph isolated from forest soil. *Int J Syst Evol Micr* **61**: 810–815.

Intergovernmental Panel on Climate Change (IPCC) (2007), Climate Change 2007: The Scientific Basis. Contribution of Working Group I to the Fourth Assessment Report of the Intergovernmental Panel on Climate Change, edited by S. Solomon et al., *Cambridge Univ. Press*, New York, USA.

Intergovernmental Panel on Climate Change (IPCC) (2013), Summary for policymakers, in Climate Change 2013: The Physical Science Basis. Contribution of Working Group I to the Fifth Assessment Report of the Intergovernmental Panel on Climate Change, edited by Stocker, T. F., Qin, D., Plattner, G. K., Tignor, M., Allen, S. K., Boschung, et al. pp. 1535. *Cambridge Univ Press*, Cambridge, UK and New York, USA.

Islam, T., Jensen, S., Reigstad, L. J., Larsen, O., Birkeland, N-K. (2008) Methane oxidation at 55 °C and pH 2 by a thermoacidophilic bacterium belonging to the *Verrucomicrobia* phylum. *P Natl Acad Sci USA* **105**: 300–304.

Jiang, Z., Xiao, T., Kuznetsov, V. L., Edwards, P. P. (2010) Turning carbon dioxide to fuel. *Phil Trans R Soc* **368**: 33343–33364.

Kalidass, B., Farhan, Ul-Haque. M., Baral, B. S., DiSpirito, A. A., Semrau, J. D. (2015) Competition between metals for binding to methanobactin enables expression of soluble methane monooxygenase in the presence of copper. *Appl Environ Microbiol* **81**(3): 1024–2031.

Kalyuzhnaya, M. G., Khmelenina, V. N., Eshinimaev, B., Sorokin, D., Fuse, H., Lidstrom, M. E., et al. (2008) Classification of halo(alkali)philic and halo(alkali)tolerant methanotrophs provisionally assigned to the genera *Methylomicrobium* and *Methylobacter* and emended description of the genus *Methylomicrobium*. *Int J Syst Evol Micr* **58**: 591–596.

Kalyuzhnaya, M. G., Yang, S., Rozova, O. N., Smalley, N. E., Clubb, J., Lamb, A., et al. (2013) Highly efficient methane biocatalysis revealed in a methanotrophic bacterium. *Nat Commun* **4**.

Karlsen, O. A., Bervem, F. S., Stafford, G. P., Larsen, O., Murrell, J. C., Jensen, H., et al. (2003) The surface-associated and secreted MopE protein of *Methylococcus capsulatus* (Bath) responds to changes in the concentration of copper in the growth medium. *Appl Environ Microb* **69**: 2386–2387.

Karthikeyan, O. P., Karthigeyan, C. P., Cirés, S., Heimann, K. (2014) Review of sustainable methane mitigation and bio-polymer production. *Crit Rev Environ Sci Technol* **45**(15): 1579–1610.

Keltjens, J. T., Pol, A., Reimann, J., Op den Camp, H. J. (2014) PQQ-dependent methanol dehydrogenases: rare-earth elements make a difference. *Appl Microbiol Biotechnol* **98**: 6163–6183.

Kenney, G. E., Rosenzweig, A. C. (2013) Genome mining for methanobactins. *BMC Biology* **11**: 17.

Khadem, A. F., Pol, A., Wieczorek, A., Mohammadi, S. S., Francoijs, K. J., Stunnenberg, H. G., Jetten, M. S. M., Op den Camp, H. J. M. (2011) Autotrophic methanotrophy in Verrucomicrobia: *Methylacidiphilum fumariolicum* SolV uses the Calvin-Benson-Bassham cycle for carbon dioxide fixation. *J bacteriol* **193**: 4438–4446.

Khadem, A. F., van Teeseling, M. C., van Niftrik, N. L., Jetten, M. S., Op den Camp, H. J., Pol, A. (2012) Genomic and physiological analysis of carbon storage in the verrucomicrobial methanotroph "*Ca.* Methylacidiphilum fumariolicum" SolV. *Front Microbiol* **3**: 345.

Khalifa, A., Lee, C. G., Ogiso, T., Ueno, C., Dianou, D., Demachi, T., et al. (2015) *Methylomagnum ishizawai* gen. nov., sp. nov., a mesophilic type I methanotroph isolated from rice rhizosphere. *Int J Syst Evol Micr* **65**: 3527–3534.

Kim, H. G., Han, G. H., Kim, D., Choi, J.-S., Kim, S. W. (2012) Comparative analysis of two types of methanol dehydrogenase from *Methylophaga aminisulfidivorans* $MP^T$ grown on methanol. *J Basic Microbiol* **52**: 141–149.

Kim, H. J., Galeva, N., Larive, C. K., Alterman, M., Graham, D. W. (2005) Purification and physical-chemical properties of methanobactin: A chalkophore from *Methylosinus trichosporium* OB3b. *Biochemistry* **44**: 5140–5148.

Kim, H. J., Graham, D. W., DiSpirito, A. A., Alterman, M. A., Galeva, N., Larive, C. K., et al. (2004) Methanobactin, a copper-acquisition compound from methane-oxidizing bacteria. *Science* **305**: 1612–1615.

Kirschke, S., Bousquet, P., Ciais, P., Saunois, M., Dlugokencky, E. J., Bergamaschi, P., et al. (2013) Three decades of methane sources and sinks: budgets and variations. *Nat Geosci* **6**: 813–823.

Knapp, C. W., Fowle, D. A., Kulczycki, E., Roberts, J. A., Graham, D. W. (2007) Methane monooxygenase gene expression mediated by methanobactin in the presence of mineral copper sources. *Proc Nat Acad Sci USA* **104**: 12040–12045.

Kojima, H., Tsutsumi, M., Ishikawa, K., Iwata, T., Mußmann, M., Fukui, M. (2012) Distribution of putative denitrifying methane oxidizing bacteria in sediment of a freshwater lake, Lake Biwa. *Syst Appl Microbiol* **35**: 233–238.

Koldkin-Gal, I., Hazan, R., Gaathon, A., Carmeli, S., Engelberg-Kulka, H. (2007) A linear pentapeptide is a quorum-sensing factor required for *mazEF*-mediated cell death in *Escherichia coli*. *Science* **318**: 652–655.

Kool, D. M., Talbot, H. M., Rush, D., Ettwig, K., Sinninghe Damsté, J. S. (2014) Rare bacteriohopanepolyols as markers for an autotrophic, intra-aerobic methanotroph. *Geochim Cosmochim Acta* **136**: 114–125.

Krentz, B. D., Mulheron, H. J., Semrau, J. D., Dispirito, A. A., Bandow, N. L., Haft, D. H., et al. (2010) A comparison of methanobactins from *Methylosinus trichosporium* OB3b and *Methylocystis* strain SB2 predicts methanobactins are synthesized from diverse peptide precursors modified to create a common core for binding and reducing copper ions. *Biochemistry* **49**: 10117–10130.

Kulczycki, E., Fowle, D. A., Knapp, C., Graham, D. W., Roberts, J. A. (2007) Methanobactin-promoted dissolution of Cu-substituted borosilicate glass. *Geobiology* **5**: 251–263.

Kuznetsova, T.A., Beschastnyi, A.P., Ponamoreva, O.N., Trotsenko, Yu.A., (2012) Purification and characterization of methanol dehydrogenase of *Methylobacterium nodulans* rhizosphere phytosymbionts. *Appl Biochem Microbiol* **48**(6): 546–551.

Lamont, I. L., Beare, P. A., Ochsner, U., Vasil, A. I., Vasil, M. L. (2002) Siderophore-mediated signaling regulates virulence factor production in *Pseudomonas aeruginosa*. *Proc Natl Acad Sci* **99**: 7072–7077.

Lapidus, A., Clum, A., LaButti, K., Kalyuzhnaya, M. G., Lim, S., Beck, D. A. C., et al. (2011) Genomes of three methylotrophs from a single niche uncover genetic and metabolic divergence of *Methylophilaceae*. *J Bacteriol* **193**: 3757–3764.

Lau, E., Fisher, M. C., Steudler, P. A., Cavanaugh, C. M. (2013) The methanol dehydrogenase gene, *mxaF*, as a functional and phylogenetic marker for proteobacterial methanotrophs in natural environments. *PLoS ONE* **8**:e56993.

Lee, J., Wu, J., Deng, Y., Wang, J., Wang, C., Wang, J., et al. (2013b) A cell-cell communication signal integrates quorum sensing and stress response. *Nat Chem Biol* **9**: 339–343.

Lee, S. J., McCormick, M. S., Lippard, S. J., Cho, U. S. (2013a) Control of substrate access to the active site in methane monooxygenase. *Nature* **494**: 380–384.

Lemos, S. S., Collins, M. L. P., Eaton, S. S., Eaton, G. R., Antholine, W. E. (2000) Comparison of EPR-visible $Cu^{2+}$ sites in pMMO from *Methylococcus capsulatus* (Bath) and *Methylomicrobium album* BG8. *Biophys J* **79**: 1085–1094.

Lidstrom, M. E. (1990) Genetics of carbon metabolism in methylotrophic bacteria. *FEMS Microbiol Rev* **7**: 431–436.

Lidstrom, M. E., Anthony, C., Biville, F., Gasser, F., Goodwin, P., Hanson, R. S., et al. (1994) New unified nomenclature for genes involved in the oxidation of methanol in Gram-negative bacteria. *FEMS Microbiol Lett* **117**: 103–106.

Lieberman, R. L., Kondapalli, K. C., Shrestha, D. B., Hakemian, A. S., Smith, S. M., Telser, J., et al. (2006) Characterization of the particulate methane monooxygenase metal centers in multiple redox states by X-ray absorption spectroscopy. *Inorg Chem* **45**: 8372–8381.

Lieberman, R. L., Rosenzweig, A. C. (2005) Crystal structure of a membrane-bound metalloenzyme that catalyses the biological oxidation of methane. *Nature* **434**: 177–182.

Lieberman, R. L., Shrestha, D. B., Doan, P. E., Hoffman, B. M., Stemmler, T. L., Rosenzweig, A. C. (2003) Purified particulate methane monooxygenase from *Methylococcus capsulatus* (Bath) is a dimer with both mononuclear copper and a copper-containing cluster. *Proc Natl Acad Sci USA* **100**: 3820–3825.

Liebner, S., Svenning, M. M. (2013) Environmental transcription of *mmoX* by methane-oxidizing Proteobacteria in a subarctic palsa peatland. *Appl Environ Microbiol* **79**: 701–706.

Lipscomb, J. D. (1994) Biochemistry of the soluble methane monooxygenase. *Ann Rev Microbiol* **48**: 371–399.

Liu, K. E., Valentine, A. M., Wang, D. L., Huynh, B. H., Edmondson, D. E., Salifoglou, A., Lippard, S. J. (1995) Kinetic and spectroscopic characterization of intermediates and component interactions in reactions of methane monooxygenase from *Methylococcus capsulatus* (Bath). *J Am Chem Soc* **117**: 10174–10185.

Lützenkirchen, J. (1988) Comparison of 1-pK and 2-pK versions of surface complexation theory by goodness of fit in describing surface charge data of hydroxides. *Environ Sci Technol* **32**: 3149–3154.

Martinho, M., Choi, D. W., DiSpirito, A. A., Antholine, W. E., Semrau, J. D., Munck, W. (2007) Mossbauer studies of the membrane-associated methane monooxygenase from *Methylococcus capsulatus* Bath: evidence for a diiron center. *J Am Chem Soc* **129**: 15783–15785.

Matsushita, K., Takahashi, K., Adachi, O. (1993) A novel quinoprotein methanol dehydrogenase containing an additional 32-kilodalton peptide purified from *Acetobacter methanolicus*: identification of the peptide as a *moxJ* product. *Biochemistry* **32**: 5576–5582.

McDonald, I. R., Murrell, J. C. (1997) The particulate methane monooxygenase gene *pmoA* and its use as a functional gene probe for methanotrophs. *FEMS Microbiol Lett* **156**: 205–210.

Merkx, M., Kopp, D. A., Sazinsky, M. H., Blazyk, J. L., Muller, J., Lippard, S. J. (2001) Dioxygen activation and methane hydroxylation by soluble methane monooxygenase: A tale of two irons and three proteins. *Angew Chem Int Ed Engl* **40**: 2782–2807.

Merkx, M., Lippard, S. J. (2002) Why OrfY? Characterization of MMOD, a long overlooked component of the soluble methane monooxygenase from *Methylococcus capsulatus* (Bath). *J Biol Chem* **277**: 5858–5865.

Meyerdierks, A., Kube, M., Kostadinov, I., Teeling, H., Glösckner, F. O., Reinhardt, R., et al. (2010) Metagenome and mRNA expression analyses of anaerobic methanotrophic archaea of the ANME-1 group. *Environ Microbiol* **12**: 422–439.

Michael, T. M., Martinko, J. M., Parker, J., Brock, T.D. (2003) Brock Microbilogie: *Specktrum akademischer Verlag*, Heidelberg, Berlin.

Milucka, J., Ferdelman, T. G., Polerecky, L., Franzke, D., Wegener, G., Schmid, M., et al. (2012) Zero-valent sulphur is a key intermediate in marine methane oxidation. *Nature* **491**: 541–546.

Miyaji, A., Kamachi, T., Okura, I. (2002) Improvement of the purification method for retaining the activity of the particulate methane monooxygenase from *Methylosinus trichosporium* OB3b. *Biotechnol Lett* **24**: 1883–1887.

Miyaji, A., Miyoshi, T., Motokura, K., Baba, T. (2011) The substrate binding cavity of particulate methane monooxygenase from *Methylosinus trichosporium* OB3b expresses high enantioselectivity for n-butane and n-pentane oxidation to 2-alcohol. *Biotech Lett* **33**: 2241–2246.

Montzka. S., Dlugokencky, E., Butler, J. (2011) Non-$CO_2$ greenhouse gases and climate change. *Nature* **476:** 43–50.

Morris, C. J., Kim, Y. M., Perkins, K. E., Lidstrom, M. E. (1995) Identification and nucleotide sequences of *mxaA*, *mxaC*, *mxaK*, *mxaL*, and *mxaD* genes from *Methylobacterium extorquens* AM1. *J Bacteriol* **177**: 6825–6831.

Morton, J. D., Hayes, K. F., Semrau, J. D. (2000) Bioavailability of chelated and soil-adsorbed copper to *Methylosinus trichosporium* OB3b. *Environ Sci Technol* **34**: 4917–4922.

Mueller, H., Skrede, A., Kleppe, G. (2005) Lipids from methanotrophic bacteria for cholesterol reduction. Patent: WO 2005004888 A1.

Murrell, J. C. (1994) Molecular genetics of methane oxidation. *Biodegradation* **5**: 145–149.

Murrell, J. C., Gilbert, B., McDonald, I. R. (2000) Molecular biology and regulation of methane monooxygenase. *Arch Microbiol* **173**: 325–332.

Murrell, J. C., McDonald, I. R., Bourne, D. G. (1998) Molecular methods for the study of methanotroph ecology. *FEMS Microbiol Ecol* **27**: 103–114.

Muzio, L. J., Kramlich, J. K. (1988) An artifact in the measurement of $N_2O$ from combustion sources. *Geophys Res Lett* **15**: 1369–1372.

Myronova, N., Kitmitto, A., Collins, R. F., Miyaji, A., Dalton, H. (2006) Three-dimensional structure determination of a protein supercomplex that oxidizes methane to formaldehyde in *Methylococcus capsulatus* (Bath). *Biochem* **45**: 11905–11914.

Nakagawa, T., Mitsui, R., Tani, A., Sasa, K., Tashiro, S., Iwama, T., et al. (2012) A catalytic role of XoxF1 as $La^{3+}$ - dependent methanol dehydrogenase in *Methylobacterium extorquens* strain AM1. *PLoS ONE* **7**: e50480.

Nguyen, H. H. T., Elliott, S. J., Yip, I. H. K., Chan, S. I. (1998) The particulate methane monooxygenase from *Methylococcus capsulatus* (Bath) is a novel copper-containing three-subunit enzyme - isolation and characterization. *J Biol Chem* **273**: 7957–7966.

Nguyen, H-HT., Shiemke, A. K., Jacobs, S. J., Hales, B. J., Lidstrom, M. E., Chan, S. I. (1994) The nature of the copper ions in the membranes containing the particulate methane monooxygenase from *Methylococcus capsulatus* (Bath). *J Biol Chem* **269**: 14995–15005.

Nielsen, A. K., Gerdes, K., Murrell, J. C. (1997) Copper-dependent reciprocal transcriptional regulation of methane oxidation genes in *Methylococcus capsulatus* Bath and *Methylosinus trichosporium* OB3b. *Mol Microbiol* **25**: 399–409.

Nojiri, M., Hira, D., Yamaguchi, K., Okajima, T., Tanizawa, K., Suzuki, S. (2006) Crystal structures of cytochrome $c_L$ and methanol dehydrogenase from *Hyphomicrobium denitrificans*: structural and mechanistic insights into interactions between the two proteins. *Biochemistry* **45**: 3481–3492.

Nunn, D. N., Day, D., Anthony, C. (1989) The second subunit of methanol dehydrogenase of *Methylobacterium extorquens* AM1. *Biochem J* **260**: 857–862.

Nunn, D., Lidstrom, M. E. (1986) Phenotypic characterization of 10 methanol oxidation mutant classes in *Methylobacterium* sp. strain AM1. *J Bacteriol* **166**: 591–597.

O'Halloran, T. V. (1993) Transition metals in control of gene expression. *Science* **261**: 715–725.

Ohara, T., Akimoto, H., Kurokawa, J., Horii, N., Yamaji, K., Yan, X., and Hayasaka, T. (2007) An asian emission inventory of anthropogenic emission sources for the period 1980–2020, *Atmos Chem Phys* **7**: 4419–4444,.

Okada, M., Sato, I., Cho, S. J., Dubnau, D., Sakagami, Y. (2006) Chemical synthesis of ComX pheromone and related peptides containing isoprenoidal tryptophan residues. *Tetrahedron* **62**: 8907–8918.

Op den Camp, H. J. M., Islam, T., Stott, M. B., Harhangi, H. R., Hynes, A., Schouten, S., Jetten, M. S. M., et al. (2009) Environmental, genomic and taxonomic perspectives on methanotrophic Verrucomicrobia. *Environ Microbiol Rep* **1**(5): 293–306.

Oubrie, A., Rozeboom, H.J., Kalk, K.H., Huizinga, E.G., Dijkstra, B.W. (2002) Crystal structure of quinohemoprotein alcohol dehydrogenase from *Comamonas testosteroni*: Structural basis for substrate oxidation. *J Biol Chem* **277**: 3727–3732.

Øverland, M., Tauson, A. H., Shearer, K., Skrede, A. (2010) Evaluation of methane-utilising bacteria products as feed ingredients for monogastric animals. *Arch Anim Nutr* **64**: 171–189.

Pagano, G., Guida, M., Tommasi, F., Oral, R. (2015) Health effects and toxicity mechanisms of rare earth elements-Knowledge gaps and research prospects. *Ecotoxicol Environ Saf* **115**: 40–48.

Parker, M. W., Cornish, A., Gossain, V., Best, D. J. (1987) Purification, crystallisation and preliminary X-ray diffraction characterisation of methanol dehydrogenase from *Methylosinus trichosporium* OB3b. *Eur J Biochem* **164**: 223–227.

Parker, R., Boesch, H., Cogan, A., Fraser, A., Feng, L., Palmer, et al. (2011) Methane observations from the greenhouse gases observing satellite: Comparison to ground-based TCCON data and model calculations. *Geophys Res Lett* **38**: L15807.

Pesch, M. L., Christl, I., Hoffmann, M., Kraemer, S. M., Kretzschmar, R. (2012) Copper complexation of methanobactin isolated from *Methylosinus trichosporium* OB3b: pH-dependent speciation and modeling. *J Inorg Biochem* **116**: 55–62.

Pesci, E. C., Milbank, J. B. J., Pearson, J. P., McKnight, S., Kende, A. S., Greenberg, E. P., et al. (1999) Quinolone signaling in the cell-to-cell communication system of *Pseudomonas aeruginosa*. *Proc Natl Acad Sci USA* **96**: 11229–11234.

Poehlein, A., Deutzmann, J. S., Daniel, R., Simeonova, D. D. (2013) Draft genome sequence of the methanotrophic *Gammaproteobacterium Methyloglobulus morosus* DSM 22980 Strain KoM1. *Genome Announc* **1**(6): e01078-13.

Pol, A., Barends, T. R. M., Dietl, A., Khadem, A. F., Eygensteyn, J., Jetten, M. S. M., Op den Camp, H. J. M. (2014) Rare earth metals are essential for methanotrophic life in volcanic mudpots. *Environ Microbiol* **16**: 255–264.

Pol, A., Heijmans, K., Harhangi, H. R., Tedesco, D., Jetten, M. S. M., Op den Camp, H. J. M. (2007) Methanotrophy below pH 1 by a new Verrucomicrobia species. *Nature* **450**: 874–878.

Prentice, I. C., Farquhar, G. D., Fasham, M. J. R., Goulden, M. L., Heimann, M., Jaramillo, V. J., et al., in Climate Change 2001: The Scientific Basis. Contribution of Working Group I to the Third Assessment Report of the Intergovernmental Panel on Climate Change. Houghton, J. T., et al., Eds. pp. 183–237. *Cambridge Univ Press*, New York, USA.

Price, S. J., Sherlock, R. R., Kelliher, F. M., McSeveny, T. M., Tate, K. R., Condron, L. M. (2004) Pristine New Zealand forest soil is a strong methane sink. *Glob Change Biol* **10**: 16–26.

Prinn, R. G., Weiss, R. F., Fraser, P. J., Simmonds, P. G., Cunnold, D. M., Alyea, F. N., et al. (2000) A history of chemically and radiatively important gases in air deduced from ALE/GAGE/AGAGE. *J Geophys Res* **105**(D14): 17751–17792.

Prinn, R. G., Weiss, R. F., Miller, B., Huang, J., Alyea, F. N., Cunnold, D. M., et al. (1995) Atmospheric trends and lifetime of trichloroethane and global hydroxyl radical concentrations based on 1978-1994 ALE/GAGE measurements. *Science* **269**: 187–192, 1995.

Puehringer, S., Metlitzky, M., Schwarzenbacher, R. (2008) The pyrroloquinoline quinone biosynthesis pathway revisited: a structural approach. *BMC Biochem* **9**: 8.

Rahalkar, M., Bussmann, I., Schink, B. (2007) *Methylosoma difficile* gen. nov., sp. nov., a novel methanotroph enriched from gradient cultivation from littoral sediment of Lake Constance. *Int J Syst Evol Micr* **57**: 1073–1080.

Rasigraf, O., Kool, D. M., Jetten, M. S. M., Sinninghe Damsté, J. S., Ettwig, K. F. (2014) Autotrophic carbon dioxide fixation via the Calvin-Benson-Bassham cycle by the denitrifying methanotroph *Methylomirabilis oxyfera*. *Appl Environ Microbiol* **80**(8): 2451–2460.

Reeburgh, W. S. (2007) Oceanic methane biogeochemistry. *Chem Rev* **107**: 486–513.

Richardson, I. W., Anthony, C. (1992) Characterization of mutant forms of the quinoprotein methanol dehydrogenase lacking an essential calcium ion. *Biochem J* **287**: 709–715.

Rosenzweig, A. C., Brandstetter, H., Whittington, D. A., Nordlund, P., Lippard, S. J., Frederick, C. A. (1997) Crystal structures of the methane monooxygenase hydroxylase from *Methylococcus capsulatus* (Bath): implications for substrate gating and component interactions. *Proteins* **29**: 141–152.

Rosenzweig, A. C., Frederick, C. A., Lippard, S. J., Nordlund, P. (1993) Crystal structure of a bacterial non-haem iron hydroxylase that catalyses the biological oxidation of methane. *Nature* **366**: 537–543.

Ruiz, A., Ogden, K. L. (2004) Biotreatment of copper and isopropyl alcohol in waste from semiconductor manufacturing. *IEEE Trans Semicond Manuf* **17**: 538–543.

Ryan, R. P., Dow, J. M. (2008) Diffusible signals and interspecies communication in bacteria. *Microbiol* **154**: 1845–1858.

Schmidt, S., Christen, P., Kiefer, P., Vorholt, J. A. (2010) Functional investigation of methanol dehydrogenase-like protein XoxF in *Methylobacterium extorquens* AM1. *Microbiology* **156**: 2575–2586.

Schnell, S., King, G. M. (1995) Stability of methane oxidation capacity to variations in methane and nutrient concentrations. *FEMS Microbiol Ecol* **17**: 285–294.

Schreiber, L., Holler, T., Knittel, K., Meyerdierks, A., Amann, R. (2010) Identification of the dominant sulfate-reducing bacterial partner of anaerobic methanotrophs of the ANME-2 clade. *Environ Microbiol* **12**: 2327–2340.

Seitzinger, S. P., Kroeze, C., Styles, R. (2000) Global distribution of $N_2O$ emissions from freshwater and coastal marine systems: Natural emissions and anthropogenic effects. *Chemosphere–Global Change Sci* **2**: 267–279.

Semrau, J. D., Chistoserdov, A., Lebron, J., Costello, A., Davagnino, J., Kenna, E., et al. (1995) Particulate methane monooxygenase genes in methanotrophs. *J Bacteriol* **177**: 3071–3079.

Semrau, J. D., DiSpirito, A. A., Yoon, S. (2010) Methanotrophs and copper. *FEMS Microbiol Rev* **34**: 496–531.

Semrau, J. D., Jagadevan, S., DiSpirito, A. A., Khalifa, A., Scanlan, J., Bergman, B. H., et al. (2013) Methanobactin and MmoD work in concert to act as the "copper-switch" in methanotrophs. *Environ Microbiol* **15**: 3077–3086.

Sharp, C. E., Martínez-Lorenzo, A., Brady, A. L., Grasby, S. E., Dunfield, P. F. (2014) Methanotrophic bacteria in warm geothermal spring sediments identified using stable-isotope probing. *FEMS Microbiol Ecol* **90**(1): 92–102.

Shiemke, A. K., Arp, D. J., Sayavedra-Soto, L. A. (2004) Inhibition of membrane-bound methane monooxygenase and ammonia monooxygenase by diphenyliodonium: implications for electron transfer. *J Bacteriol* **186**: 928–937.

Sikkeland, L. I., Thorgersen, E. B., Haug, T., Mollnes, T. E. (2007) Complement activation and cytokine response by BioProtein, a bacterial single cell protein *Clin Exp Immunol* **148**(1): 146–152.

Silverman, J., Resnick, S. M., Mendez, M. (2014) Making fuel e.g. diesel fuel involves converting biomass from culture primarily comprising single carbon-metabolizing non-photosynthetic microorganism into oil composition and refining the oil composition into a fuel. Patent: US2014024872-A1, US2014024872-A1, C10G-003/00 201411.

Sirajuddin, S., Barupala, D., Helling, S., Marcus, K., Stemmler, T. L., Rosenzweig, A. C. (2014) Effects of zinc on particulate methane monooxygenase activity and structure. *J Biol Chem* **289**(31): 21782–21794.

Sivan, O., Antler, G., Turchyn, A. V., Marlow, J. J., Orphan, V. J. (2014) Iron oxides stimulate sulfate-driven anaerobic methane oxidation in seeps. *Proc Natl Acad Sci USA* **111**(40): E4139–E4147.

Skovran, E., Palmer, A. D., Rountree, A. M., Good, N. M., Lidstrom, M. E. (2011) XoxF is required for expression of methanol dehydrogenase in *Methylobacterium extorquens* AM1. *J Bacteriol* **193**: 6032–6038.

Smith, D. D. S., Dalton, H. (1989) Solubilization of methane monooxygenase from *Methylococcus capsulatus* (Bath). *Eur J Biochem* **182**: 667–671.

Smith, S. J., Edmonds, J. A., Hartin, C. A., Mundra, A., Calvin, K. V. (2015) Near-term acceleration in the rate of temperature change. *Nat Clim Change* **5**(4): 333–336.

Smith, S. M., Rawat, S., Telser, J., Hoffman, B. M., Stemmler, T. L., Rosenzweig, A. C. (2011) Crystal structure and characterization of particulate methane monooxygenase from *Methylocystis* species strain M. *Biochemistry* **50**: 10231–10240.

Sommerhalter, M., Lieberman, R. L., Rosenzweig, A. C. (2005) X-ray crystallography and biological metal centers: Is seeing believing? *Inorg Chem* **44**: 770–778.

Springer, A. L., Auman, A. J., Lidstrom, M. E. (1998) Sequence and characterization of *mxaB*, a response regulator involved in regulation of methanol oxidation, and of *mxaW* a methanol-regulated gene in *Methylobacterium extorquens* AM1. *FEMS Microbiol Lett* **160**: 119–124.

Springer, A. L., Chou, H. H., Fan, W. H., Lee, E., Lidstrom, M. E. (1995) Methanol oxidation mutants in *Methylobacterium extorquens* AM1: identification of new genetic complementation groups. *Microbiology* **141**: 2985–2993.

Springer, A. L., Morris, C. J., Lidstrom, M. E. (1997) Molecular analysis of *mxbD* and *mxbM*, a putative sensor-regulator pair required for oxidation of methanol in *Methylobacterium extorquens* AM1. *Microbiology* **143**: 1737–1744.

Springer, A. L., Ramamoorthi, R., Lidstrom, M. E. (1996) Characterization and nucleotide sequence of *pqqE* and *pqqF* in *Methylobacterium extorquens* AM1. *J Bacteriol* **178**: 2154–2157.

Stafford, G., Scanlan, J., McDonald, I., Murrell, J. C. (2003) *ropN*, *mmoR* and *mmoG*, genes involved in regulating the expression of soluble monooxygenase in *Methylosinus trichosporium* OB3b. *Microbiology* **149**: 1771–1784.

Stanley, S. H., Prior, S. D., Leak, D. J., Dalton, H. (1983) Copper stress underlies the fundamental change in intracellular location of methane mono-oxygenase in methane-oxidizing organisms - studies in batch and continuous cultures. *Biotechnol Lett* **5**: 487–492.

Stirling, D. I., Colby, J., Dalton, H. (1979) A comparison of the substrate and electron-donor specificity of the methane monooxygenase from three strains of methane oxidizing bacteria. *Biochem J* **177**: 362–364.

Stokke, R., Roalkvam, I., Lanzen, A., Haflidason, H., Steen, I. H. (2012) Integrated metagenomic and metaproteomic analyses of an ANME-1-dominated community in marine cold seep sediments. *Environ Microbiol* **14**: 1333–1346.

Stolyar, S., Costello, A. M., Peeples, T. L., Lidstrom, M. E. (1999) Role of multiple gene copies in particulate methane monooxygenase activity in the methane-oxidising bacterium *Methylococcus capsulatus* Bath. *Microbiology* **145**: 1235–1244.

Subak, S., Raskin, P., Von Hippel, D. (1993) National greenhouse gas accounts: Current anthropogenic sources and sinks. *Clim Chang* **25**: 15–58.

Summer, K. H., Lichtmannegger, J., Bandow, N., Choi, D. W., DiSpirito, A. A., Michalke, B. (2011) The biogenic methanobactin is an effective chelator for copper in a rat model for Wilson disease. *J Trace El Med Biol* **25**: 36–41.

Takano, E. (2006) γ-butyrolactones: Streptomyces signaling molecules regulating antibiotic production and differentiation. *Curr Opin Microbiol* **9**: 287–294.

Tavormina, P. L., Hatzenpichler, R., McGlynn, S., Chadwick, G., Dawson, K.S., Connon, S.A. et al. (2015) *Methyloprofundus sedimenti* gen. nov., sp. nov., an obligate methanotroph from ocean sediment belonging to the "deep sea-1" clade of marine methanotrophs. *Int J Syst Evol Microbiol* **65**: 251–259.

Thauer, R. K. (2011) Anaerobic oxidation of methane with sulfate: on the reversibility of the reactions that are catalyzed by enzymes also involved in methanogenesis from CO2. *Curr Opin Microbiol* **14**: 292–299.

Theisen, A. R., Ali, M. H., Radajewski, S., Dumont, M. G., Dunfield, P. F., McDonald, I. R., et al. (2005) Regulation of methane oxidation in the facultative methanotroph *Methylocella silvestris* BL2. *Mol Microbiol* **58**: 682–692.

Tinberg, C. E., Lippard, S. J. (2010) Oxidation reactions performed by soluble methane monooxygenase hydroxylase intermediates Hperoxo and Q proceed by distinct mechanisms. *Biochemistry* **49**: 7902–7912.

Toyama, H., Chistoserdova, L., Lidstrom, M. E. (1997) Sequence analysis of *pqq* genes required for biosynthesis of pyrroloquinoline quinone in *Methylobacterium extorquens* AM1 and the purification of a biosynthetic intermediate. *Microbiology* **143**: 595–602.

Traxler, M. F., Seyedsayamdost, M. R., Clardy, J., Kolter, R. (2012) Interspecies modulation of bacterial development through iron competition and siderophore piracy. *Mol Microbiol* **86**: 628–644.

Trotsenko, I. A., Doronina, N. V., Khmelenina, V. N. (2005) Biotechnological potential of methylotrophic bacteria: a review of current status and future prospects. *Prikl Biokhim Mikrobiol* **41**(5): 495–503.

Tsubota, J., Eshinimaev, B. Ts., Khmelenina, V. H., Trotsenko, Y. A. (2005) *Methylothermus thermalis* gen. nov., sp. nov., a novel moderately thermophilic obligate methanotroph from a hot spring in Japan. *Int J Syst Evol Micr* **55**: 1877–1884.

Valentine, A. M., LeTadic-Biadatti, M. H., Toy, P. H., Newcomb, M., Lippard, S. J. (1999) Oxidation of ultrafast radical clock substrate probes by the soluble methane monooxygenase from *Methylococcus capsulatus* (Bath) *J Biol Chem* **274**: 10771–10776.

Van Groenigen, J. W., Velthof, G. L., Oenema, O., Van Groenigen, K. J., Van Kessel, C. (2010) Towards an agronomic assessment of $N_2O$ emissions: A case study for arable crops. *Eur J Soil Sci* **61**(6): 903–913.

Van Spanning, R. J., Wansell, C. W., De Boer, T., Hazelaar, M. J., Anazawa, H., Harms, N., et al. (1991) Isolation and characterization of the *moxJ*, *moxG*, *moxI*, and *moxR* genes of

*Paracoccus denitrificans*: inactivation of *moxJ*, *moxG*, and *moxR* and the resultant effect on methylotrophic growth. *J Bacteriol* **173**: 6948–6961.
Ve, T., Mathisen, K., Helland, R., Karlsen, O. A., Fjellbirkeland, A., Røhr, Å. K., et al. (2012) The *Methylococcus capsulatus* (Bath) secreted protein, MopE*, binds both reduced and oxidized copper. *PLoS ONE* **7**(8): e43146.
Vigliotta, G., Nutricati, E., Carata, E., Tredici, S. M., De Stefano, M., Pontieri, P., et al. (2007) *Clonothrix fusca* Roze 1896, a filamentous, sheathed, methanotrophic *γ-proteobacterium*. *Appl Environ Microbiol* **73**: 3556–3565.
Vorobev, A. V., Baani, M., Doronina, N. V., Brady, A. L., Liesack, W., Dunfield, P. F., et al. (2011) *Methyloferula stellata* gen. nov., sp nov., an acidophilic, obligately methanotrophic bacterium that possesses only a soluble methane monooxygenase. *Int J Syst Evol Micr* **61**: 2456–2463.
Vorobev, A., Jagadevan, S., Baral, B. S., Dispirito, A. A., Freemeier, B. C., Bergman, B. H., Bandow, N. L., Semrau, J. D. (2013) Detoxification of mercury by methanobactin from *Methylosinus trichosporium* OB3b. *Appl Environ Microb* **79**: 5918–5926.
Wackett, L. P., Professor, M. (2014) Methanotroph biotechnology. *Microb Biotechnol* **7**(1): 86–87.
Wallar, B. J., Lipscomb, J. D. (1996) Dioxygen activation by enzymes containing binuclear non-heme iron clusters. *Chem Rev* **96**: 2625–2657.
Wallar, B. J., Lipscomb, J. D. (2001) Methane monooxygenase component B mutants alter the kinetics of steps throughout the catalytic cycle. *Biochemistry* **40**: 2220–2233.
Wang, F. P., Zhang, Y., Chen, Y., He, Y., Qi, J., Hinrichs, K-U., Zhang, X-X., Xiao, X., Boon, N. (2014) Methanotrophic archaea possessing diverging methane-oxidizing and electron-transporting pathways. *ISME J* **8**: 1069–1078.
Wartiainen, I., Grethe Hestnes, A., McDonald, I. R., Svenning, M. M. (2006a) *Methylocystis rosea* sp. nov., a novel methanotrophic bacterium from Arctic wetland soil, Svalbard, Norway (78u N). *Int J Syst Evol Microbiol* **56**: 541–547.
Wartiainen, I., Hestnes, A. G., McDonald, I. R., Svenning, M. M. (2006b) *Methylobacter tundripaludum* sp. nov., a methane-oxidizing bacterium from arctic wetland soil on the Svalbard islands, Norway (781N). *Int J Syst Evol Micr* **56**: 109–113.
Whittenbury, R. A., Krieg, N. R. (1984) Family IV. *Methylococcaceae*. In Krieg and Holt (Editors), *Bergey' s manual of systematic bacteriology*. Williams and Wilkins Co, Baltimore, 256–261.
Whittenbury, R., Phillips, K. C., Wilkinson, J. G. (1970) Enrichment, isolation and some properties of methane-utilizing bacteria. *J Gen Microbiol* **61**: 205–218.
Williams, P. A., Coates, L., Mohammed, F., Gill, R., Erskine, P. T., Coker, A., et al. (2005) The atomic resolution structure of methanol dehydrogenase from *Methylobacterium extorquens*. *Acta Crystallogr D Biol Crystallogr* **61**: 75–79.
Winzer, K., Hardie, K. R., Williams, P. (2002) Bacterial cell-to-cell communication: sorry, can't talk now – gone to lunch! *Curr Op Microbiol* **5**: 216–222.
Wise, M. G., McArthur, J. V., Shimkets, L. J. (2001) *Methylosarcina fibrata* gen. nov., sp. nov., and *Methylosarcina quisquiliarum* sp. nov., novel type I methanotrophs. *Int J Syst Evol Micr* **51**: 611–621.Kalyuzhnaya, M. G., Stolyar, S. M., Auman, A. J., Lara, J. C., Lidstrom, M. E., Chistoserdova, L. (2005) *Methylosarcina lacus* sp. nov., a methanotroph from Lake

Washington, Seattle, USA, and emended description of the genus *Methylosarcina*. *Int J Syst Evol Micr* **55**: 2345–2350.
Wu, M. L., Ettwig, K. F., Jetten, M. S., Strous, M., Keltjens, J. T., van Niftrik, L. (2011) A new intra-aerobic metabolism in the nitrite-dependent anaerobic methane-oxidizing bacterium *Candidatus* 'Methylomirabilis oxyfera'. *Biochem Soc Trans* **39**: 243–248.
Wu, M. L., Wessels, H. J., Pol, A., Op den Camp, H. J., Jetten, M. S., van Niftrik, L., et al. (2015) An XoxF-type methanol dehydrogenase from the anaerobic methanotroph '*Candidatus Methylomirabilis oxyfera*'. *Appl Environ Microbiol* **81**(4): 1442–1451.
Xavier, K. B., Miller, S. T., Lu, W., Kim, J. H., Rabinowitz, J., Pelczer, I., et al. (2007) Phosphorylation and processing of the quorum-sensing molecule autonducer-2 in enteric bacteria. *ACS Biol* **2**: 128–136.
Xia, Z. X., Dai, W. W., He, Y. N., White, S. A., Mathews, F. S., Davidson, V. L. (2003) X-ray structure of methanol dehydrogenase from *Paracoccus denitrificans* and molecular modeling of its interactions with cytochrome $c_{551i}$. *J Biol Inorg Chem* **8**: 843–854.
Xia, Z. X., Dai, W. W., Xiong, J. P., Hao, Z. P., Davidson, V. L., White, S., et al. (1992) The three-dimensional structures of methanol dehydrogenase from two methylotrophic bacteria at 2.6-angstrom resolution. *J Biol Chem* **267**: 22289–22297.
Xia, Z. X., He, Y. N., Dai, W. W., White, S. A., Boyd, G. D., Mathews, F. S. (1999) Detailed active site configuration of a new crystal form of methanol dehydrogenase from *Methylophilus* W3A1 at 1.9 Å resolution. *Biochemistry* **38**: 1214–1220.
Xia, Z., Dai, W., Zhang, Y., White, S. A., Boyd, G. D., Mathews, F. S. (1996) Determination of the gene sequence and the three-dimensional structure at 2.4 angstroms resolution of methanol dehydrogenase from *Methylophilus* W3A1. *J Mol Biol* **259**: 480–501.
Xin, J. Y., Cui, J. R., Niu, J. Z., Hua, S. F., Xia, C. G., Li, S. B., Zhu, L. M. (2004) Production of methanol from methane by methanotrophic bacteria. *Biocatal Biotransform* **22**: 225–229.
Yajima, A. (2014) Recent progress in the chemistry and chemical biology of microbial signaling molecules: quorum-sensing pheromones and microbial hormones. *Tetrahedron Lett* **55**(17): 2773–2780.
Yoon, S., Carey, J. N., Semrau, J. D. (2009) Feasibility of atmospheric methane removal using methanotrophic biotrickling filters. *Appl Microbiol Biotechnol* **83**: 949–956.
Zahn, J. A., DiSpirito, A. A. (1996) Membrane-associated methane monooxygenase from *Methylococcus capsulatus* (Bath). *J Bacteriol* **178**: 1018–1029.
Zhang, C., Li, Q., Zhang, M., Zhang, N., Li, M. (2013) Effects of rare earth elements on growth and metabolism of medicinal plants. *Acta Pharm Sin B* **3**: 20–24.
Zhang, M., Lidstrom, M. E. (2003) Promoters and transcripts for genes involved in methanol oxidation in *Methylobacterium extorquens* AM 1. *Microbiology* **149**: 1033–1040.
Zischka, H., Lichtmannegger, J., Schmitt, S., Jagemann, N., Schulz, S., Wartini, D., et al. (2011) Liver mitochondrial membrane crosslinking and destruction in a rat model of Wilson disease. *J Clin Invest* **121:** 1508–1518.